Hydrogeophysical quantification of infiltration and recharge through soil-filled sinkholes using Time Domain Reflectometry and Electrical Resistivity Tomography

Benjamin Farley Schwartz

Dissertation submitted to the faculty of the Virginia Polytechnic Institute and State University in partial fulfillment of requirements for the degree of

Doctor of Philosophy
in
Geosciences

Committee
Madeline E. Schreiber, Chair
Thomas J. Burbey
W. Lee Daniels
J. Donald Rimstidt
William B. White

November 16, 2007
Blacksburg, VA

Keywords: mantled karst, deep drainage, potential recharge, karst hydrology, concentrated recharge, diffuse recharge

Hydrogeophysical quantification of infiltration and recharge through soil-filled sinkholes using Time Domain Reflectometry and Electrical Resistivity Tomography

Benjamin Farley Schwartz

ABSTRACT

This dissertation presents the results of a detailed physical and hydrogeophysical study of two soil-filled sinkholes mantled by ancient New River fluvial terrace deposits. Research was performed at the Virginia Tech Kentland Experimental Farms in Whitethorne, Virginia, USA between fall 2003 and spring 2007, and focused on characterizing infiltration, deep drainage, and recharge through soil-filled sinkholes. Using hydrogeophysical methods, the spatial and temporal distribution of soil moisture was modeled and potential recharge was quantified in two soil-filled sinkholes.

Access-tube time domain reflectometry (TDR) was used to derive one-dimensional (1-D) soil moisture profiles. During access-tube installation, 470 soil samples were obtained from depths between 0.3 and to 9.0 m and characterized both physically and chemically. Using these data, a TDR calibration method was developed. Physio-chemical, TDR moisture, and 1-D electrical resistivity tomography (ERT) data were used to derive a numerically optimized form of Archie's Law which was used to convert ERT measurements into volumetric soil moisture. These results led to development of 2-D ERT-derived distributions of soil moisture in three transects across the two sinkholes in two terraces. Potential recharge was quantified using time-series ERT data with comparison to modeled cumulative potential evapotranspiration (PET) and cumulative precipitation between May 17 and October 9, 2006. The patterns of ERT-derived potential recharge values compared well with those expected from PET and precipitation data. Over the monitoring period from late spring to early fall during this study, results showed that a period of intense rain followed by a 31-day period of consistent rain, in which the rate of precipitation was equal to or exceeded PET, were the only periods in which significant amounts of potential recharge occurred (from 19 to 31% of cumulative precipitation during the study). Spatial distributions of ERT-derived moisture clearly revealed that significant amounts of infiltration occurred on sinkhole flanks and bottoms. Runoff during periods of intense rain flowed to the topographically lowest point in the sinkholes where it infiltrated and resulted in localized zones of enhanced infiltration and potential recharge to the water table.

DEDICATION

This dissertation would not have been completed without the understanding and unwavering support of my wonderful wife, Corinne Schwartz.

Cori, I dedicate this dissertation to you.
Thank you for all your sacrifices.

ACKNOWLEDGMENTS

Though the following pages may seem to be excessive in length, it is, in fact, impossible for me to thank all those who have helped throughout my life and more recent education. Since I am preparing to begin what I hope will be a productive and exciting career, I feel I should acknowledge at least some of the many who have helped me reach this point in my life.

Through the support and guidance of an excellent researcher and incredible advisor, Madeline Schreiber, I have not only completed a Ph.D. in Geosciences, but feel I am well prepared to begin my own career as a researcher, educator and advisor. Maddy, thank you for working with me, guiding me, and giving me the freedom to pursue research directions which had little in common with your existing research: Only now do I understand how uncommon this is. I will always be grateful for the opportunity to have worked with such a superb mentor and researcher and can only hope to follow your example in my future endeavors.

I thank my committee members Tom Burbey, Lee Daniels, Don Rimstidt and Will White for their teaching, collaboration, support and guidance over the last four and a half years. It has been a rich and fulfilling period for me and your advice and support have always been appreciated. I am very fortunate to have had such an exceptional committee. Jim Spotilla has also been an invaluable source of advice and generosity during my graduate work at Virginia Tech. I appreciate the discussions we have had regarding research topics unrelated to my dissertation work, as well as your willingness to share critical equipment.

Without friends and family, life would not be such a beautiful experience. This has certainly been true for me and I especially thank my wife Cori, my son Zachary, my parents Connie and Leonidas, and my brothers Aedin, Baron, and Nathaniel for helping to make me the person I am today, for being such good friends, and for being a great and tolerant family. I also thank the many friends I have made in the Geosciences Department, Blacksburg, and elsewhere, who have encouraged and supported me during my education. The life of a graduate student may be one of financial poverty, but it is wonderfully rich in friendship, collaboration, and assistance: many thanks to all of you.

Mike and Trudy Nicholson are not only wonderful friends, but have also been a second family to me since I met them in 1994. After I left a 4-year job working for Mike as a precision CNC machinist to attend college, they generously and unexpectedly contributed to my undergraduate education. Their only request was that I do the same for others in the future if I am able. Mike and Trudy: know that your generosity will be paid forward many times over.

I owe an especially warm thanks to all the incredible friends I have made during nearly 20 years of caving. Through you I have come to understand what friendship really means. Fun, sweat, tears, blood and mud brought us together and keep us together; no matter how small the obstacle. Your contagious intellect and unstoppable drive to explore, document, and understand the world beneath our feet have always inspired me and are reasons I chose a path of geoscience research and speleology. What could be a better place to study the earth than inside it? I am so very fortunate to count my wife Cori as one of these wonderful friends I met while caving. Mike Ficco, Nevin and Judy Davis, Phil and Charlotte Lucas, Gregg Clemmer and Tommy Shifflett deserve special mention for being friends, co-conspirators, and even transportation before I was old enough to drive! I also thank all those who compose the Butler Cave Conservancy Society and the unofficial ‘Omega group’ for never-ending adventures and stimulating conversations. I look forward to the next 20 years!

My undergraduate advisor at Radford University, Bill Anderson, was an excellent teacher and an early inspiration to learn more about hydrogeology and connections between surface water and groundwater. I appreciate his advice, insights, and our discussions during and since my studies at Radford. I thank Bill and Rhett Herman (also at Radford) for opening my eyes to geophysics as a tool for characterizing near-surface hydrogeologic processes. While at Radford, I also had the privilege of learning from and working with Jonathan Tso. Jon is a tireless and truly exceptional teacher. I am fortunate to have been part of a graduating class in which the epic 'Tso Trilogy' of Structural Geology, Petrology, and Field Methods was an integral part. These were truly the most difficult, enjoyable, and stimulating classes I participated in as an undergraduate. Jon also helped me appreciate that, even though they rarely host caves, non-carbonate rocks are immensely interesting!

For the past 6 years, Wil Orndorff has been a constant and unwavering proponent of my abilities as a student and researcher. I am continually amazed by Wil's deep understanding of and insight into geologic processes in the Appalachians and his renaissance approach to science and the bigger picture. I have truly enjoyed working and collaborating with Wil on many different projects and look forward to continuing to do so in the future. Thank you, Wil. I hope all that sunshine was worth it!

Being a graduate student at Virginia Tech has been one of the most enriching periods of my life and I have thoroughly enjoyed every minute of my time here; though some of it can only be enjoyed retroactively! The entire Geosciences department has supported me in so many ways, and for this I thank each and every person in it. The office staff deserves special recognition for dealing with the day-to-day problems that students like me bring to them. From navigating the complicated and ever changing university rules and regulations, to sending out a message alerting us to free food in the mailroom, they have been unwavering in their caring and support. Thank you all.

The staff at Virginia Tech Kentland Farms helped me by not only providing access to the farm for my research, but by accommodating my research in any way possible. I thank them all.

I also recognize the generous financial support of the many organizations that have supported my research and studies through grants and fellowships. I hope your confidence in my abilities has been rewarded. I am very grateful for support from: US Department of Education GAANN Fellowship, Virginia Water Resources Research Center, Cave Conservancy Foundation, Cave Conservancy of the Virginias, Cave Research Foundation, National Speleological Society, Geological Society of America, Southeast Division of the Geological Society of America, West Virginia Association for Cave Studies, Virginia Tech Department of Geosciences, and Virginia Tech Graduate Research Development Program.

ATTRIBUTIONS

Chapter two was submitted as a manuscript to *Soil Science Society of America Journal* "Schwartz, B.F., Schreiber, M.E., Pooler, P.S., and Rimstidt, J.D., *Methods for obtaining accurate access-tube TDR moisture in deep heterogeneous soils*. B.F. Schwartz was responsible for conceiving the project, collecting, interpreting, and analyzing all samples and data, preparing figures and writing the manuscript. M.E. Schreiber helped by clarifying text and reviewing the manuscript. P.S. Pooler assisted with multiple linear regression statistical analysis and performed categorical linear regression modeling. P.S. Pooler also contributed to a figure illustrating the categorical linear regression results. J.D. Rimstidt assisted with statistical and error analyses and manuscript review.

Chapter three was written as a manuscript in preparation for submission to a peer-reviewed journal. B.F. Schwartz was responsible for conceiving the project, collecting, interpreting, and analyzing all data, preparing all figures and writing the manuscript. M.E. Schreiber helped clarify the text and reviewed the manuscript. T. Yan performed numerical optimization of Archie's Law using U-Code and provided documentation for and assistance in interpretation of the model results. W. L. Daniels helped clarify a figure describing soil horizons at the Kentland Experimental Farms.

Chapter four was written as a manuscript in preparation for submission to a peer-reviewed journal. B.F. Schwartz was responsible for conceiving the project, collecting, interpreting, and analyzing all data, preparing all figures and writing the manuscript. M.E. Schreiber helped clarify the text and figures and reviewed the manuscript.

TABLE OF CONTENTS

LIST OF FIGURES

LIST OF TABLES

GRANT INFORMATION

US Department of Education GAANN Fellowship
Virginia Water Resources Research Center
Cave Conservancy Foundation
Cave Research Foundation
National Speleological Society
Geological Society of America
West Virginia Association for Cave Studies
Virginia Tech Graduate Research Development Program
Virginia Tech Department of Geosciences

CHAPTER 1

INTRODUCTION

Sinkholes are often the most visible features in karst terrains and are an integral component of most karst systems in the eastern United States. Sinkholes formed by dissolution are generally considered to be part of the epikarst, which is a complex, diverse, and very heterogeneous zone lying between the land surface and underlying un-weathered carbonate bedrock (Klimchouk, 2004). Factors such as bedrock lithology and structures, climate, and soil cover all play important roles in the development of different epikarst properties and morphologies. For similar reasons, sinkholes themselves are complex, diverse and heterogeneous, both with respect to their physical properties and their geographic distribution. Within the classification of sinkholes created by dissolution (as opposed to collapse sinkholes), there is one type which is of special interest to many: the soil-filled sinkhole. In many agricultural regions, soil-filled sinkholes are often subtle features which are utilized for agriculture in a similar manner as the surrounding areas. There are many unresolved questions concerning the ability of these sinkholes to transport water and dissolved contaminants into underlying aquifers, whether better management practices (BMPs) should be implemented within the sinkholes, and, if so, how to best define the area in which to apply these BMPs. At the root of all these questions is the basic issue of whether soil-filled sinkholes transmit water and contaminants to the underlying aquifer more or less efficiently than surrounding areas. Common sense indicates that they should be more efficient in transmission of water and contaminants; though there is little empirical evidence to support this conclusion.

The research presented in this dissertation focuses on characterizing and quantifying the spatial and temporal distribution of infiltration and recharge in sinkholes with thick soil mantles. In particular, I studied volumetric soil moisture changes in two sinkholes in two sinkhole plains which developed in ancient New River terrace deposits on the Virginia Tech Kentland Experimental Farms in Montgomery County, southwest Virginia, USA. The weathered deposits in these terraces are the source of most of the thick soils overlying carbonate bedrock at the study site. Soil mantles range in thickness from 3 m to greater than 12 m and, due to their parent materials, are highly heterogeneous with regard to texture and physio-chemical properties.

As with many proposed research projects, answering specific research questions was not as straightforward a task as was initially envisaged. The problem of measuring soil moisture at the field site seemed fairly straightforward until fieldwork began. Some of the difficulties encountered were related to limitations with instrument installation methods, instrument calibration difficulties, heterogeneities in soils, and an unexpectedly deep soil profile. These difficulties led to the development of new methods for installing instrumentation and calibrating measurements, for measuring the spatial distribution of soil moisture in very thick and heterogeneous soil profiles, and for quantifying infiltration and potential recharge at the field-scale. This dissertation is organized into three main chapters, prepared as three separate manuscripts, which are currently either in review or in preparation for submission to scientific journals. The papers are described below.

METHODS FOR OBTAINING ACCURATE ACCESS-TUBE TDR MOISTURE IN DEEP HETEROGENEOUS SOILS

Time domain reflectometry (TDR) is an accepted method for measuring soil moisture, and access-tube TDR is commonly used to measure 1-D soil moisture profiles up to 3 m in depth. However, the technique has several limitations which are related to TDR's insensitivity to certain fractions of soil moisture (Jacobsen and Schjonning, 1993), and methods which were unsuitable for installing access-tubes to depths of up to 9 m (Whalley et al., 2004). Chapter 2 of this dissertation presents methods I developed to install TDR access-tubes in deep soils and to later calibrate access-tube derived TDR measurements. To obtain correct soil moisture values using TDR, I developed a physico-chemical method for calibrating access-tube TDR soil moisture measurements using measured soil properties from 470 soil samples. I present two important findings: 1) that access-tube TDR soil moisture measurements are not representative of true soil moisture content in most soil textures and cannot be used to accurately calculate volumetric soil moisture without calibration, and 2) that TDR moisture measurements can be calibrated to true moisture content by multiple linear or categorical linear regression modeling of several important physical and chemical parameters. The calibration dominantly corrects for water which is partially undetectable by TDR due to various physical and chemical mechanisms of water immobilization. The model was used to calibrate time-series measurements by first applying the calibration equation which correct for the physico-chemical effects. A final calibration of time-

series measurements was then obtained by adding the change in uncalibrated TDR moisture at the time of interest relative to the TDR moisture reading at the time of initial measurement and calibration. This method makes two important assumptions: 1) that the TDR probe is accurately measuring 'free' moisture content and any subsequent changes in moisture content, and 2) that the TDR-undetectable moisture content remains essentially constant.

LINKING FIELD SCALE ELECTRICAL RESISTIVITY TOMOGRAPHY AND TIME DOMAIN REFLECTOMETRY DERIVED SOIL MOISTURE

1-D quantification of soil moisture distribution using TDR showed that significant field-scale heterogeneities existed in both sinkholes, which prevented simple 2-D modeling of soil moisture. Because ERT measurements in unsaturated soils are sensitive to soil moisture (Shuyun and Yeh, 2004; Sreedeep and Singh, 2005), I used 2-D ERT data as the foundation for obtaining 2-D soil moisture measurements. Chapter 3 presents research which resulted in a method for quantitatively measuring soil moisture in 2-D field-scale profiles. Using data derived in part from the TDR calibration work, I converted the 2-D ERT data into 2-D models of volumetric soil moisture using a modified and numerically optimized form of Archie's law (Shah and Singh, 2005) which includes ERT-derived bulk conductivity measurements, percent clay, and pore water conductivity estimates using one of two methods: soluble salts or an extractable cation proxy. The extractable cation model produced slightly better results. The results suggested that both proxy methods are suitable substitutes for actually measuring pore-water conductivity: a time consuming and expensive task. When calibrated to TDR-derived soil moisture measurements, my final results showed that field-scale 2-D ERT profiles can successfully be converted into 2-D soil moisture models with one standard deviation in soil moisture of $\pm$ 6%. The ability to convert field scale ERT measurements into profiles of soil moisture is a valuable tool for quantitatively assessing soil moisture distribution in soils and the methods discussed in this chapter are also applicable to time-series and 3-D moisture modeling at a variety of scales.

QUANTIFYING POTENTIAL RECHARGE THROUGH THICK SOILS IN MANTLED SINKHOLES USING ERT DATA

Quantifying infiltration through soil-filled agricultural sinkholes is an important step towards characterizing how this type of karst feature contributes to recharge entering karst aquifers.

Understanding the spatial and temporal distribution of infiltration and recharge is critical information for modeling water quantity and quality (Bohlke, 2002; de Vries and Simmers, 2002). This is especially important at the intermediate or field scale, as this is the scale at which many water quality problems exist. Chapter 4 presents methods for quantifying field-scale infiltration and potential recharge using time-series ERT data. Expanding on the methods and results presented in chapters 2 and 3, I used time-series ERT data from May 17 to October 9, 2006, cumulative precipitation records, and cumulative modeled potential evapotranspiration (PET) to quantify rates and amounts of infiltration and potential recharge through the two soil-filled sinkholes. Although the results of this study are specific to the study site, several important conclusions were reached. First, infiltration and potential recharge occurs via several mechanisms in soil-filled sinkholes and can be divided into two components: 1) rapid infiltration via macropores, and 2) diffuse infiltration through the porous unsaturated soils. The methods presented here were used to measure diffuse infiltration, although high temporal resolution of ERT can produce better resolution of rapidly infiltrating water. Second, soil-filled sinkholes at this study site clearly contribute significant amounts of recharge via both rapid and diffuse mechanisms. During normal conditions, this type of sinkhole should probably be modeled as an environment closer to that which exists on topographic highlands around sinkholes: a region of potentially rapid infiltration and recharge via macropores, but with a significant diffuse recharge component as well. Intense rains causing overland flow enhance the volume of infiltration at the lowest points in the sinkholes. This indicates that under these conditions soil-filled sinkholes should still be treated as regions with greater potential for contamination than the surrounding uplands.

REFERENCES

Bohlke, J.-K. 2002. Groundwater recharge and agricultural contamination. Hydrogeology Journal 10:153-179.

de Vries, J.J., and I. Simmers. 2002. Groundwater recharge: an overview of processes and challenges. Hydrogeology Journal 10:5-17.

Jacobsen, O.H., and P. Schjonning. 1993. A laboratory calibration of time domain reflectometry for soil water measurement including effects of bulk density and texture. Journal of Hydrology:147-157.

Klimchouk, A.B. 2004. Towards defining, delimiting and classifying epikarst: Its origin, processes and variants of geomorphic evolution. Speleogenesis and Evolution of Karst Aquifers www.speleogenesis.info 2.

Shah, P.H., and D.N. Singh. 2005. Generalized Archie's Law for Estimation of Soil Electrical Conductivity. Journal of ASTM International 2:1-20.

Shuyun, L., and T.-C.J. Yeh. 2004. An integrative approach for monitoring water movement in the vadose zone. Vadose Zone Journal 3:681-692.

Sreedeep, S., and D.N. Singh. 2005. Estimating unsaturated hydraulic conductivity of fine-grained soils using electrical resistivity measurements. Journal of ASTM International 2:1-11.

Whalley, W.R., R.E. Cope, C.J. Nicholl, and A.P. Whitmore. 2004. In-field calibration of a dielectric soil moisture meter designed for use in an access tube. Soil Use and Management 20:203-206.

CHAPTER 2

Methods for obtaining accurate access-tube TDR moisture in deep heterogeneous soils

[1]Benjamin F. Schwartz*, [1]Madeline E. Schreiber, [2]Penelope S. Pooler, [1]J. Donald Rimstidt
[1] Department of Geosciences
4044 Derring Hall
[2] Department of Statistics
Virginia Polytechnic and State University
Blacksburg, VA 24060
Phone: 1-540-231-7287 Fax: 1-540-231-3386
beschwar@vt.edu
*Corresponding author

Methods for obtaining accurate access-tube TDR moisture in deep heterogeneous soils

ABSTRACT

Hydrologic characterization of the vadose zone requires accurate measurements of soil moisture in a variety of soil textures. Time-domain reflectometry (TDR) instruments are commonly used to obtain soil moisture. Although there are advantages to using TDR, certain types of instruments pose challenges, including proper installation and calibration, which must be overcome. The principal objective of this study was to develop a new method for obtaining and calibrating access-tube TDR measurements in deep heterogeneous soils. Using two regression techniques, physical and chemical property-based calibrations were developed to predict soil moisture and explain unexpectedly large differences between TDR and field moisture values. Results provide insight into which physical and chemical parameters are most important for TDR calibration and lead us to propose new protocols for interpreting access-tube TDR moisture measurements. Differences between TDR moisture and gravimetric field moisture were almost entirely controlled by physical and chemical soil properties; indicating that our access-tube TDR probe likely produced an accurate measurement of 'free' but not the undetectable soil moisture. The undetectable fraction is controlled by physical and chemical properties and is a nearly static parameter at the depths and time scales considered in this study. Changes in TDR measurements after the initial calibration represent changes in the 'free' moisture content. Our calibration equations used easily obtained parameters to predict accurate soil moisture values in a wide range of soil textures. Approximately 95% of the soil moisture values predicted using our calibration equations had residuals of less than $\pm$ 10% soil moisture. We also developed a cost-effective method for installing access tubes which minimized problems related to air gaps and soil structure disturbances in deep soil profiles. This greatly increases the utility of TDR to be used as a tool for characterizing vadose zone hydrology in thick heterogeneous soils.

INTRODUCTION

Quantifying the spatial and temporal distribution of moisture in unsaturated porous media is critical to characterizing and modeling flow in the vadose zone. A variety of tools and methods have been developed to measure soil moisture in-situ. Because of its ability to acquire data quickly, and its relative safety when compared to nuclear methods (e.g., neutron probe), several different types of time domain reflectometry (TDR) probes are commonly used to measure soil moisture. Moisture measurements using TDR are derived by converting the measured bulk dielectric constant of a material, such as moist soil, into volumetric water content. Most TDR instruments are designed for long-term installation and continuous monitoring at shallow depths and are installed by inserting pronged wave-guides directly into the soil of interest, generally into the wall of a dug pit which is backfilled after installation. When deep vertical moisture profiling is required, this type of probe is not a practical option (Whalley et al., 2004). For these conditions, access-tube style TDR probes have been developed which allow moisture profiling using a single instrument that is raised and lowered inside an access-tube installed in the soil. Measurements are obtained without direct contact between the instrument and the soil of interest. Access-tube instruments can be used both for long-term installation and continuous monitoring of soil moisture or to obtain a single reading at a specific depth. From a hydrologic perspective, the main advantages of using an access-tube TDR probe include the ability to measure soil moisture profiles to greater depths and to obtain high spatial resolution using a single instrument.

Although TDR methods are useful in terms of their ease of use and ability to take measurements quickly, there are complications and challenges with using and installing TDR instruments. Modeling temporal variations in soil moisture profiles first requires the ability to accurately measure moisture in a variety of soil textures and over a range of depths. Thus, the most important question that must be asked when using TDR is: how accurate are the resulting soil moisture values? If TDR moisture values differ from gravimetrically obtained field moisture measurements, what are the reasons for this discrepancy? The only way to address these questions is through TDR calibration.

The traditional method for calibrating TDR measurements has been to use an empirical function which describes the relationship between moisture content and the bulk dielectric constant of a

soil (Topp et al., 1980). Alternatively, some researchers have calibrated TDR moisture measurements to soil moisture measured gravimetrically and/or with a neutron probe (Evett and Steiner, 1995; Laurent et al., 2005). With the TRIME probe used in this study, an initial calibration is applied to TDR measurements via an internally stored standard calibration equation that is assumed to be suitable for use in a wide range of mineral soils and will determine soil moisture values with a stated accuracy of $\pm$ 2 to 3% (IMKO, 2006a). It is also assumed that deviations from the standard equation are relatively small when measurements are made in different soil types: resulting in errors of only a few percent of soil moisture by volume.

For soils in which the standard calibration equations are not suitable, material-specific calibrations of TDR measurements to measured soil moisture values can be performed using one of several methods. For shallow soils, the most common material-specific method is to sample the soil of interest and develop a secondary empirical calibration equation in a laboratory setting by collecting multiple pairs of TDR moisture and volumetric moisture content measurements for individual soil samples (Chandler et al., 2004; Jacobsen and Schjonning, 1993). This method may be suitable for use in settings where a few samples from a relatively homogeneous field site will produce acceptable calibration results for soils in the area of interest. Unfortunately, the method is extremely time-consuming and is not practical for calibrating many individual TDR moisture measurements obtained in deep heterogeneous profiles. Additionally, for access-tube instruments, this method requires a very large soil sample which is very difficult to obtain in deep soils. A further limitation of this method is that it does not attempt to quantify the effects that various physical and chemical soil parameters have on the dielectric properties of a soil, and the resulting effects on TDR moisture measurements. As a result, it cannot be generally applied to estimate moisture in heterogeneous soils.

Another method for material specific calibration is to use a dielectric mixing model in which the modeled bulk dielectric constant is related to the individual dielectric values of specific components of the soil system including air, water, mineral grains and bound water (Dobson et al., 1985). By assuming a constant dielectric value for each parameter, a modeled value for soil moisture can be derived. However, in complex heterogeneous environments, variations in soil

texture, moisture content, mineral properties, and a variety of soil chemistry parameters make this type of model very difficult to apply.

A third method involves relating the bulk dielectric constant to soil moisture using volumetric water content, depth, and bulk density values determined from cores taken in a pit excavated adjacent to an access-tube (Whalley et al., 2004). In very heterogeneous conditions found at many field sites or in situations where significant depths are involved, this type of approach may not be practical either.

Although all the techniques discussed above have successfully been used to calibrate TDR measurements in relatively shallow soil environments, they are generally inappropriate or impractical for access-tube TDR measurements in deeper heterogeneous soils. Thus, after recognizing large differences between our TDR and field moisture values, the primary objective of this study was to develop a calibration protocol for access-tube TDR measurements based on statistical analyses of physical and chemical properties obtained from each of our soil samples. Our methods can not only be used to calibrate access-tube TDR measurements in similar settings but also to evaluate the relative influence of individually measured parameters (e.g., percent clay).

FIELD SITE

Our research site at the Virginia Tech Kentland Experimental Farms in Montgomery County, Virginia contains two well-developed sinkhole plains formed in ancient New River terraces (**Figure 2.1a**). Most sinkholes are broad and relatively shallow, allowing easy access for agricultural activities, and contain no bedrock outcrops. Thick terrace deposits mantle sinkholes with soils characterized as weathered fluvial terrace materials deposited by the ancient New River, which have developed over the underlying Cambrian aged Elbrook Formation limestone and dolostone bedrock. Soils are classified by the USDA-NRCS as Guernsey silt loam, Unison and Braddock soils, and Unison and Braddock cobbly soils (USDA-NRCS, 2006). Both sinkhole plains have numerous sinkholes of similar size and shape. Following initial characterization work of six sinkholes, two sinkholes were chosen for more detailed study. Sinkhole #1 is in a higher and older terrace deposit and contains highly weathered soils to depths

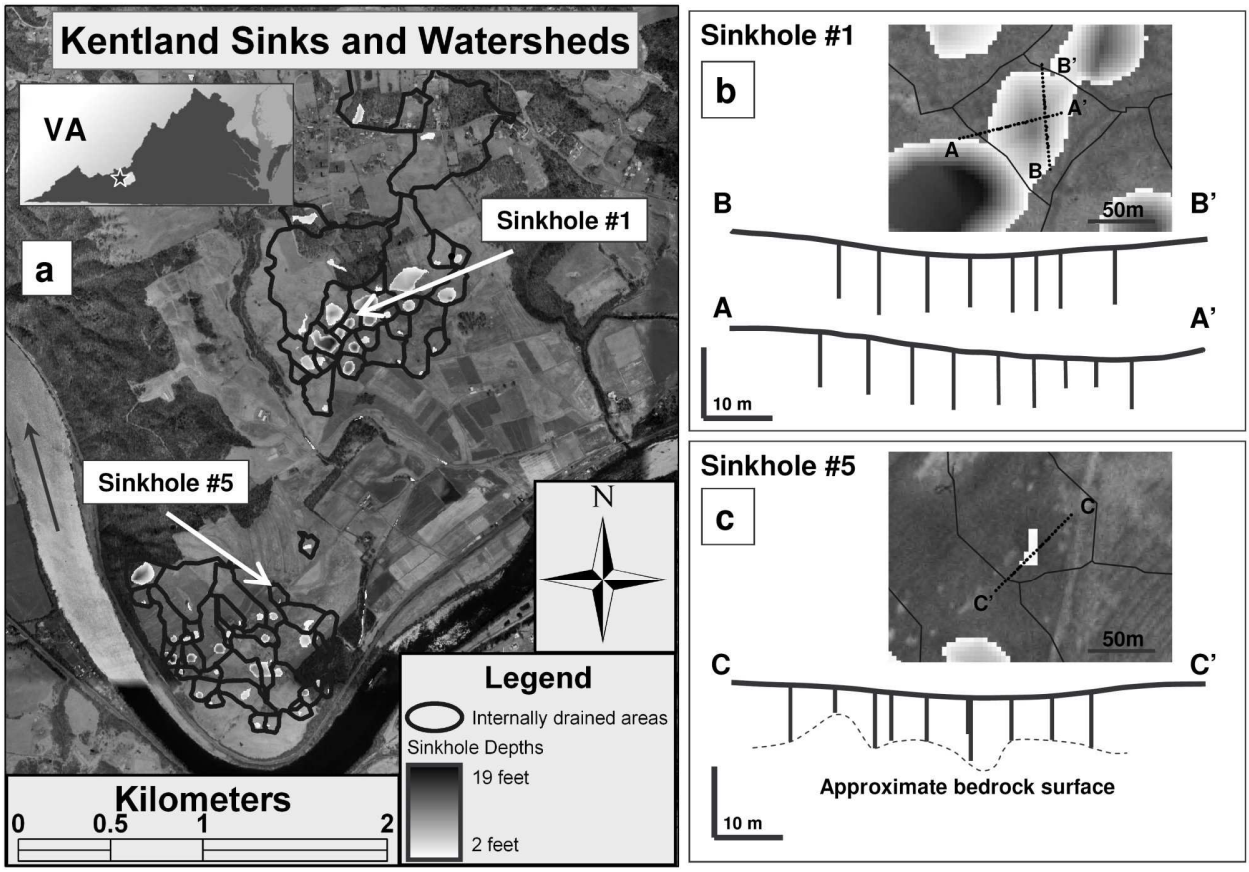

Figure 2.1 Study area and sinkhole transects

a) Virginia Tech Kentland Experimental Farms at Whitethorne, Virginia, USA. Figure 2.1a shows study sinkholes #1 and #5 and catchment areas (adjacent polygons) for each sinkhole within the two sinkhole plains. Aerial imagery © 2002 Commonwealth of Virginia. Sinkhole #1 is in the higher, older terrace. b) and c) show the location and orientation of instrumentation installed in transects across both sinkholes. Upper image in the diagrams is a map view of the sinkhole, while the lower portion of the diagrams shows profile views of monitoring wells, TDR access-tubes and other instrumentation installed along each transect. Note that depth of bedrock was not determined in Sinkhole #1.

of more than 40 feet (12.2 m). Sinkhole #5 is formed in a much lower and younger terrace and contains less weathered soils. In Sinkhole #5, bedrock was reached in nearly all augered holes at depths between 11 and 25 feet (3.4 and 7.6m) below land surface.

MATERIALS AND METHODS

Time Domain Reflectometry

At our field site, we used a TRIME T3-50 IPH Tube Access Probe TDR unit (manufactured by IMKO of Germany) connected to a laptop computer to measure and record uncalibrated percent moisture by volume. This instrument converts the pseudo-transit-time (which is related to the bulk dielectric constant) of a high frequency electromagnetic pulse into an approximate TDR moisture value using a factory-set internal calibration. Our instrument's internal calibration relates pseudo-transit-time to soil moisture using a standard equation in the form of (1). θ_{TDR} = TDR soil moisture [%] and t_p = pseudo transit-time.

$$\theta_{TDR} = -50.18321 + 0.769028 t_p - 4.19107 \cdot 10^{-3} t_p^2 + 1.185743 \cdot 10^{-5} t_p^3 - 1.613228 \cdot 10^{-8} t_p^4 + 8.57611 \cdot 10^{-12} t_p^5 \qquad (1)$$

Equation (1) is used by IMKO to initially calibrate each TRIME T3-50 IPH probe. After the initial calibration is performed, an instrument-specific calibration is then applied. Separate material specific calibrations can later be applied by the user. However, the instrument does not allow bulk dielectric constant values or pseudo-transit-times to be measured or recorded directly, and the final internal calibration coefficients are not accessible by the user. The T3-50 IPH probe has a stated maximum region of influence of 2.4 inches (60 mm) radially along the short axis of an oval field, and 6.3 inches (160 mm) on the long axis (MESA-Systems, 2006). Although multiple measurements at different angular orientations can be averaged to obtain a better estimate of soil moisture at a given depth, only one oriented reading was taken each time TDR moisture measurements were collected, as field experiments at our site showed little variation resulting from changes in angular orientation. Vertically, the T3-50 IPH probe measures the average moisture content over a depth interval of approximately 6 inches (15.24 cm).

Access-tube installation

TDR measurements for this study were collected from access-tubes installed in three transects across the two sinkholes between June, 2005 and May, 2006. Transects cross the low point of each sinkhole and radiate outwards to the edges (**Figure 2.1b** and **c**). Locations were chosen based on results of previous electrical resistivity tomography (ERT) surveys which indicated linear features such as 'valleys' in subsurface soil properties. The TDR transects follow and cross these features which, when more completely understood, will aid in future hydrologic characterization and modeling efforts at the site.

Transects consist of 15 access-tubes for two transects in sinkhole #1 and 8 access-tubes for the remaining transect in sinkhole #5. To install the access-tubes, a 2-inch (5.08 cm) mud-auger, custom manufactured to bore a 2.375-inch (6.03 cm) diameter hole, was used with threaded extensions to hand auger twenty-three holes to depths between 12 and 30 feet (3.6 and 9.1 meters). Schedule 40, 2.375-inch (6.03 cm) outer diameter PVC access-tubes were installed in the vertically augered holes. Access-tubes consist of standard threaded and o-ring sealed-joint PVC well-casing sealed on the bottom with a glued PVC well-point to seal the bottom. Care was taken to minimize air gaps between access-tubes and the surrounding soil. This is critical for obtaining accurate TDR readings because the dielectric constant of air is significantly lower than that of damp soils. Relatively small air gaps can thus produce significant errors in TDR measurements. During installation, access-tubes fit very snugly in augered holes to depths of 3 to 5 feet (0.9 to 1.5m). Below this, the fit was tight enough to require significant steady force to install, with resistance caused primarily by increasing friction between the tube and damp clay-rich soils, and compressed air in the augered hole beneath the sealed bottom of the access-tube. As a result of the tight fit and minimal vibration during installation, air gaps and soil disturbances around our access-tubes are assumed to be minimal.

The depth of individual holes was limited by cobbles or bedrock encountered and/or practical limits of hand-augering and sampling in deeper holes. To pass obstructing cobbles, we constructed a rock-breaking tool that could be threaded onto the auger stem to break smaller cobbles and permit a deeper hole to be augered.

After installation, access-tubes were completed by digging a shallow hole around the top of the tube and cutting the access-tube off just below ground surface. A removable end-cap was then used to seal the top of the tube. A protective cover consisting of a 12-inch (30.5 cm) length of 4-inch (10.2 cm) diameter Schedule 40 PVC pipe with an end-cap was then driven into the ground around the upper portion of the access-tube until the end-cap was flush with the ground surface (**Figure 2.2**). This was necessary to protect the access-tube from farming activities at the field-site. We recognize that this will influence long-term moisture measurements in the uppermost portion of the moisture profile.

Soil sampling

During augering for access-tube installation, volumetric soil samples were collected at one-foot (30 cm) intervals in most holes, with some holes having a two-foot (61 cm) sample interval. Sample lengths were taken by carefully measuring the depth of the auger stem before and after filling the auger, and not by measuring the length of the augered soil sample itself. Sample lengths averaged 5.0 inches (12.7 cm) and were recorded for use in volume calculations. Sample volume was calculated by multiplying the augered depth of each sample by the augered cross-sectional area (28.6 cm^2). To preserve original field moisture content, each soil sample was removed from the auger and placed in a labeled zippered polyethylene bag for later lab analysis. A field-log recording depth and thickness of each soil horizon encountered included details on soil color, difficulty in augering, approximate soil texture, relative moisture content, and amount and type of gravel or cobbles observed. After installing each access-tube, TDR moisture measurements were immediately recorded at 6-inch (15.2 cm) depth intervals in the access-tube.

Sample analysis

Each sample was weighed to the nearest 0.01 g prior to drying in an oven at 105°C until repeated weighing showed no further weight loss. A final oven-dry weight was then recorded. Percent moisture by volume (field moisture) and dry bulk density were calculated using final oven-dry weight, initial weight and the sample volume. For all calculations, the density of water was assumed to be 1 g cm^{-3}. Dried samples were prepared for further physical and chemical analyses by passing the fine-earth component through a 2.0 mm sieve. The coarse (> 2.0 mm) fraction

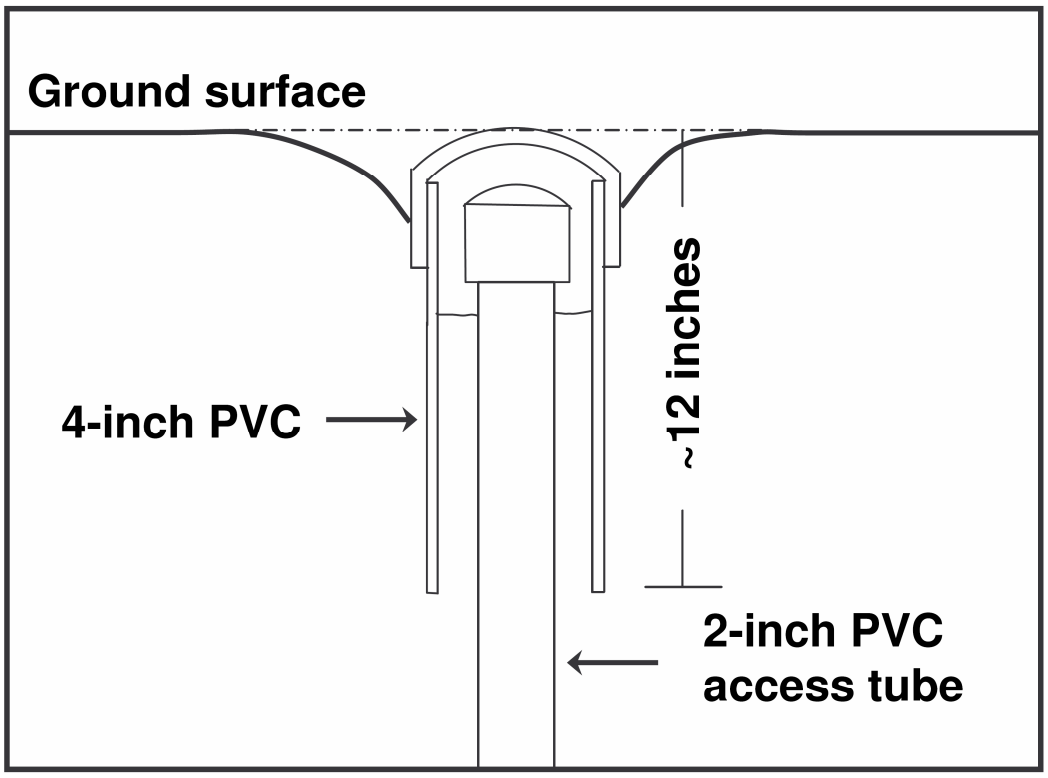

Figure 2.2 Access-tube completion and protection
Diagram showing how access-tubes are completed after installation. A four-inch PVC pipe and end cap protects the top of the access-tube from farm equipment and animals while minimizing interference with natural infiltration around the access-tube.

remaining was weighed and recorded as gravel. The fine-earth portion was mixed and retained for particle size analysis (PSA).

PSAs were performed on each sample using the ASTM 152H hydrometer method using a procedure slightly modified from the method described in Dane (2002). Modifications consisted of collecting hydrometer and temperature readings at intervals of 1, 5, 15, 30, 60, 180, 240, ~480 and ~1,440 minutes. Each hydrometer reading was corrected for the temperature recorded at the time of measurement. This eliminated the need for thermal equilibration in a sedimentation cabinet or temperature controlled water bath. Temperature variations were very small in our lab environment during these measurements. Each PSA used 40.00 g of oven-dried (105°C) $\leq$2.0 mm soil. Percent clay was calculated by plotting the percent of sediment in suspension at each time vs. the log of particle size in microns. For each sample, the equation from a best-fit regression line was used to calculate the amount of clay in each sample. Assuming that clay is composed of all sediments $\leq$ 2 µm, percent clay in suspension is calculated by substituting 2 for particle size in the regression equation.

Percent sand was measured by thoroughly washing each sample through a 53 µm sieve and drying the retained sand at 105°C. The dried sediments were shaken on the sieve to remove any remaining silt or clay. The sand fraction was then weighed and recorded. Percent silt was calculated by difference from the initial 40.0 g sample of $\leq$2.0 mm material.

Traditional PSAs do not measure sand, silt and clay percentages as portions of a bulk soil volume, but instead as a portion of the fine-earth ($\leq$ 2.0 mm) component only. After performing PSAs, we adjusted the percentages of each particle size fraction to include the percentage of gravel measured in the bulk sample. The weight of gravel (> 2.0 mm particles) was recorded when each bulk sample was passed through a 2.0 mm sieve. We chose to include percent gravel in our PSAs because higher rock and gravel content will significantly decrease the bulk dielectric constant and therefore influence the TDR measured moisture content.

A split of each sample was analyzed for standard soil chemical parameters, including pH, BpH (buffer pH, a measure of a soil's natural buffering capacity), acidity, base saturation, Ca

saturation, Mg saturation, K saturation, estimated Cation Exchange Capacity (CEC), total soluble salts (TSS), organic matter (by loss on ignition), and the following extractable nutrients: P, K, Ca, Mg, Zn, Mn, Cu, Fe, and B. Analyses were performed by the Virginia Tech Soil Testing and Plant Analysis Laboratory using the methods described in Mullins (2005).

Statistical analysis

We examined the relationship between TDR moisture readings and actual moisture content using two different regression models. In the first model, we predicted true field moisture using TDR moisture readings and a number of other continuous variables that specify the physical and chemical properties of each sample. This is a standard multiple linear regression (MLR) model which uses the observed numeric values for all of the significant variables in each sample to derive the best estimate of the true moisture content in each respective sample. In this type of regression model the null hypothesis for each possible explanatory variable is that it is not useful in predicting true field moisture. Each variable is treated identically and its importance or lack thereof in the model does not change the interpretation of other variables' importance in the final model.

The second model we used is another type of MLR which uses categorical variables (rather than continuous variables). This method is called categorical linear regression (CLR) and is sometimes referred to as a parallel lines model (Ramsey and Schafer, 1997). In contrast with MLR, a CLR model focuses primarily on the linear relationship between TDR moisture readings and true moisture content within specific categories of physical and chemical parameters. This is done by converting each of the physical and chemical property variables to a categorical variable. The categories we developed for each of the pertinent variables were based on knowledge of how each factor affects the accuracy of TDR moisture readings and represent a defined range of values for each parameter. For example, we divided percent clay into four categories of <15%, 15 to <30%, 30 to <45%, and $\geq$45%. This variable conversion allows us to use TDR readings to predict actual moisture within small, relatively homogeneous subsets of the data. If TDR moisture is significant in explaining field moisture in this model, then the null hypothesis for each of the other categories is that the relationship between TDR moisture and field moisture is the same in that category subset as it is in the baseline category for that variable.

Using the first model, a basic MLR calibration equation for TDR moisture readings was derived using the following statistical analysis software packages: SAS software for general statistical analysis, Analyse-it for graphing and general statistical analysis, and SAS-JMP software for cross-correlation analysis (Analyse-it, Analyse-it for Microsoft Excel; JMP, 1989-2005; SAS, 2000-2004). Prior to MLR modeling, Pearson correlation coefficients and cross correlation plots were used to eliminate from the model variables that showed significant correlation with other variables. Additionally, nearly all chemical parameters are log-normally distributed and were log transformed prior to statistical analysis. Forward, backward and stepwise MLR analysis procedures were used to determine significant variables with a p-value of <0.05. This list was refined to include the fewest variables possible by retaining only those which, when included in the regression model, contributed significantly to the final R^2 value and are most commonly obtained during soil analyses. The same software packages were used in developing and refining the CLR model.

A few statistical outliers were removed from the data prior to development of a final model. These points were identified by examining the distribution of residuals and removing data which were more than 4 standard deviations from the mean. Additional data were removed prior to regression modeling because of known measurement errors due to installation problems of one access-tube. Other points were removed if they were known to be associated with very small soil samples obtained in very cobbly intervals where the true sample volume was highly uncertain and the corresponding TDR measurement was almost certainly affected by surrounding large cobbles. These cobbles are generally not represented in the PSA for a soil sample because they were too large to be sampled. As a result, their effect can not easily be considered in statistical models.

Error analysis

Propagation of measurement errors is useful for understanding how well a statistical model can reasonably fit the data. This prevents over-fitting of the data by addition of more variables than are needed. An error analysis was performed for all variables we used in both statistical models. Because CLR is a type of MLR, equation (2) can be used to estimate propagated errors in both

CLR and MLR models. We modified a standard model of fractional error to derive an equation which propagates errors weighted using the mean parameter value and the regression coefficient:

$$\delta X = \sqrt{(\delta a\,\mu_a\eta_a)^2 + (\delta b\,\mu_b\eta_b)^2 + \cdots + (\delta n\,\mu_n\eta_n)^2} \qquad (2)$$

Where μ_n represents the mean of a variable used and η_n represents the regression coefficient for that variable.

Estimating errors can be challenging because many instruments and methods do not have well-defined errors associated with them. In all cases we use either a stated ± value or our own estimate of measurement error and assume that these values represent one standard deviation from the median measurement for that parameter.

Random errors also occur due to the heterogeneous conditions at our field site. For example, significant errors can result from proximity of the TDR probe to undetected large cobbles, bedrock or small natural voids during measurement. These errors can not be quantified and there is no way of knowing which readings are affected by these factors. As a result, they are assumed to be randomly distributed. These errors should express themselves as a standard deviation of the residuals for the regressed data that is higher than the standard deviation estimated through measurement of error propagation. These residuals should also be normally distributed.

RESULTS

Table 2.1 summarizes the physical and chemical characteristics of the soil samples collected for our study. We compared the mean, range, and standard deviation of values for parameters obtained from soils in sinkhole #1 and sinkhole #5 to broadly examine differences in physical and chemical properties between the two sites. The most significant differences between data shown for sinkholes #1 and #5 in **Table 2.1** were that sinkhole #5 has finer-grained soils (more clay and silt), higher CEC, and contains higher levels of Ca and Mg. Higher extractable Ca and Mg reflect the fact that most access-tubes in sinkhole #5 were augered to bedrock where soils contain significant amounts of weathered carbonates. In sinkhole #1, none of the access-tubes

reached bedrock and none of the samples contained weathered carbonates. Dominantly fluvial sediments are likely the reason for the generally coarser-grained soils sampled in sinkhole #1.

Our particle size analyses placed soil samples within eight of the 12 soil textures as defined by the USDA NRCS (Schoeneberger, 2002), with most being clay and/or silt dominated (**Figure 2.3**). Samples from sinkhole #5 tend to have higher clay and silt content than those in sinkhole #1 and correspondingly lower sand and gravel content. Bulk density values average 1.42 g cm^{-3} for all samples and show no correlation with depth in either sinkhole. This was not unexpected as soil profiles in similar clay-rich soils have also been shown to have approximately constant or decreasing bulk density values with depth (Kool et al., 1986). In many soils, bulk density tends to increase with depth as a result of compaction. In clay-rich soils, this trend can be significantly reduced or not observed at all.

Multiple linear regression

A simple linear regression of TDR moisture values against measured field moisture values produced an R^2 statistic of 0.23 (**Figure 2.4**a), indicating that there is not a simple linear relationship between TDR moisture measurements and field moisture values. Furthermore, non-linear trends were not visible in the data and other models (such as polynomial or exponential) did not result in a better relationship. For this case, and with a large set of physical and chemical parameters potentially affecting the TDR moisture versus field moisture relationship, MLR analysis was a more appropriate method than simple linear regression. Normal distribution of standardized residuals is another important test of whether linear regression models are appropriate. **Figure 2.5** shows normal distribution of standardized residuals, indicating that MLR models are suitable for all three data sets. If this were not the case, either non-linear regression techniques should be used or the data must be transformed prior to regression.

For the MLR model, data were analyzed both as a single group and divided by study sinkhole into two groups. Pearson cross-correlation statistics and cross-correlation plots were constructed to identify parameters that should be removed from the variable set or not included if a related parameter is included. For example, because the percentages of gravel, sand, silt and

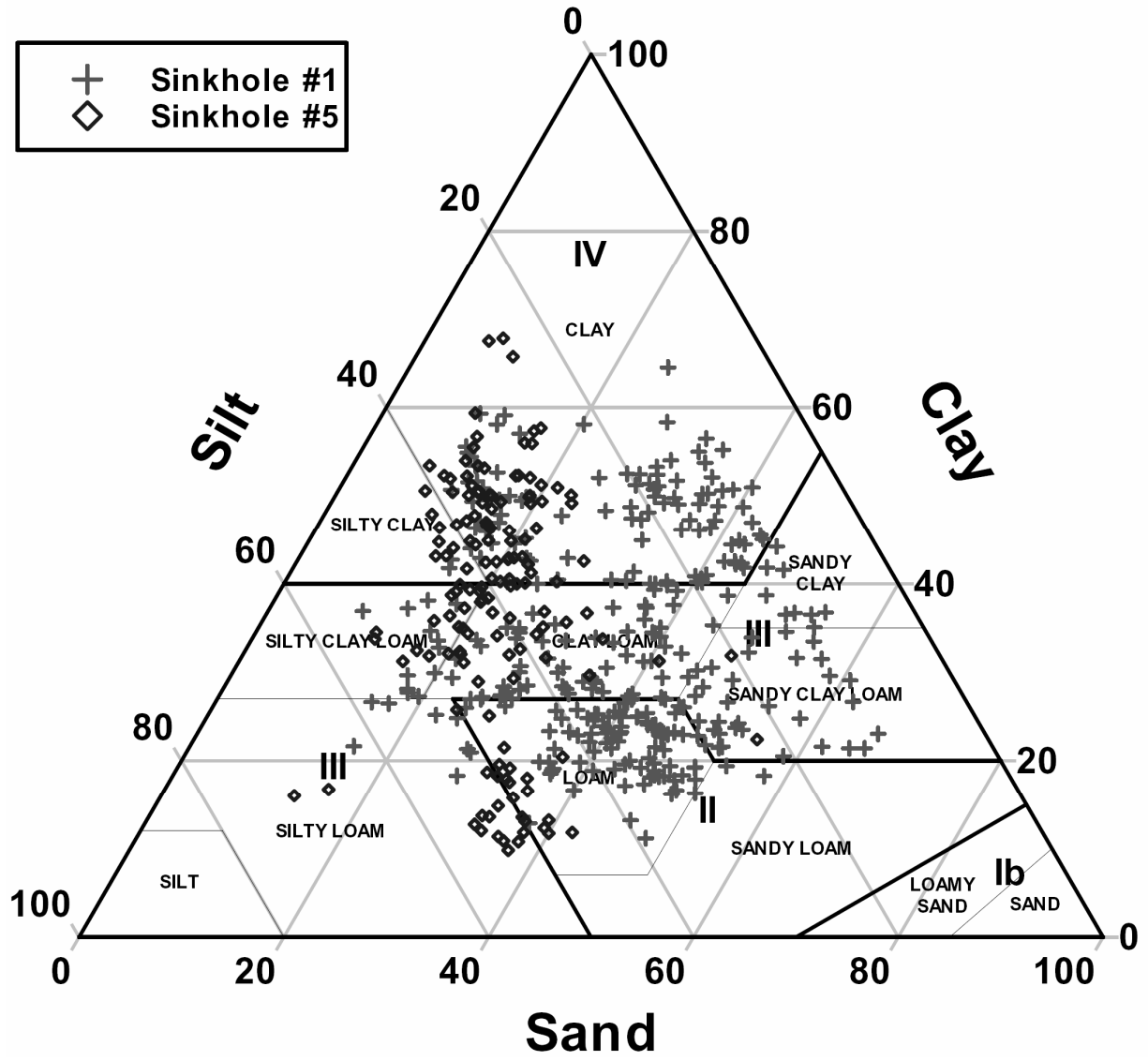

Figure 2.3 USDA soil texture with all samples plotted

Soil classification diagram showing the heterogeneity in USDA soil textural properties for samples collected in both sinkholes. Crosses [+] are from sinkhole #1 and diamonds [◊] are samples from sinkhole #5.

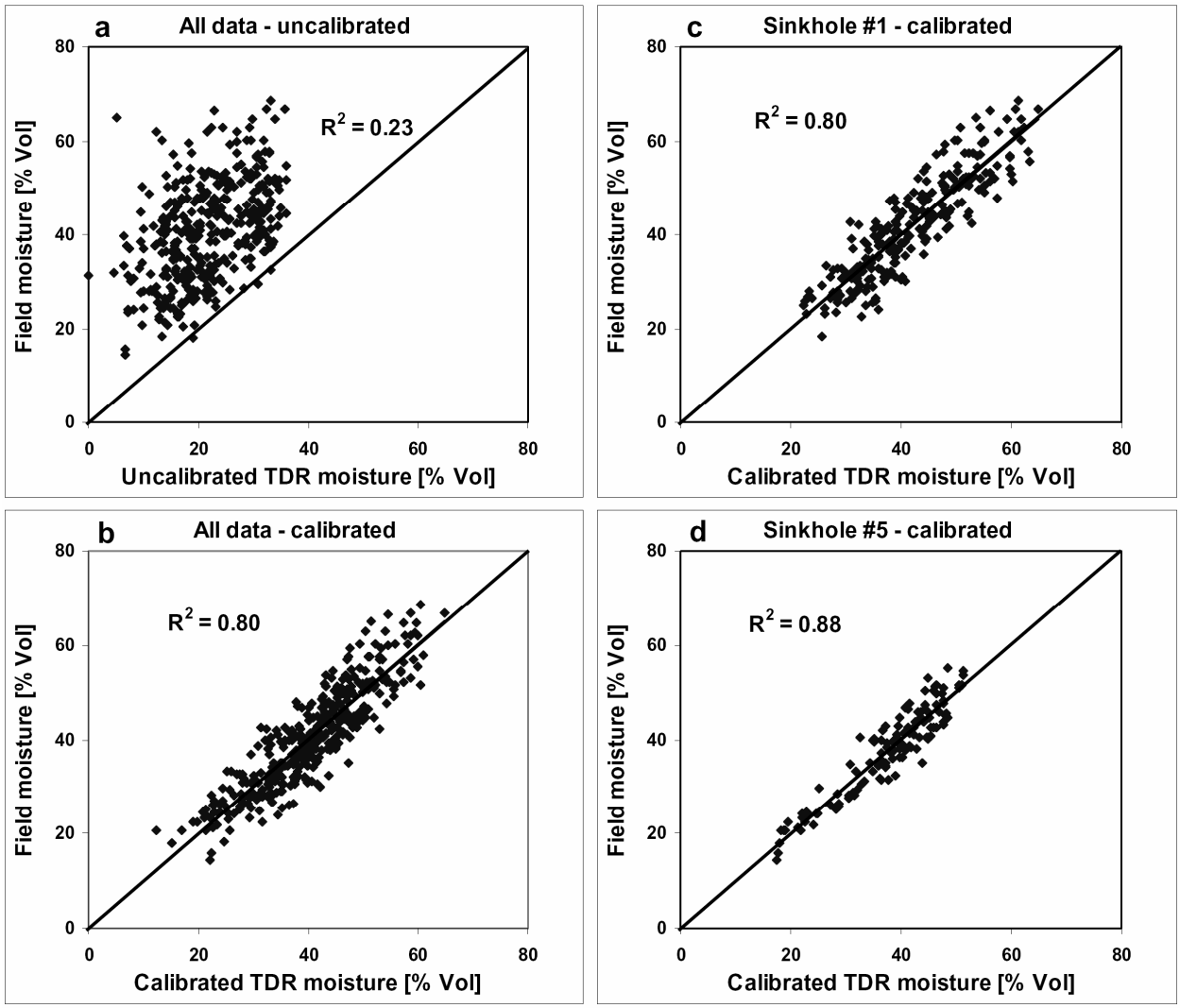

Figure 2.4 Plot of calibration fits using MLR

Diagrams showing: a) un-calibrated TDR moisture readings vs. laboratory-measured field moisture values, b) all calibrated data vs. field moisture, c) calibrated data for sinkhole #1 vs. field moisture, and d) calibrated data for sinkhole #5 vs. field moisture. Diagonal lines represent a 1:1 relationship between calibrated TDR values and field moisture.

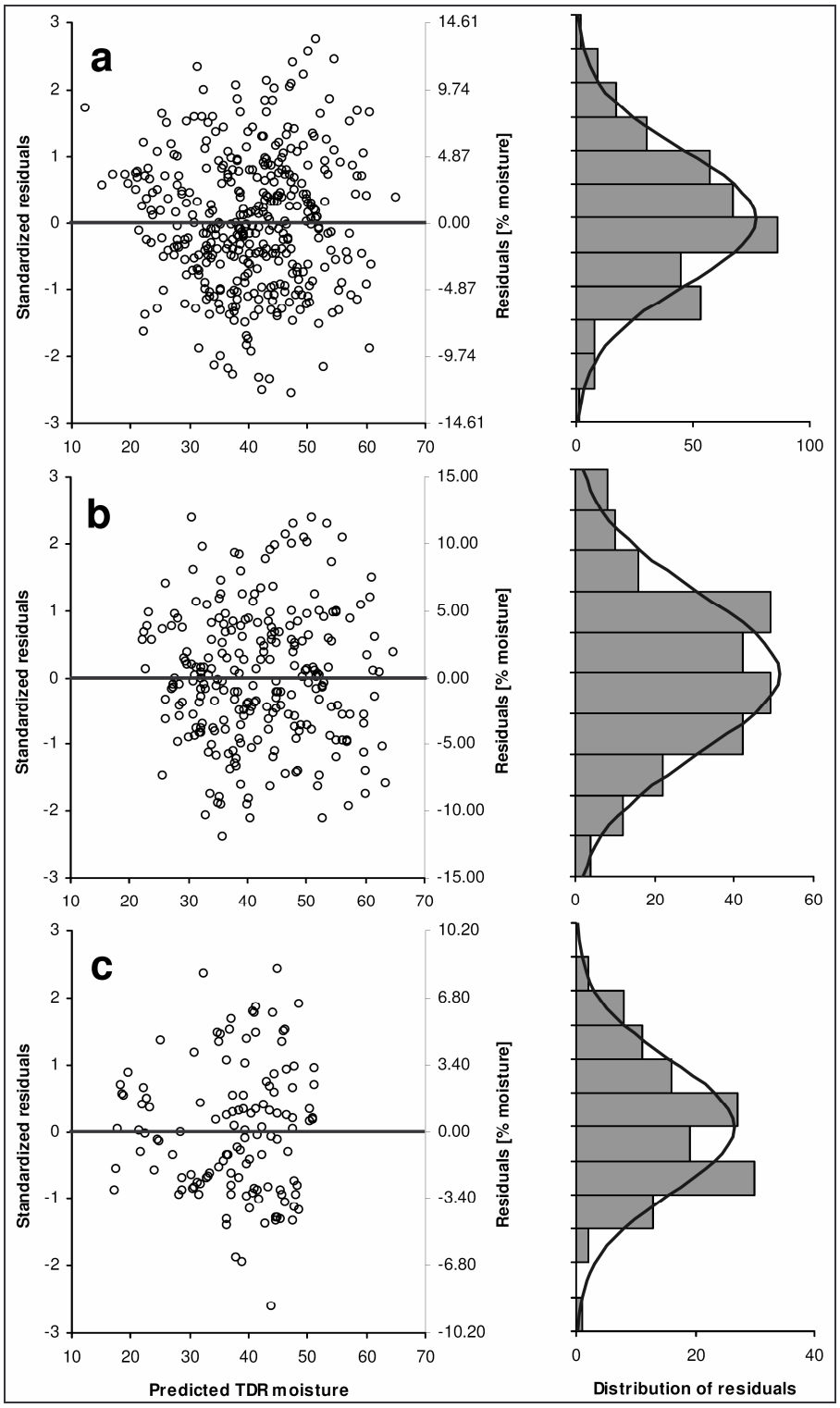

Figure 2.5 Distribution of residuals for MLR results
Distribution of standardized residuals for a) all data, b) sinkhole #1, and c) sinkhole #5. Left plots show distribution of residuals in standardized units (left axis) as well as % moisture (right axis). Right plots show a frequency histogram with a normal distribution curve.

clay sum to 100% for each sample, they should not be simultaneously included in the regression model. MLR was then used to obtain baseline calibration results using TDR moisture and key physical and chemical soil parameters. Common variables included in MLR models for all three groups of data are: TDR moisture, percent clay, depth, percent silt, bulk density, estimated Cation Exchange Capacity (CEC), and log of % calcium saturation (**Table 2.2**). Of these six variables, percent clay and depth explained much of the difference between TDR readings and measured field moisture. Inclusion of these two variables alone increased the R^2 statistic to approximately 80% of the final R^2 value for each model.

Percent clay affects TDR moisture values due to the fact that water molecules bound between clay particles of certain mineralogies tend to be less responsive to TDR measurement (Sabburg et al., 1997), which decreases the bulk dielectric constant, thereby decreasing the resulting TDR moisture value. In essence, the bound water molecules are not able to freely move and interact with the electromagnetic pulse produced by the TDR probe during measurement, thereby limiting the ability of the probe to detect the bound water. This is reflected in our data by positive regression coefficients for percent clay (**Table 2.2**).

The influence of installation depth on TDR-moisture values is important to recognize and estimate when using access-tube style TDR probes. This has been recognized by other researchers (Whalley et al., 2004) who concluded that near-surface disturbances of soil structure were caused by access-tube installation. The disturbances resulted in increased air gaps and air-filled fractures, which decreased the bulk dielectric constant. In our study, repeated insertion and extraction of an auger, no matter how carefully it was done, inevitably led to slight borehole enlargement (especially at or near the surface) and possible soil structure disturbances. Both factors effectively reduce the bulk dielectric constant by introducing air gaps around the access-tube. At greater depths, these factors and related effects are greatly reduced because of fewer disturbances related to augering. However, when we examined the effect depth has on our TDR moisture readings we observed the opposite effect. Instead of the negative correlation found by Whalley, et al (2004), (indicating the influence of air gaps and increased soil disturbances near the surface), we found a strong positive correlation with depth (**Table 2.2**). Although this is good evidence that our access-tube installation methods do not affect TDR measurements, we are

not yet able to fully explain the reasons for this relationship and leave this topic open for further investigation. A possible explanation is that the amount of water bound by various clay minerals is increasing with depth. Moisture content increased systematically with depth in moisture profiles.

Estimated CEC was included in our MLR model because an increase in CEC increases the bulk dielectric constant (Garrouch and Sharma, 1994). This results in increased TDR moisture values, which is reflected by the negative coefficient for CEC values in our calibration equations. The log of percent calcium saturation was included in the model because of its statistical significance and because calcium concentration has also been shown to affect TDR readings (Vogeler, 2001) by increasing the bulk dielectric constant. This is again reflected by the negative correlation coefficient (**Table 2.2**).

Because bulk density is related to mineral grain properties and porosity, there is a theoretical basis for its effect on the bulk dielectric constant (Roth et al., 1990). While bulk density had a relatively small influence on TDR moisture values in our work, we included it in our calibration model because it is statistically significant and is a parameter which is relatively easy to measure. Other field-based studies have shown similar results where bulk density had little or no influence on TDR readings (Whalley et al., 2004). Even some lab-based research has shown relatively insignificant effects of bulk density on bulk dielectric constant (Jacobsen and Schjonning, 1993). The reason for the relative insignificance of bulk density in field conditions and in certain lab experiments, when theoretical and some lab work indicate the opposite should be true, is the subject of debate and one that has not yet been resolved in the literature.

In addition to analyzing the data as a single set and divided by study sinkhole (**Table 2.2**), we also performed MLR analyses on data sets grouped by soil texture (results not shown). In some cases better fits were obtained using this method while in other cases poorer fits were achieved. In most cases fewer variables were required to obtain a final regression model. Because there was not an overall improvement in calibration results, and our soils are highly heterogeneous with respect to physical and chemical properties, we have chosen to use the entire data set and only divide it with respect to sinkhole. This is justified because the sinkholes sampled are

widely separated and are formed in river terraces of different ages and composition. It also allowed us to compare differences between the two sinkholes and the entire data set.

Regression statistics for three baseline MLR calibration models which include the same parameters in each model are presented in **Table 2.2**. With the exception of TDR moisture, p-values of <0.005 indicate that all variables are significant. From the results of the MLR analysis, we derived the baseline calibration equations (3), (4) and (5) for each data set using regression coefficients for each parameter.

For the entire data set:

$$\Theta = \left(0.053 - \left(0.062 \cdot \theta TDR\right) + \left(0.881 \cdot C\right) - \left(0.609 \cdot D\right) + \left(0.442 \cdot S\right) + \left(8.542 \cdot \sigma_b\right) - \left(2.988 \cdot CEC\right) - \left(7.210 \cdot \log Ca\right)\right) \quad (3)$$

For sinkhole #1:

$$\Theta = \left(0.921 - \left(0.102 \cdot \theta TDR\right) + \left(0.917 \cdot C\right) - \left(0.621 \cdot D\right) + \left(0.439 \cdot S\right) + \left(5.206 \cdot \sigma_b\right) - \left(2.806 \cdot CEC\right) - \left(4.282 \cdot \log Ca\right)\right) \quad (4)$$

For Sinkhole #5:

$$\Theta = \left(7.879 + \left(0.045 \cdot \theta TDR\right) + \left(0.627 \cdot C\right) - \left(0.508 \cdot D\right) + \left(0.291 \cdot S\right) + \left(14.235 \cdot \sigma_b\right) - \left(1.347 \cdot CEC\right) - \left(14.361 \cdot \log Ca\right)\right) \quad (5)$$

Where Θ = baseline calibrated soil moisture *[%]*, θTDR = TDR moisture *[%]*, C = percent clay, D = depth [ft], S = percent silt, σ_b = bulk density [g/cm^3], CEC = Cation Exchange Capacity [meq/100g], and $log\ Ca$ = log of percent calcium saturation [%]**.** Equation (3) is the baseline calibration equation for the entire data set, (4) is for data from sinkhole #1 and (5) is for data from sinkhole #5. It is important to note that the coefficients in these calibration equations are specific only to this instrument which contains an internal factory-set standard calibration equation. Knowing the instrument's internal calibration is not important for obtaining a secondary calibration equation using our methods. It is, however, important that internal calibrations not be changed during subsequent calibration and data collection work. If our results are used to calibrate other's TDR measurements without performing a similar statistical analysis, care should be taken to understand the relationship between our calibration equations (3, 4, and 5) and the TDR moisture measurement's relationship to the pseudo transit-time equation (1). **Figure 2.6** shows a vertical moisture profile of uncalibrated and calibrated moisture content compared with gravimetrically measured soil moisture.

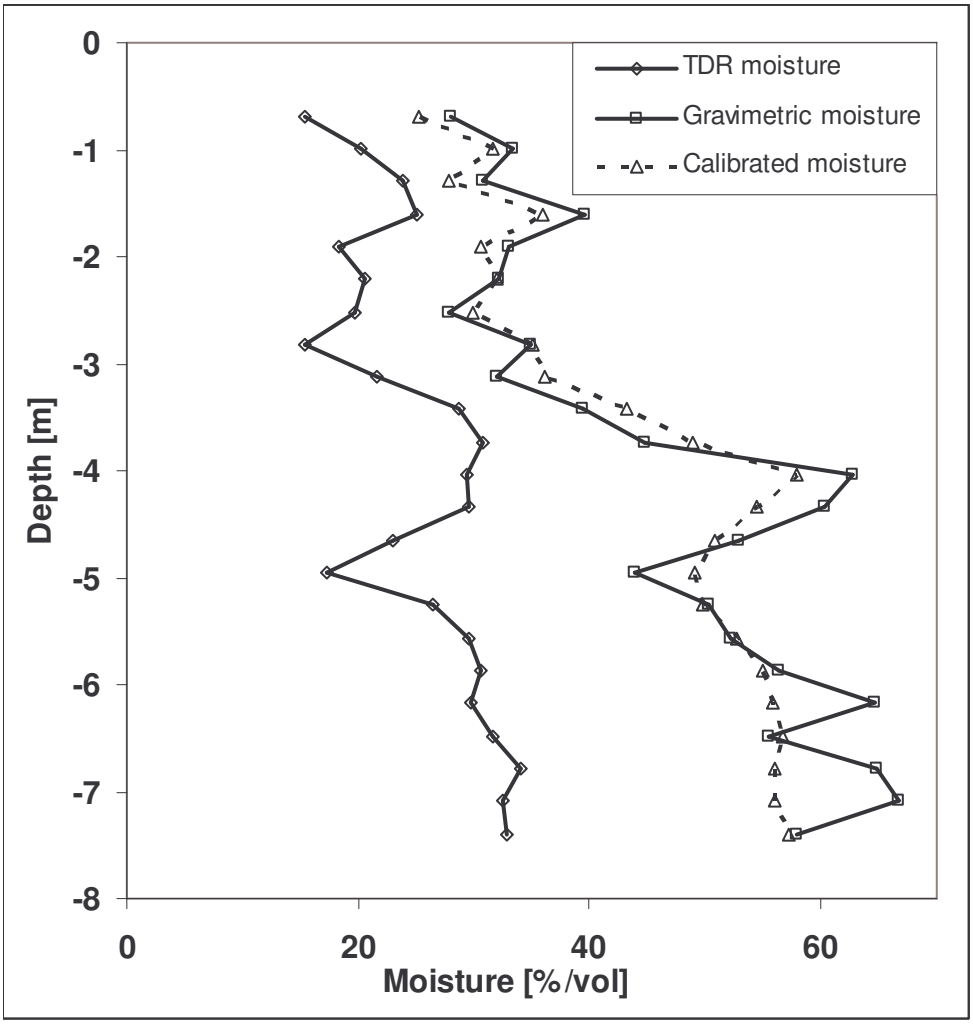

Figure 2.6 Comparison of TDR, gravimetric, and calibrated TDR soil moisture. Figure showing an example of a 1-dimensional moisture profile with depth. Solid line with diamonds represents uncalibrated TDR moisture, solid line with squares represents gravimetrically measured soil moisture, and dashed line represents the MLR-model calibrated TDR moisture.

Error! Reference source not found.**a, b** and **c** show how the R^2 statistic increases as the standard deviation of residuals decreases with inclusion of additional variables in the MLR calibration model. Both the R^2 and the standard deviation were important criteria in choosing the number of parameters we kept in our final models. Sequential addition of TDR moisture, % clay, depth, % silt, bulk density, CEC, and log % Ca saturation did not increase the R^2 statistic more than 0.015 per variable added. Because the standard deviation of residuals is not less than the weighted propagated error estimate in each model (shown by the horizontal lines in Error! Reference source not found.), we conclude that we have not included more parameters than are reasonable in the regression model and have not over-fitted the model.

Figure 2.4 (**b, c** and **d**) illustrates the improved fit of calibrated TDR moisture data using our final calibration equations compared to un-calibrated data (**Figure 2.4a**). Compared to the R^2 of 0.23 for uncalibrated TDR moisture *vs.* field moisture, the R^2 values are: for all data, 0.80; for sinkhole #5, 0.88; for sinkhole #1, 0.80.

Categorical linear regression (CLR)

CLR modeling produced results that are very similar to MLR results, though TDR moisture is more significant in the categorical model and the coefficient for TDR moisture is larger (**Table 2.3**). This result indicates that there is a slightly stronger relationship between TDR moisture and the measured field moisture than is shown using MLR. Although the results show TDR moisture has more influence on the final calibrated data than in MLR, the coefficient for TDR moisture is still small. As with the MLR results, this supports the idea that access-tube TDR measurements are measuring 'free' moisture and the difference between TDR moisture and field moisture is primarily due to the effects of chemical and physical soil properties. The results of our CLR modeling are shown in **Table 2.3** and **Figure 2.8** Fit and residual distribution for CLR results . The baseline calibrated fit for all data points using CLR is very similar to that achieved with MLR. The R^2 statistic is 0.75 *vs.* 0.80 and residuals are normally distributed (**Figure 2.8** Fit and residual distribution for CLR results).

The baseline CLR model includes 7 categorical variables other than TDR moisture which are statistically significant ($Pr > |t| \leq 0.05$): depth, % clay, % sand, bulk density, log Ca saturation,

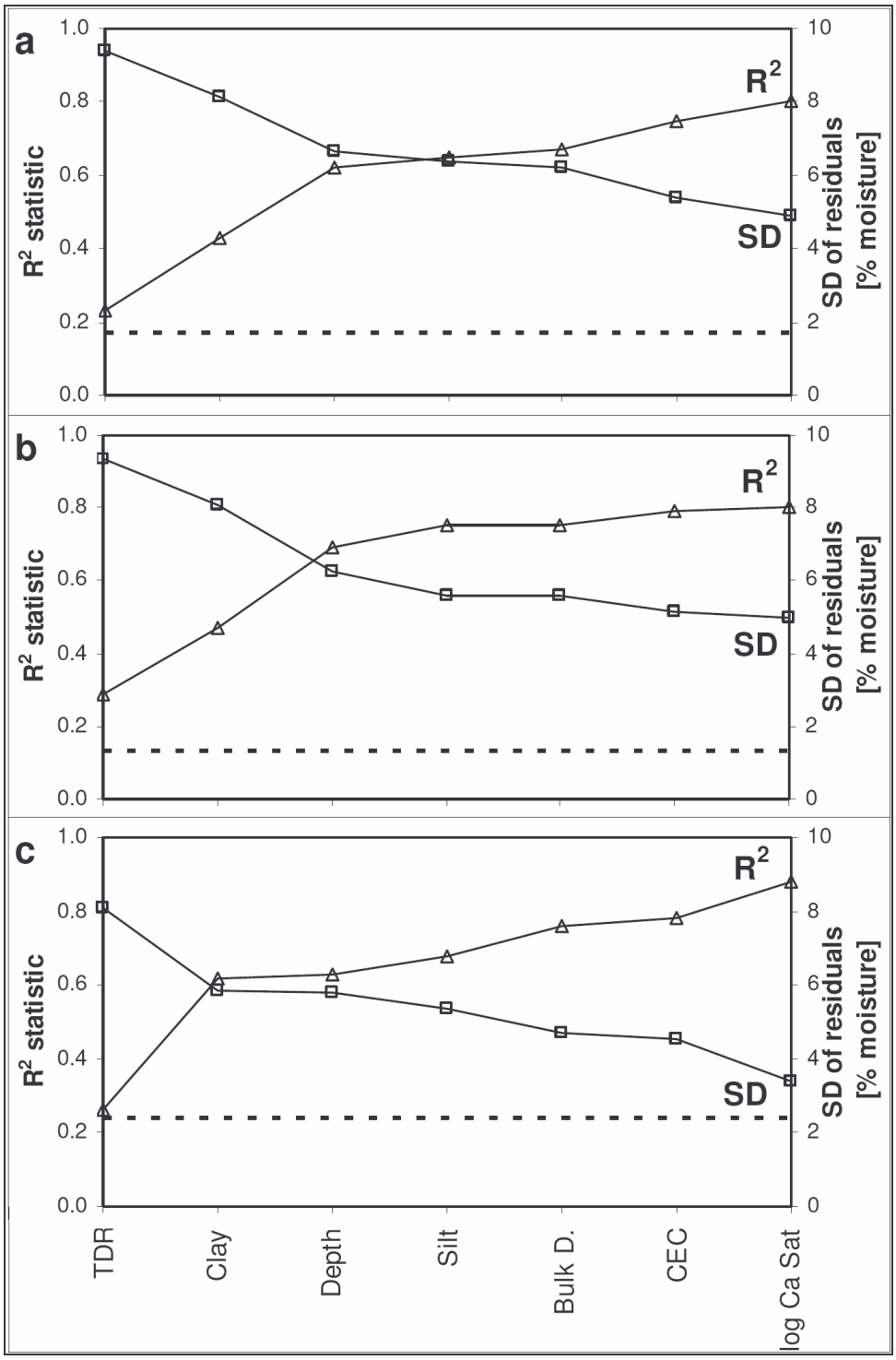

Figure 2.7 Change in MLR calibration fit with additional variables
Diagrams showing for a) complete data set, b) sinkhole #1, and c) sinkhole #5, how regression statistics increase (triangles) and the standard deviation of moisture residuals (squares) decrease with addition of variables. Lower horizontal dashed lines in each plot indicate weighted propagated error estimates based on the relative influence of each variable in the regression model.

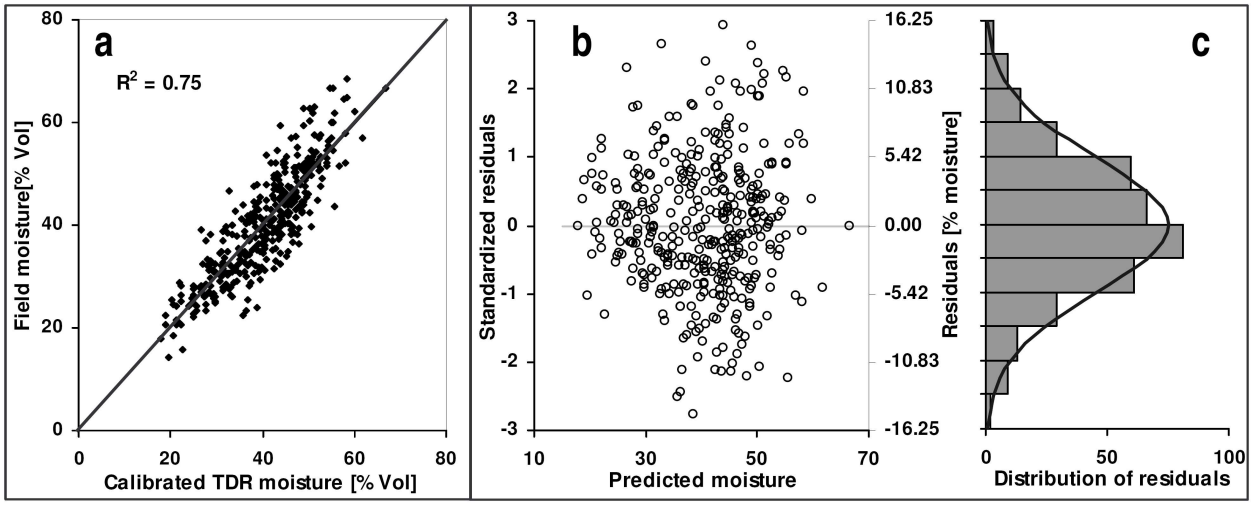

Figure 2.8 Fit and residual distribution for CLR results

Diagram showing field moisture values *vs.* calibrated TDR moisture values resulting from the categorical regression model a). Plots b) and c) show standardized residuals and residual distribution for the categorical regression model.

estimated CEC, and % organic matter. These are the same variables that were significant in the MLR model except that % sand is included instead of % silt in the CLR model (because of greater significance), and % organic matter is significant enough to include in the CLR model. Organic matter has been shown to have effects similar to those of clay on the bulk dielectric constant (Jacobsen and Schjonning, 1993), which is shown in our CLR results by positive parameter estimates for both variables (**Table 2.3**).

The baseline CLR calibration method differs slightly from the MLR method which uses a single linear equation for all data included in the model. In CLR results, each category is matched with a parameter estimate. Parameter estimates for each category are summed to obtain a calibrated moisture value. As an example, to calculate a baseline calibrated moisture value for a sample with the following parameter values (TDR moisture = 15.4, depth = 2.25, % clay = 13.14, % sand = 47.02, bulk density = 1.52, log Ca Sat = 1.73, CEC = 2.5, % organic matter = 1), each parameter is first assigned a category. Using our categories and regression results presented in **Table 2.3**, the baseline calibrated moisture value (Θ) is calculated by summing the following: [27.39 (intercept term) + (0.214 x 15.4) (TDR term) + 0 + 0 - 9.11 + 3.47 - 7.03 + 0 + 4.10]. Using parameter estimates in the same order as listed above, this produces a baseline calibrated moisture value of 22.13%. Zero values represent parameter estimates for data within a baseline category and are included as place-holders in this example. Non-zero parameter estimates represent differences between the relationship within a category and the corresponding baseline category.

Although it would be difficult to show all the categorical subsets specified in the model, we use two of the more important variables in an example which illustrates the essential benefit of the CLR approach. **Figure 2.9** Relationships between variables using CLR shows the relationship between TDR moisture readings and field moisture values in each of the depth and percent clay category subsets. This figure shows both the observed data and the estimated regression relationship each in subset. Although the regression lines shown are not parallel, our model analyses found that an additional model term allowing these slopes to be distinctly defined for each category was insignificant.

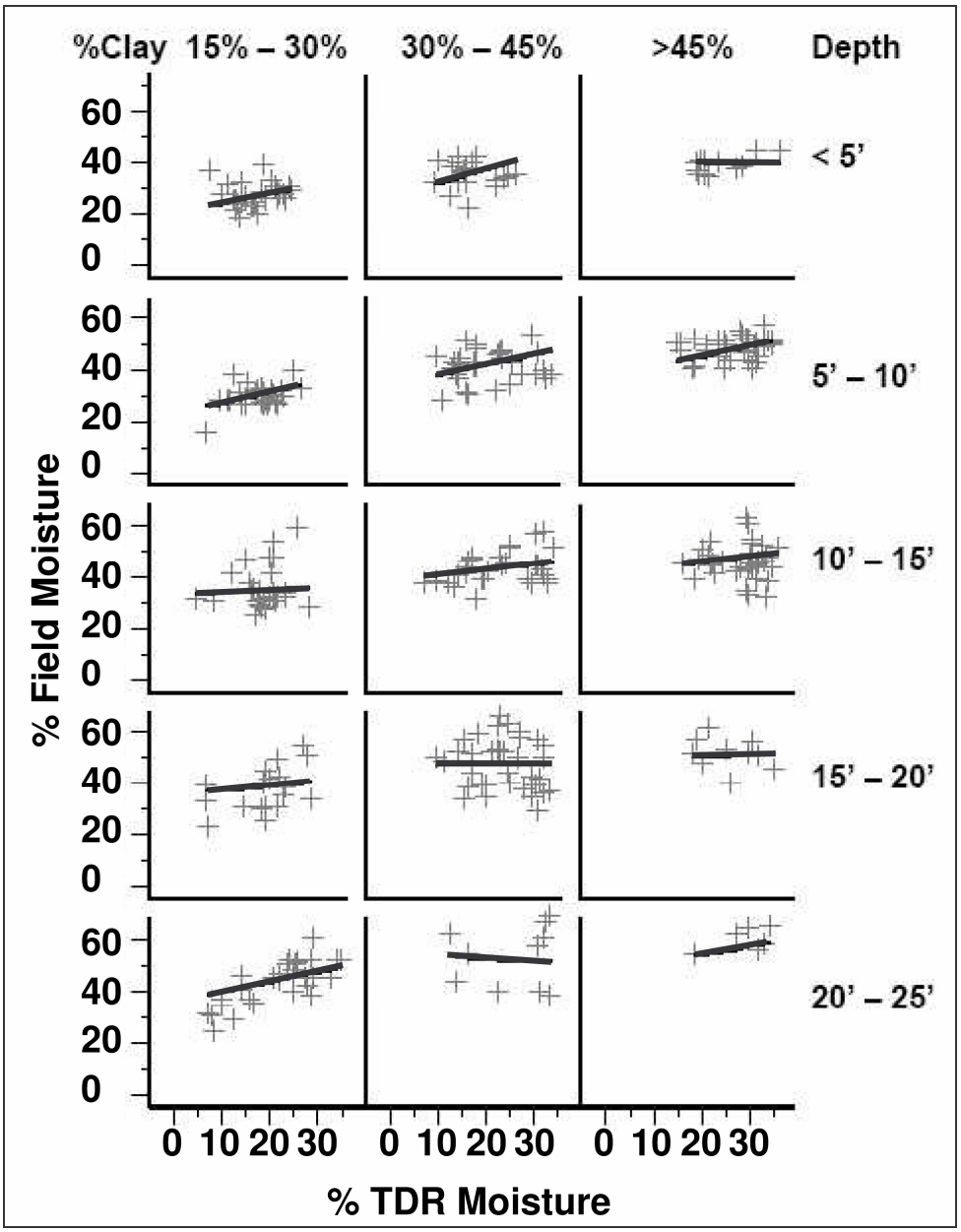

Figure 2.9 Relationships between variables using CLR
Diagram showing the relationship between TDR moisture and field moisture within each of the depth and percent clay category subsets. The lowest category for percent clay and the deepest category for depth have both been excluded because they contained either no or very few observations (<5 obs.). Actual observations are indicated by grey [+] symbols. The regression relationship between TDR moisture and field moisture in each subset is illustrated by the black lines.

Effects of bound water on TRIME TDR moisture readings

The fact that TDR moisture had low significance in the derivation of the baseline calibration equation was surprising as we expected there to be a much stronger relationship between TDR moisture and field moisture. The lack of a strong relationship indicates that the difference between TDR moisture readings and gravimetric soil moisture is the result of something other than a systematic error in the factory calibration. An alternate explanation for the insignificance of TDR moisture in the regression models is that the range of moisture values measured for each soil texture is somewhat limited. Increasing the range of moisture values measured in each texture may have revealed a stronger relationship, but we were not able to investigate this possibility as we were limited by field conditions.

Perhaps the most important implication of TDR moisture having low significance in the regression models is that the measured TDR moisture content is an accurate measurement of the 'free' water in open pores and that the difference between TDR moisture and field moisture is dominantly due to physical properties of the soil controlling the bound water content which is undetectable by the TDR probe. To a lesser extent, the difference is also influenced by chemical effects on the bulk dielectric constant. As a result, any calibration to correct for this difference would not be influenced by the measured TDR moisture. This is a logical assumption since the TDR probe is designed and calibrated at the factory to measure this 'free' fraction of moisture in a soil and is not calibrated to correctly measure moisture in soils with high clay content or high salinity. With this in mind it becomes clear that, in certain soils, TDR moisture measurements may only be useful for measuring and monitoring changes in this 'free' moisture; a point which is not widely discussed in the literature. The remaining bound moisture can reasonably be assumed to remain constant in deep soil profiles where the influence of evapotranspiration is minimal.

Calibrating time-series TDR measurements after baseline calibration is established

Regression modeling indicated that the difference between θTDR and gravimetrically measured soil moisture can almost entirely be explained by the effects of the physical and chemical parameters of the soil. Because θTDR had little influence on the baseline calibrated moisture

values, changes in θTDR observed after the very first measurement (θTDR_i, which was used to develop the baseline calibration) can be interpreted to primarily represent changes in the 'free' moisture content. Using this rationale, our model for calibrating subsequent θTDR measurements (θTDR_t) obtained at the same point is relatively simple and consists of adding the measured change in θTDR ($\theta TDR_t - \theta TDR_i$) to the baseline calibrated value (Θ).

As an example, consider the initial uncalibrated TDR measurement (θTDR_i) which was collected immediately after access tube installation, and a subsequent TDR measurement (θTDR_t) obtained at time t. The baseline calibration equation is applied to θTDR_i to obtain the baseline calibrated moisture content (Θ). The calibrated moisture value at some time t (Θ_t) for the measurement θTDR_t is obtained by adding the difference between the subsequent and initial θTDR measurements to Θ:

$$\Theta_t = \Theta + (\theta TDR_t - \theta TDR_i) \quad (6)$$

DISCUSSION

Calibration of TDR measurements

Determining how physical and chemical parameters can explain the difference between field TDR moisture measurements and gravimetric moisture measurements from soil samples was the primary objective of this study. We believe that equation (3) represents a general calibration equation that can be used to adjust TRIME T3-50 IPH TDR moisture measurements when the required physical and chemical soil parameters are also measured. Calibrated values for subsequent TDR measurements at the same location can then obtained by applying equation (6). Although we believe that our results are broadly applicable, the effects of certain physical and chemical parameters on soil moisture should be evaluated at individual field sites to obtain the most accurate soil moisture measurements. As an example, this is especially true if the clay mineralogy is significantly different, as clay minerals have widely variable capacities for bound water.

Our results highlight parameters which best explain differences between field moisture and TDR measurements in all three data sets, using two regression methods. They also emphasize that instrument-programmed material-specific calibration equations will not produce accurate results

in heterogeneous soil profiles. Our baseline calibration methods are, in essence, a material specific calibration for each TDR measurement. In equation (3), coefficients represent the results of using MLR on the larger set of 383 samples. While the coefficients for equations (4) and (5) are somewhat different from equation (3), the values are similar and tend to bracket the coefficients in equation (3). This supports the idea that, for this TDR instrument, equation (3) is a general MLR calibration model suitable for use in texturally heterogeneous soils with similar chemical properties.

The CLR results can also be used as a general calibration method. We chose to model the data using CLR and include the results because CLR emphasizes different relationships within the data. For example, in MLR, the relationship between TDR moisture and field moisture is not emphasized and can be diminished by stronger relationships between other variables in the model. Using a CLR model allowed us to emphasize the relationship between TDR moisture and field moisture while examining it over the ranges (which are divided into categories) of each additional variable. Results of the CLR model corroborate the results of our MLR modeling and support the notion that discrepancies between gravimetrically measured TDR moisture are not detected using a factory installed calibration equation. The amount of bound, or undetectable, water in our soils is controlled almost entirely by physical and chemical parameters.

Our results can be used as a guide for evaluating the relative importance of soil parameters when performing similar calibration work in the future. The first four parameters (% clay, depth, % silt, and bulk density) are relatively easy to obtain during basic physical characterization of a soil sample and, depending on the goals of a study using access-tube TDR, may provide an acceptable initial calibration. Aside from depth, these parameters are related to soil texture and the associated dielectric properties of mineral grains, porosity, and the effects of bound water in clays. Adding additional parameters such as CEC and log % Ca saturation (which are easily obtained with a routine soil chemical analysis) allows some of the more important dielectric effects of soil chemistry to also be incorporated in the model.

Because a standard soil chemical analysis usually measures many parameters, rather than specific parameters such as CEC and % Ca saturation, using the additional parameters in

regression modeling is easy and economical. We investigated how additional chemical parameters might further improve our regression models. Results indicated that additional parameters did improve the calibration fit by small but statistically significant increments for each group of data. Parameters which were significant (at p-values of <.005) in one or more of the models were pH, log Mn, Organic Matter, and log % K saturation. Ultimately, we decided that inclusion of these parameters was not justified because of relatively small increases in R^2 values (.01 to .015 per parameter) or because of indications that cross-correlation may be a problem. For example, pH and log Ca saturation have a Pearson correlation coefficient of 0.75. However, these results indicate that many other chemical factors are subtly influencing TDR measurements and, depending on the situation, may deserve inclusion in a final regression model. This is not surprising considering that many chemical parameters can alter the dielectric properties of the pore waters being measured.

The accuracy of our baseline calibration models varies depending on data grouping (all data *vs.* division by sinkhole). This is likely the result of differences in random error distribution in TDR measurements that can not be quantified such as proximity of the probe to cobbles or natural voids. Measurements made in soils with more undetected cobbles would result in larger variability in the regressed data. This is supported in our data by the fact that sinkhole #1 contained the most cobbles encountered and also has the highest residual variability in the calibrated moisture values. The results of our baseline MLR models predict a one standard-deviation accuracy of ±4.87, ±5.00 and ±3.40% in volumetric moisture for (3), (4) and (5), respectively. With the CLR model, one standard-deviation in residuals is $\pm$5.42% in volumetric soil moisture. Using our methods, and understanding that random heterogeneities in a field setting will introduce significant variability, we believe that achieving better calibration results is unlikely. For example, achieving an R^2 of 0.99 would not be reasonable considering the natural variability in the system as well as the effects of propagated errors. However, as outlined above, small improvements may be possible by including additional chemical parameters in a regression model.

INSTALLATION

The manufacturer-recommended method for installing TDR access-tubes is to use specialized tools and an auger inside the access-tube to bore a hole approximately the same diameter as the inside of the access tube. Augering is done in short increments and the access tube is then hammered downward from the top (IMKO, 2001). The augered hole is enlarged to the outer diameter of the access-tube as surrounding soils are 'shaved' off by a special cutting head that protects the end of the access-tube. This results in a tight fit between the soil and the tube. In addition to physical limitations on installation depth for this method, there are also practical reasons why it is not suitable for certain soils. Whalley (2004) reported evidence that vibrations from hammering caused significant disturbances in soil structures and probably introduced air gaps around upper portions of the tube. In the clay-rich soils at our field sites and with practice, our method of augering a hole first and then slowly pushing the access-tube into the hole seems to have overcome both of these limitations. Pushing slippery PVC access tubes steadily downward can be quite challenging. We used a long loop of 1-inch tubular nylon climbing webbing as a clamp and a long lever to apply steady downward force on the access-tube. As the tube slid downward, the clamp was moved incrementally upwards and the process repeated until the tube was installed. This method would not be ideal in soils where stability of the augered hole is an issue.

Other researchers have installed access-tubes composed of various plastics as well as fiberglass (Laurent et al., 2005). We used schedule 40, 2.375-inch (6.03 cm) diameter, PVC threaded well-casing access-tubes because they are relatively inexpensive, can be smoothly joined without the need for a connector that increases the outer diameter of the tube, and are sturdy enough to resist damage while applying significant steady force during installation. Additionally, the T3-50 IPH probe is designed for use in schedule 40 PVC pipe. For deep access-tubes, this type of tube and installation method combination seems to be ideal.

Recommended installation methods

Based on our experiences, we suggest the following method for installing access-tubes that will permit accurate TDR measurements at depths up to (and possibly greater than) 30 feet (9.1 m) and will allow subsequent calibration. First, a hole should be augered that is the same diameter

as the access tube. During augering, volumetric soil samples should be collected at intervals that correspond to planned TDR measurement depths. These soil samples can later be used to obtain the parameters used in our MLR and CLR results. Second, the access tube should be installed with careful, steady downward pressure rather than hammering. Last, TDR moisture measurements should be collected immediately after access tube installation.

CONCLUSIONS

Our study shows the importance of calibrating TDR moisture readings to obtain accurate field moisture values from an access-tube instrument in environments where a wide range of soil properties are encountered. To obtain accurate field-moisture values, a large set of soil samples can be characterized and statistically analyzed to determine which parameters significantly influence the bulk dielectric constant of soil. Our baseline MLR calibration model uses TDR moisture, % clay, depth, % silt, bulk density, CEC, and log % Ca saturation to predict an initial field moisture value at each sample point. Minor improvements to the fit of each model were made by adding two or three statistically significant chemical parameters. While these parameters probably do influence the bulk dielectric constant of moist soils, they did not make a large enough difference in our regression results for us to confidently include them in our final MLR models.

Our baseline CLR model uses TDR moisture, depth, % clay, % sand, bulk density, log % Ca saturation, estimated CEC, and % organic matter. As with MLR, minor improvements could be made to the fit of the model, but additional categorical variables did not make large enough differences for us to include them in our final categorical model. The CLR model did not produce significantly different calibration results from the MLR (**Figure 2.8** Fit and residual distribution for CLR results *vs.* **Figure 2.4** and **Figure 2.5**). However, it did reinforce the conclusions reached using MLR, which were that the differences between TDR moisture and field moisture values are primarily the result of effects due to physical and chemical properties.

While TDR calibration for access-tube measurements is a potentially difficult exercise, it can and should be done if TDR will be used to measure soil moisture in heterogeneous soils – especially those with high clay content. We have determined which parameters best explain discrepancies

between access-tube TDR and gravimetrically measured moisture measurements so that others might use this information to design sampling and calibration methodologies in the most time and cost-effective manner.

In our study, un-calibrated access-tube TDR moisture measurements significantly and consistently underestimated true field moisture values (**Figure 2.4a**). In our MLR and CLR model results, TDR moisture has a very small and statistically insignificant effect on initial calibrated moisture values in our analyses (p-values are all > 0.05). This leads us to the conclusion that large differences between measured TDR moisture values and corresponding gravimetrically measured soil moisture values are due to the effects of (dominantly) physical and (to a lesser extent) chemical soil properties on soil moisture which the TDR probe we used is not able to detect.

After a baseline calibration is applied, subsequent TDR measurements in the same location can be calibrated using equation (6). This method assumes that temporal changes in uncalibrated TDR measurements are the result of changes in 'free' soil moisture and that bound moisture remains essentially constant over time in deep profiles, is mostly undetectable by the TDR probe, and is accounted for by using the baseline calibration.

ACKNOWLEDGEMENTS

We would like to acknowledge funding for this research from: US Department of Education GAANN Fellowship, Virginia Water Resources Research Center, Cave Conservancy Foundation, Cave Research Foundation, National Speleological Society, Geological Society of America, West Virginia Association for Cave Studies, and the Virginia Tech Graduate Research Development Program. We would also like to thank Dr. Rolf Becker and Mr. Timo Camek at IMKO for their generous technical assistance and advice. We thank Ankan Basu, Mike Beck, Lee Daniels, Beth Diesel, Bruce Dunlavy, Frank Evans, Brad Foltz, Marty Griffith, Mary Harvey, Ashley Hogan, Danielle Huminicki, Stuart Hyde, Rachel Lauer, Steve Nagle, Jeanette Montrey, Wil Orndorff, Zenah Orndorff, Dave Rugh, Cori and Zachary Schwartz, Jim Spotila, Brett Viar, Dongbo Wang, and Brad White for their assistance both in the field and in the lab.

REFERENCES

Analyse-it for Microsoft Excel. Leeds, UK. See http://www.analyse-it.com/.

Chandler, D.G., M. Seyfried, M. Murdock, and J.P. McNamara. 2004. Field Calibration of Water Content Reflectometers. Soil Science Society of America Journal 68:1501-1507.

Dane, J.H., Topp, G.C., (ed.) 2002. Methods of soil analysis. Part 4: physical methods, pp. 1-1692. Soil Science Society of America, Madison, Wisconsin.

Dobson, M.C., F.T. Ulaby, M.T. Hallikainen, and M.A. El-Rayes. 1985. Microwave dielectric behavior of wet soils - part II: dielectric mixing models. IEEE Transactions on Geoscience and Remote Sensing GE-23:35-46.

Evett, S.R., and J.L. Steiner. 1995. Precision of neutron scattering and capacitance type soil water content gauges from field calibration. Soil Science Society of America Journal 59:961-968.

Garrouch, A.A., and M.M. Sharma. 1994. The influence of clay content, salinity, stress and wettability on the dielectric properties of bring saturated rocks: 10 Hz to 10 MHz. Geophysics 59:909-917.

IMKO. 2001. TRIME-FM User Manual - 22 pgs.

IMKO. 2006a. Micromodultechnik GmbH. Theoretical aspects on measuring moisture using TRIME, Ettlingen, Germany.

IMKO. 2006b. Theoretical aspects on measuring moisture using TRIME - pages 33-55.

Jacobsen, O.H., and P. Schjonning. 1993. A laboratory calibration of time domain reflectometry for soil water measurement including effects of bulk density and texture. Journal of Hydrology:147-157.

1989-2005. Version 6. SAS Institute Inc, Cary, NC.

Kool, J.B., K.A. Albrecht, J.C. Parker, and J.C. Baker. 1986. Physical and chemical characterization of the Groseclose Soil Mapping Unit. Virginia Agricultural Experiment Station Bulletin 86-4:75.

Laurent, J., P. Ruelle, L. Delage, A. Zairi, B.B. Nouna, and T. Adjim. 2005. Monitoring soil water content profiles with a commercial TDR system: comparative field tests and laboratory calibration. Vadose Zone Journal 4:1030-1036.

MESA-Systems. 2006. 50mm Tube Access Probes specifications [Online] http://www.mesasystemsco.com/product.asp?id=6#.

Mullins, G.L., Heckendorn, S. E. 2005. Draft Copy of Laboratory Procedures - Publication 452-881. Virginia Tech Soil Testing Laboratory, Blacksburg.

Ramsey, F.L., and D.W. Schafer. 1997. The statistical sleuth: a course in methods of data analysis. Duxbury Press, Belmont, CA.

Roth, K., R. Schulin, H. Fluhler, and W. Attinger. 1990. Calibration of Time Domain Reflectometry for Water Content Measurement Using a Composite Dielectric Approach. Water Resources Research 26:2267-2273.

Sabburg, J., J.A.R. Ball, and N.H. Hancock. 1997. Dielectric behavior of moist swelling clay soils at microwave frequencies. IEEE Transactions on Geoscience and Remote Sensing 35:784-787.

SAS Institute Inc. 2000-2004. SAS 9.1 Software. SAS Institute Inc, Cary, NC.

Schoeneberger, P.J., Wysocki, D. A., Benham, E. C., and Broderson, W. D. (editors). 2002. Field book for describing and sampling soils, Version 2.0. 2.0 ed. Natural Resources Conservation Service, National Soil Survey Center, Lincoln, NE.

Topp, G.C., J.L. Davis, and A.P. Annan. 1980. Electromagnetic determination of soil water content: measurements in coaxial transmission lines. Water Resources Research 16:574-582.

USDA-NRCS. 2006. Web Soil Survey [Online] (verified September 4, 2006).

Vogeler, I. 2001. Copper and Calcium Transport through an Unsaturated Soil Column. Journal of Environmental Quality 30:927-933.

Whalley, W.R., R.E. Cope, C.J. Nicholl, and A.P. Whitmore. 2004. In-field calibration of a dielectric soil moisture meter designed for use in an access tube. Soil Use and Management 20:203-206.

Table 2.1
Mean, standard deviation, and range (minimum and maximum) values for physical and chemical characteristics of 383 soil samples used for calibrating TDR moisture measurements.

		All data n = 382			Sinkhole #1 n = 253			Sinkhole #5 n = 129		
Parameter	Units	Mean	Std Dev	Range	Mean	Std Dev	Range	Mean	Std Dev	Range
TDR Moisture	vol. %	21.68	7.46	0.00, 36.10	20.80	7.27	0.00, 35.90	23.41	7.55	6.50, 36.10
Field Moisture	vol. %	40.53	10.72	14.31, 68.62	41.96	11.06	18.38, 68.62	37.70	9.42	14.31, 55.01
Depth	feet	-11.38	6.63	-28.25, -1.25	-12.48	7.00	-28.25, -1.25	-9.20	5.23	-21.25, -1.25
Bulk Density	g/cm^3	1.42	0.27	0.76, 2.54	1.51	0.26	0.89, 2.54	1.25	0.19	0.76, 1.88
Clay	% bulk sample	34.5	12.7	8.6, 67.8	33.3	11.8	13.1, 59.0	36. 9	14.2	8.6, 67.8
Silt	% bulk sample	33.3	11.3	8.7, 71.0	30.5	11.6	8.7, 62.0	39.0	8.2	19.6, 71.0
Sand	% bulk sample	29.5	12.4	6.3, 66.0	33.9	11.8	9.2, 66.0	21.0	8. 5	6.3, 46.0
Gravel	% bulk sample	2.6	4.6	0.0, 30.0	2.4	4.7	0.0, 30.0	3.1	4.4	0.0, 23.0
pH	pH	4.93	0.41	4.20, 6.59	4.81	0.37	4.20, 6.44	5.17	0.39	4.39, 6.59
BpH	BpH	5.98	0.24	5.29, 6.61	5.93	0.25	5.35, 6.61	6.07	0.21	5.29, 6.49
Est CEC	meq/100g	4.52	1.34	0.90, 8.50	4.15	1.18	0.90, 7.70	5.25	1.36	2.00, 8.50
log % Ca Sat	%	1.23	0.35	0.54, 1.88	1.12	0.34	0.54, 1.88	1.47	0.23	0.69, 1.85
log % Mg Sat	%	1.17	0.30	0.38, 1.68	1.06	0.28	0.38, 1.67	1.40	0.18	0.91, 1.68
log % K Sat	%	0.41	0.20	-0.50, 0.88	0.35	0.02	-0.05, 0.86	0.51	0.14	0.11, 0.88
log K	(mg/kg)	1.64	0.19	1.20, 2.08	1.55	0.16	1.20, 2.03	1.81	0.10	1.46, 2.08
log Ca	(mg/kg)	2.17	0.37	1.36, 3.01	2.02	0.34	1.36, 3.01	2.47	0.24	1.73, 3.01
log Mg	(mg/kg)	1.89	0.34	0.85, 2.58	1.74	0.28	0.85, 2.32	2.19	0.24	1.49, 2.58
log Zn	(mg/kg)	-0.23	0.46	-1.00, 2.00	-0.38	0.27	-1.00, 1.39	0.064	0.59	-0.70, 2.00
log Mn	(mg/kg)	0.86	0.60	-1.00, 2.32	0.69	0.58	-1.00, 1.98	1.20	0.46	-0.10, 2.32
log Cu	(mg/kg)	-0.45	0.23	-1.00, 0.85	-0.42	0.22	-1.00, 0.85	-0.51	0.24	-1.00, -0.05
log Fe	(mg/kg)	1.22	0.19	0.72, 1.69	1.25	0.21	0.72, 1.69	1.16	0.15	0.91, 1.51
OM	% bulk sample	1.24	0.44	0.40, 2.80	1.15	0.41	0.40, 2.30	1.41	0.43	0.50, 2.80
Phosphorus	(mg/kg)	4.33	12.49	2.00, 185.00	3.44	11.65	2.00, 185.00	6.08	13.89	2.00, 118.00
Boron	(mg/kg)	0.11	0.025	0.10, 0.20	0.10	0.017	0.10, 0.20	0.11	0.034	0.10, 0.20
Acidity	%	55.59	26.25	0.00, 92.70	65.20	25.12	0.00, 92.70	36.66	16.27	0.40, 77.40
Soluble Salts	ppm	45.03	25.23	1.00, 179.00	36.20	18.65	1.00, 115.00	62.40	27.43	26.00, 179.00

Table 2.2
Final regression statistics for each data set. Top table shows statistics when all data are included in a single model. Bottom tables show statistics resulting from division of data by sinkhole. Correlation coefficients, p-values and measurement errors for each parameter are listed. SD = standard deviation of residuals [% moisture]. One standard deviation in % moisture for weighted error propagation are also shown. Errors shown are either estimated or obtained from published sources (Dane, 2002; IMKO, 2006b)

All Data						
Variable	Coefficient	p-value	Error %	Source for error value		
Intercept	0.053	0.9862			n	382
TDR Moisture	-0.062	0.1919	2	IMKO report	R^2	0.80
Clay	0.881	<0.0001	0.5	Dane and Topp	SD of residuals	4.83
Depth	-0.609	<0.0001	0.35	Estimated	Weighted error	1.70
Silt	0.442	<0.0001	1	Dane and Topp		
Bulk Density	8.542	<0.0001	5	Estimated		
Est CEC	-2.988	<0.0001	10	Estimated		
Log Ca Sat	-7.210	<0.0001	10	Estimated		
Sinkhole #1						
Variable	Coefficient	p-value	Error %	Source for error value		
Intercept	0.921	0.8196			n	253
TDR Moisture	-0.102	0.1240	2	IMKO report	R^2	0.80
Clay	0.917	<0.0001	0.5	Dane and Topp	SD of residuals	4.95
Depth	-0.621	<0.0001	0.35	Estimated	Weighted error	1.34
Silt	0.439	<0.0001	1	Dane and Topp		
Bulk Density	5.206	0.0025	5	Estimated		
Est CEC	-2.806	<0.0001	10	Estimated		
Log Ca Sat	-4.282	<0.0001	10	Estimated		
Sinkhole #5						
Variable	Coefficient	p-value	Error %	Source for error value		
Intercept	7.879	0.1042			n	129
TDR Moisture	0.045	0.4140	2	IMKO report	R^2	0.88
Clay	0.627	<0.0001	0.5	Dane and Topp	SD of residuals	3.40
Depth	-0.508	<0.0001	0.35	Estimated	Weighted error	2.40
Silt	0.291	<0.0001	1	Dane and Topp		
Bulk Density	14.235	<0.0001	5	Estimated		
Est CEC	-1.347	<0.0001	10	Estimated		
Log Ca Sat	-14.361	<0.0001	10	Estimated		

Table 2.3
Parameter estimates, standard error, and t-statistics for categorical variables in the categorical regression model.

Variable and Category	Parameter Estimate	Standard Error	t Value	Pr > | t |
Intercept	27.399	2.158	12.7	<0.0001
TDR Moisture	0.214	0.052	4.11	<0.0001
Depth (<5 feet)	0.000			
Depth (5 to <10 feet)	2.621	0.933	2.81	0.0052
Depth (10 to <15 feet)	3.961	0.978	4.05	<0.0001
Depth (15 to <20 feet)	7.732	1.026	7.54	<0.0001
Depth (20 to <25 feet)	11.205	1.190	9.42	<0.0001
Depth (≥25 feet)	15.061	2.761	5.45	<0.0001
% Clay (<15)	0.000			
% Clay (15 to <30)	5.302	1.546	3.43	0.0007
% Clay (30 to <45)	11.598	1.561	7.43	<0.0001
% Clay (≥45)	13.447	1.756	7.66	<0.0001
% Sand (<20)	0.000			
% Sand (20 to <40)	-4.713	0.844	-5.59	<0.0001
% Sand (≥40)	-9.109	1.159	-7.86	<0.0001
Bulk Density (<1.25) g cm^{-3}	0.000			
Bulk Density (1.25 to <1.75) g cm^{-3}	3.473	0.746	4.66	<0.0001
Bulk Density (≥1.75) g cm^{-3}	5.399	1.200	4.50	<0.0001
Log % Ca Sat. (<1)	0.000			
Log % Ca Sat. (1 to <1.5)	-3.117	0.733	-4.25	<0.0001
Log % Ca Sat. (≥1.5)	-7.030	0.827	-8.50	<0.0001
Est CEC [meq/100g] (<3)	0.000			
Est CEC [meq/100g] (3 to <5)	-2.346	0.996	-2.36	0.0191
Est CEC [meq/100g] (5 to <6)	-6.206	1.164	-5.33	<0.0001
Est CEC [meq/100g] (≥6)	-7.294	1.353	-5.39	<0.0001
% Organic Matter (<1)	0.000			
% Organic Matter (1 to <1.5)	4.101	0.917	4.47	<0.0001
% Organic Matter (≥1.5)	5.040	1.120	4.50	<0.0001

CHAPTER 3

Linking Field Scale Electrical Resistivity Tomography and Time Domain Reflectometry Derived Soil Moisture

Benjamin F. Schwartz[1], Madeline E. Schreiber[1] and Tingting Yan[2]
[1]Department of Geosciences
Virginia Polytechnic and State University
Blacksburg, VA 24060
[2]Intera, Inc., Austin, TX 78754

ABSTRACT

Electrical Resistivity Tomography (ERT) and Time Domain Reflectometry (TDR) were used to simultaneously measure resistivity and soil moisture at an experimental field site with the objective of developing a non-invasive method for measuring 2-D soil moisture profiles in unsaturated zones. Using the field data, we developed a model using a modified form of Archie's Law, which uses bulk conductivity derived from ERT readings, pore water conductivity, and percent clay content of soils, to convert 2-D ERT profiles into 2-D soil moisture profiles. We numerically optimized and calibrated the model using 1-D access-tube Time Domain Reflectometry (TDR) derived soil moisture measurements. Results show that the model can be successfully applied to highly heterogeneous soils, and thus provides a useful tool for measuring 2-D soil moisture at a variety of field sites.

INTRODUCTION

Measuring and modeling soil moisture in unsaturated environments is difficult due to the complexity of unsaturated hydrogeologic systems and difficulties associated with obtaining accurate and spatially representative measurements of soil moisture in a heterogeneous environment. Tools commonly used for measuring soil moisture include Time Domain Reflectometry (TDR) and neutron probes. However, the challenge in using these tools is that previous work has shown that TDR and neutron methods produce measurements of soil moisture that can be inaccurate without material specific calibrations for many soil textures (Dane, 2002; Jacobsen and Schjonning, 1993; Schwartz et al., *In review;* Yao et al., 2004).

Theoretical, field, and lab-based studies have documented that relationships exist between various physical properties in the unsaturated zone (such as moisture content) and geophysical measurements (Auerswald et al., 2001; Kalinski and Kelly, 1993; Kalinski et al., 1993; Maulem

and Friedman, 1991; Titov et al., 2004). The advantage of using geophysical tools such as electrical resistivity tomography (ERT) or ground penetrating radar (GPR) is that they provide a non-invasive method for measuring or inferring soil characteristics, such as soil moisture. A limitation of many of these studies is that they often rely on a single geophysical technique to quantify soil properties, and thus lack methods for verification or validation.

Laboratory studies correlating geophysical measurements and soil properties (e. g., soil resistivity *vs.* soil moisture) are by nature conducted at small scales. Thus, a limitation of these studies is that the strong correlation observed between electrical and physical parameters is often related to the scale of measurement and the level of control over the experiment. In general, lab-scale soil resistivity *vs.* soil moisture experiments generate results which are not reproducible in the field due to problems such as heterogeneities in large-scale natural systems and decreasing resolution of geophysical measurements with depth. As an example, Kalinski and Kelly (1993) were able to show excellent correlation between measured soil electrical resistivity and volumetric soil moisture at the centimeter scale. Achieving similar results using field-scale measurements would not be possible because of lower resolution at larger scales and uncertainties related to poorly characterized heterogeneities in physical and chemical properties which influence electrical properties.

In the field, geophysical techniques have been used to non-invasively characterize unsaturated soil hydrology with varying degrees of success (Kalinski and Kelly, 1993; Lambot et al., 2004; Michot et al., 2003; Zhou et al., 2001). In contrast with lab-scale studies, field-scale geophysical studies of unsaturated soils are frequently qualitative rather than quantitative. For example, one promising method for inferring soil moisture in the field is electrical resistivity tomography (ERT), which has been used in a variety of geologic settings to study temporal variability in soil moisture (Barker and Moore, 1998; Daily and Ramirez, 2000; Hauck and Scheuermann, 2005). Use of ERT to measure temporal variations in soil moisture assumes that changes in soil resistivity result from some change of unknown magnitude in soil moisture, and that wetting or drying soils will result in decreasing or increasing resistivity values, respectively. Although ERT is a very useful tool, there are several limitations to using ERT as a stand-alone method for measuring soil moisture. For example, simply converting raw resistivity data into soil moisture values is next to impossible without a more detailed understanding of the physical and chemical properties of the subsurface. Likewise, developing a resistivity *vs.* soil moisture calibration

curve on an in-situ sample is hindered by the difficulties associated with accurately and simultaneously measuring both of these parameters in the subsurface.

There are additional challenges to conducting field-scale studies using geophysical methods to estimate soil moisture. First, there are practical issues such as variable resolution of non-intrusive measurement techniques (e.g., GPR and ERT), penetration depth being dependent on physical conditions (e.g., high clay content limits the effective depth of penetration for GPR), and the physical difficulty and cost associated with directly measuring hydrogeologic parameters in unsaturated environments. Integrative approaches which combine geophysical modeling and hydrogeologic data yield better results (Shuyun and Yeh, 2004). Results of this type of approach emphasize the value of incorporating hydrogeologic data in geophysical models.

Spatial and temporal distribution of soil moisture also needs to be addressed. In the field, relatively small-scale direct measurements of soil moisture and physical properties are the only scale at which these parameters may be collected in-situ, especially if the system being studied is not destroyed in the process of collecting the information. This means that interpolation, extrapolation, and other methods of modeling these properties (e.g., geophysical techniques) are the only alternatives for obtaining larger-scale coverage for the parameters of interest. For example, TDR measurements can provide an estimate of soil moisture within a region extending only tens of centimeters of the probe - a definite limitation in situations where the region of interest is actually tens of meters. Conversely, techniques such as ERT provide geophysical evidence of physical properties in the subsurface at many different scales and resolutions. However, directly interpreting the ERT results in terms of a parameter such as soil moisture becomes extremely difficult without additional information. This is where linking two or more data sets such as large scale ERT measurements, and small scale soil moisture measurements and physical properties can be useful.

The primary objective of this study was to develop a method for converting field-scale 2-D ERT profiles into 2-D soil moisture profiles. We approached this research problem by investigating links between small-volume (cm-scale) moisture measurements from access-tube Time Domain Reflectometry (TDR), and large volume (meter-scale) electrical measurements made using 2-D Electrical Resistivity Tomography (ERT). Developing methods for linking ERT and TDR would be useful for unsaturated zone characterization as ERT gives 2-D coverage of a study area and

can model variations in subsurface properties which may not be detected using 1-D methods such as TDR. In addition, if 2-D ERT can be used to estimate soil moisture in heterogeneous soils, it would provide an excellent tool for non-invasive characterization of almost any unsaturated soil system.

FIELD SITE

Our research site at the Virginia Tech Kentland Experimental Farms in Montgomery County, Virginia contains two well-developed sinkhole plains formed in ancient New River terraces **(Figure 3.1a)**. The sinkholes are generally broad and shallow, allowing easy access for agricultural activities, and contain no bedrock outcrops. Thick terrace deposits mantle sinkholes with soils characterized as weathered fluvial terrace materials deposited by the ancient New River, which have developed over the underlying Cambrian aged Elbrook Formation limestone and dolostone bedrocks. Soils are classified by the USDA-NRCS as Guernsey silt loam, Unison and Braddock soils, and Unison and Braddock cobbly soils (USDA-NRCS, 2006). Both sinkhole plains have numerous sinkholes of similar size and shape. Two sinkholes were chosen for more detailed analysis in our study. Sinkhole #1 is in a higher and older terrace deposit and contains highly weathered soils to depths exceeding 40 feet (12.2 m). Sinkhole #5 is formed in a lower and younger terrace and contains soils which are not as mature. In Sinkhole #5, bedrock was reached in most augered holes at depths between 11 and 25 feet (3.4 and 7.6m) below land surface.

METHODS

Sinkhole characterization

We characterized the physical and chemical properties of the sinkholes by collecting and analyzing soil samples at 12-inch (30.5 cm) intervals during access tube installation. Samples were also collected at larger intervals during installation of deeper monitoring wells (10 to 12m). Except for one monitoring well in sinkhole #1, water levels were not detected in any of the wells. A well in sinkhole #1 had <1m of water in it for a short time after installation, which was more than a year before the ERT and TDR measurements used in this study were collected. The absence of water in the monitoring wells since then is likely the result of considerably drier conditions since the wells were installed and is evidence that saturated conditions were remained well below the bottom of all TDR access tubes. Detailed topographic surveys performed in each

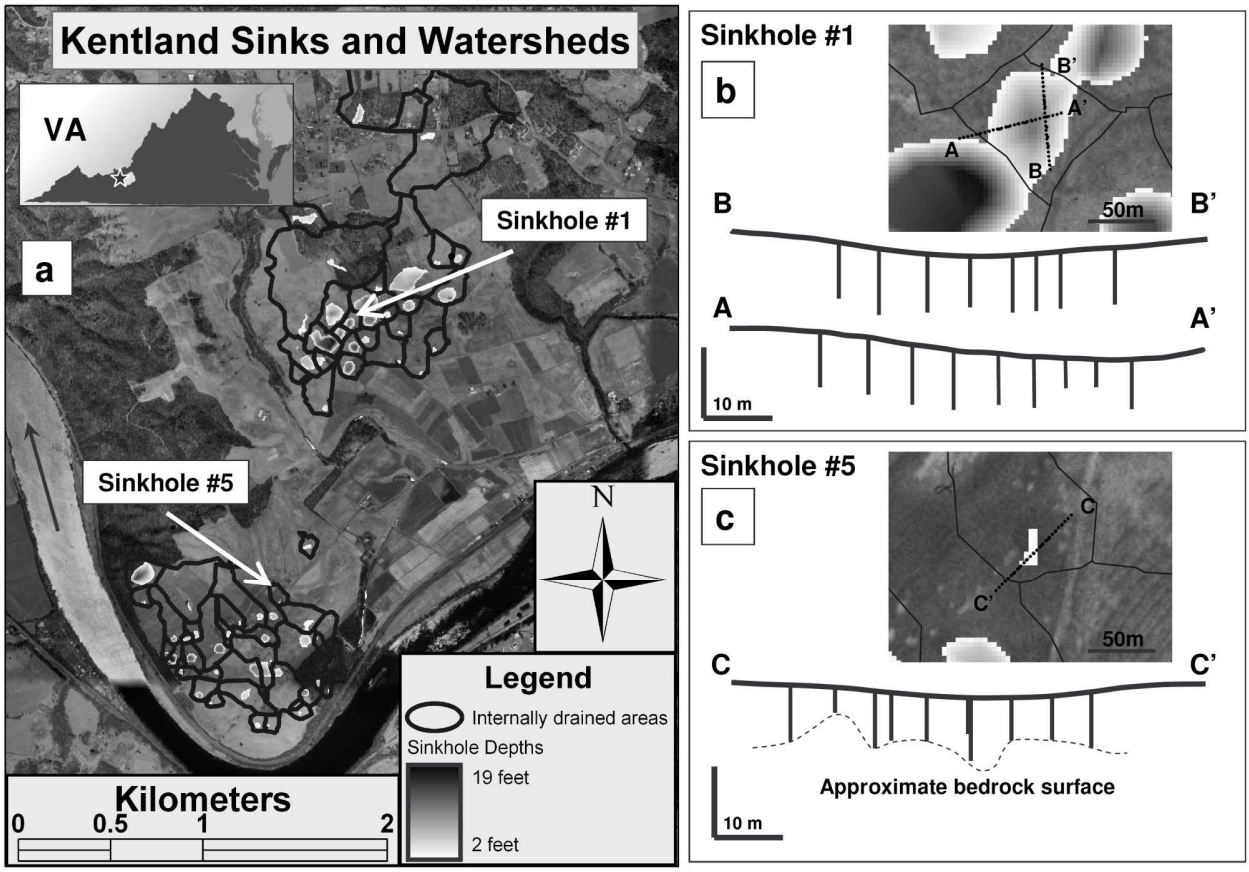

Figure 3.1 Field site and ERT transect locations

a) Virginia Tech Kentland Experimental Farms at Whitethorne, Virginia, USA. **Figure 3.1a** shows study sinkholes #1 and #5 and catchment areas (adjacent polygons) for each sinkhole within the two sinkhole plains. Aerial imagery © 2002 Commonwealth of Virginia. Sinkhole #1 is in the higher, older terrace. b) and c) show surface topography and the location and orientation of instrumentation installed in transects across both sinkholes. Upper image in the diagrams is a map view of the sinkhole, while the lower portion of the diagrams shows profile views of monitoring wells, TDR access-tubes and other instrumentation installed along each transect. Note that depth of bedrock was not determined in Sinkhole #1.

sinkhole include elevations and locations of all monitoring wells, access tubes, and ERT electrodes.

Soil Analyses

Soil moisture was determined gravimetrically for each soil sample by drying in an oven at 105°C until repeated weighing showed no further weight loss. Percent soil moisture by volume and dry bulk density were calculated using final oven-dry weight, initial weight and the sample volume. Particle size analyses (PSAs) were performed on each sample using the ASTM 152H hydrometer method described in Dane (2002) to measure percent clay. Percent sand was then measured by thoroughly washing each sample through a 53 μm sieve and drying the retained sand at 105°C. The dried sediments were shaken on the sieve to remove any remaining silt or clay. The sand fraction was then weighed and recorded. Percent silt was calculated by difference from the initial 40.0 g sample of $\leq$2.0 mm material. A split of each sample was analyzed for standard soil chemical parameters, including pH, BpH (buffer pH, a measure of a soil's natural buffering capacity), acidity, base saturation, Ca saturation, Mg saturation, K saturation, estimated Cation Exchange Capacity (CEC), total soluble salts (TSS), organic matter (by loss on ignition), and the following Mehlich 1 extractable nutrients: P, K, Ca, Mg, Zn, Mn, Cu, Fe, and B. Analyses were performed by the Virginia Tech Soil Testing and Plant Analysis Laboratory using the methods described by Mullins (2005).

Time Domain Reflectometry

We used a TRIME T3-50 IPH Tube Access Probe TDR unit (manufactured by IMKO of Germany) connected to a laptop computer in the field to measure and record uncalibrated percent moisture by volume. The TRIME T3-50 IPH probe is specially designed for use in PVC access-tubes which allow vertical moisture profiles to be measured by lowering the instrument inside tubes to the desired depths. We installed a total of 23 access tubes (made of Schedule 40, 2.375-inch (6.03 cm) outer diameter PVC) in two transects across sinkhole #1 and one transect across sinkhole #5. Each access-tube consists of standard threaded and o-ring-sealed-joint PVC well-casing sealed at the bottom with a glued PVC well-point.

TDR measurements for this study were collected at six-inch (15.2 cm) depth intervals in each access tube and then adjusted to represent calibrated field moisture values using calibration equations which were developed using select physical and chemical parameters of the soils (see

(Schwartz et al., *In review*)). The calibration was required because our TDR moisture measurements significantly and consistently underestimated soil moisture. Briefly, we used a multiple linear regression model to calibrate the TDR measurements to gravimetrically measured moisture content. In addition to TDR moisture, the model includes effects of the following physical and chemical parameters which were obtained from the soil sample analyses: percent clay, depth, percent silt, bulk density, cation exchange capacity, and log of percent calcium saturation.

Electrical Resistivity Tomography

ERT data for this study were collected by measuring three 2-D dipole-dipole ERT profiles on May 17, 2006 (1-D access-tube TDR soil moisture profiles were also measured on the same day in all of the access-tubes). The dipole-dipole array was chosen because of its reported sensitivity to the soil- bedrock interface (Zhou et al., 2000). Prior to measurements, three permanent arrays of 25 carbon electrodes each were installed in transects across the study sinkholes using 3m electrode spacing. The transects lie directly over and along the TDR access-tube transects (**Figure 3.1 b, and c**). Electrodes are 12 inches (30.5 cm) in length and are electrically coupled to the surrounding soils using alternating compacted layers of bentonite clay and native soil in a 13 inch (33 cm) augered hole. Electrodes were protected from disturbance by farming activities by installing the electrodes slightly below the ground surface and covering them with a removable PVC cap. A Campus Geopulse DC electrical resistivity meter with a 240m long, 25 take-out cable was used to measure ERT profiles. ERT data were processed using the EarthImager 2D software package from Advanced Geosciences, Inc (Advanced Geosciences, 2005). The software converts measured apparent resistivity values into a modeled distribution of subsurface resistivity values through the use of an iterative resistivity inversion model.

LINKING ERT AND TDR DERIVED SOIL MOISTURE

Archie's Law

Examination of ERT measurements vs. TDR-derived soil moisture (**Figure 3.2**) reveals that there is no clear simple relationship between them. Potential difficulties in finding a relationship include different ERT-moisture relationships for soils with different physical or chemical properties, and issues related to both the scale of ERT vs. TDR measurements and the decreasing resolution of ERT with depth. As examples: percent clay will significantly affect both electrical properties and moisture content of soils; and the scale of TDR-measurement is 15 cm or less

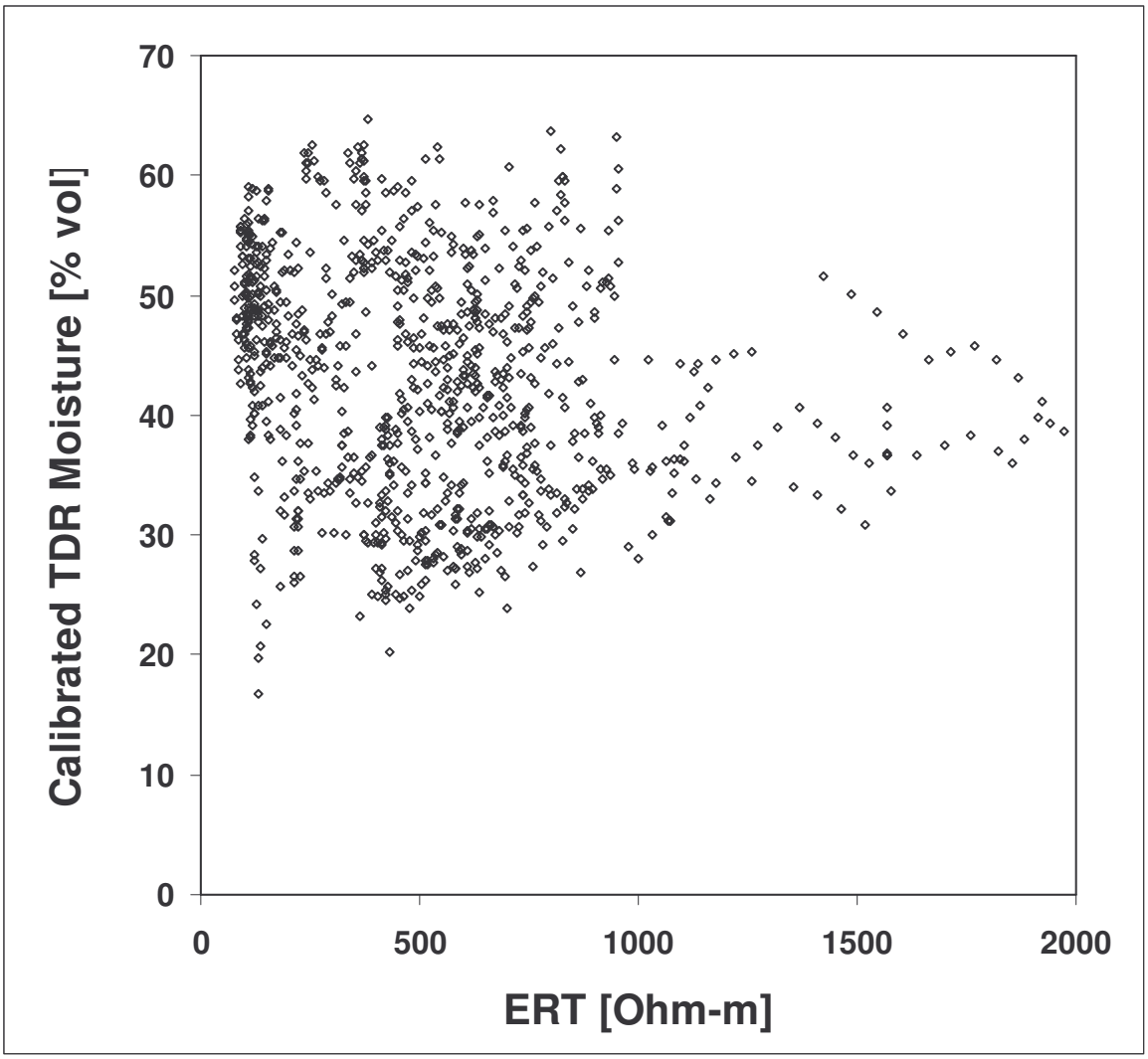

Figure 3.2 Plot of uncalibrated ERT vs. calibrated TDR moisture
Plot illustrating the original relationship between our calibrated TDR soil moisture values and modeled ERT data.

from the probe while ERT is modeling electrical properties at a much larger scale. To investigate a possible relationship between ERT and TDR-derived soil moisture, we utilized a numerically optimized and modified form of Archie's Law to derive soil moisture from ERT measurements. Archie's Law was originally developed and used to link borehole resistivity logs with porosity of surrounding petroleum reservoir rocks (Archie, 2003). Since then, variations of this relationship have been developed which also explain the relationship between electrical properties of a material and certain physical properties, such as porosity of saturated materials or moisture content in unsaturated soils. As an example, a modified form of Archie's Law has been developed by Shah and Singh (2005) to describe the relationship between electrical resistivity and soil moisture:

$$\sigma_b = c \cdot \sigma_w \cdot \theta^m \quad \textbf{(1)}$$

Where σ_b is bulk conductivity, σ_w is pore water conductivity, θ is moisture content, and c and m are fitting parameters that depend primarily on the particle size characteristics of the soil. Shah and Singh (2005) also proposed the following empirical relationships between c and m, and the clay content of a soil.

$$c = 0.6 \cdot Clay^{0.55} \quad \textbf{(2)}$$

$$m = 0.92 \cdot Clay^{0.2} \quad \textbf{(3)}$$

Where clay is expressed as percent by volume and is $\geq$ 5%. For clay contents of less than 5% these parameters become constants: c = 1.45 and m = 1.25. Shah and Singh (2005) relate fitting factors c and m to volumetric soil moisture through: $\sigma_b/\sigma_w = 1/F = c \cdot \theta^m$, where F is a formation factor.

We rearranged terms in **(1)** to solve for θ, which results in:

$$\theta = \left(\sigma_b / c \cdot \sigma_w\right)^{1/m} \quad \textbf{(4)}$$

Further refinement of the modified Archie's Law

To use **(4),** which would allow us to relate ERT values to the 1-D TDR-derived soil moisture measurements [θ_{TDR}] from our field site, we needed to measure or estimate σ_w, σ_b, *c*, *m*, and clay. We obtained estimated values of σ_b from the inverse of our modeled ERT values [σ_b = 1/ ERT] for the locations which correspond to θ_{TDR} measurements. Because our θ_{TDR} data are obtained from 1-D profiles, we extracted 1-D ERT data from 2-D ERT profiles which correspond to the θ_{TDR} measurement locations. Linear interpolation was then used to generate 1-D ERT data at the

same data intervals as our θ_{TDR} measurements, which are at six inch (15.2 cm) depth intervals. Clay contents for these locations were measured (as described above in Chapter 2) in 470 soil samples collected during TDR access-tube installation.

Issues related to comparing moisture measurements at different scales are difficult to address. TDR measurements represent small-volume measurements (not more that 15 cm from the probe), while ERT measurements were made using 3 m electrode spacings with a dipole-dipole array. Because of the difference in scale, the ERT-derived moisture measurements represent a 'smoother' model of the subsurface and do not accurately represent small-scale heterogeneities. Conversely, TDR is very sensitive to small-scale heterogeneities and may, in many cases, be over-emphasizing small-scale heterogeneities which have little effect on bulk soil moisture: particularly those related to small voids of cobbles. Reducing the electrode spacing for ERT arrays would have increased the resolution of the model and its sensitivity to small-scale heterogeneities without significantly changing the bulk characteristics of the model. However, because we installed permanent electrode arrays, modifying the spacing was not practical after the experiments began. In future work we would reduce the electrode spacing to obtain a higher resolution over the depth of physical characterization - perhaps 10 to 12 m rather than 15 to 20 m. While this research does not investigate the physical or theoretical limitations of comparing these two types of measurements at two different scales, it does show that a reasonable model can be obtained by using data which represent two different scales of measurement.

Accurately measuring σ_w is very difficult, even using direct measurement methods such as extraction of pore water or soil-paste electrical conductivity methods (Rhoades et al., 1989). The soil-paste method relates the electrical conductivity of a saturated soil paste to the extracted pore-water conductivity. Because we were unable to extract and measure pore water conductivity directly on our samples, and the soil paste method was deemed too time intensive for use on each sample, we estimated σ_w using the two different methods described below.

Soluble salts as a proxy for σ_w

The first method we used for estimating σ_w involved converting the soluble salts (SS) measurements from the soil analyses into electrical conductivity values. The original lab measurement used to calculate SS values is an electrical conductivity measurement [siemens x 10^{-5}] of a 1:2 (vol/vol) soil-water mixture (Mullins, 2005). SS is then converted into ppm in a

1:1 solution by multiplying EC by 6.4 x 2. The conversion factor from siemens to ppm is 6.4 and 2 is the dilution factor. This method assumes a KCl standard. By reversing this calculation, and then converting siemens x 10^{-5} to units of S/m, we can approximate the pore water conductivity. Obviously, the true pore water conductivity in the field would have differed from this estimate since the original soil moisture content was not a consistent 50 percent by volume in all samples. We also recognize that pore water conductivity values change over time and will not remain identical to what they were at the time our soil sample were collected. However, we believe it is reasonable to assume relatively small changes (especially at greater depths) for most samples.

One limitation we encountered with this proxy is that the SS values for our soils are so low that many of the original conductivity measurements on 1:2 soil-water mixtures were at or below the detection limit of the conductivity meter and were therefore simply reported as being the lowest measurable conductivity value. This means that samples with low pore water conductivity are assigned an SS value that over-predicts conductivity, which influences later calculations of σ_w.

Extractable Cations as a proxy for σ_w

Because the soluble salts proxy was complicated by low detection limits, we used a second proxy for pore water conductivity which assumes there is some relationship between certain extractable cations and equilibrium or near-equilibrium pore water conductivity in a soil sample. Each of the soil samples collected during TDR access-tube installation were subjected to a soil chemical analysis, which includes measurement of Mehlich 1 extractable cations (P, K, Ca, Mg, Zn, Mn, Cu, Fe, B) (Mullins, 2005). Extractable basic cations in our soil samples are dominated by Ca and Mg (~80%) so we chose to use these cations based on the assumption that they will also control pore water conductivity. The sum of Ca and Mg (reported in the soil analyses as ppm in soil, or mg/kg) was divided by 640 to convert from ppm to conductivity in the extracted solution, and then by 10 to reduce the number to an order of magnitude that would be more representative of actual pore-water conductivity values. If a relationship does exist between extractable cations and σ_w, this value can reasonably be assumed to be a proxy for σ_w.

Further justification for the use of extractable cations was found in the relationship between cations, depth, and clay mineralogy (which strongly influences cation exchange capacity (CEC) of clay-rich soils) at our field site. In additional to the textural heterogeneity at our field site, soils are also heterogeneous in terms of mineralogy for all sediment size fractions. For clay

minerals in particular, Harris et al (1980) reported that a site in the upper terrace (assumed to be equivalent to sinkhole #1) contained clays which were dominated by kaolinite, hydroxy interlayered vermiculite, and vermiculite, with kaolinite and vermiculite increasing with depth and hydroxy interlayered vermiculite decreasing with depth. The depth of investigation in their study was limited to 2.5 m, so it is unclear what trends might exist below this depth, but one indication that the kaolinite and vermiculite content may remain constant at depths greater than 2.5 m in sinkhole #1 is the fact that extractable Ca and Mg tend to decrease sharply with depth to around 3m before remaining essentially constant with depth below 3m **(Figure 3.3)**. Since hydroxy interlayered vermiculite and vermiculite have a very high CEC compared to kaolinite, we hypothesize that one reason for nearly constant extractable Ca and Mg at depths below 3 m may simply be a nearly constant CEC with depth. A slight decrease in CEC with depth may be only related to slightly decreasing clay content with depth, but with no appreciable changes in the mineralogy-related CEC **(Figure 3.4)**. Without a more detailed investigation of clay mineralogy in our samples, the true relationships between extractable cations, CEC and clay mineralogy at our site is difficult to determine. Significantly higher values of extractable Ca + Mg near the surface are probably related to the application of agricultural lime. Interestingly, the Ca + Mg profile from the access tube installed in the bottom of sinkhole #1 does not show a decreasing trend in Ca + Mg (**Figure 3.3**). An explanation for this could be that rainwater (especially overland flow) is preferentially infiltrating at the bottom of the sinkhole (an observation supported by physical observations during heavy rain events) and has carried these cations downward during infiltration after application of lime at the surface.

Optimizing the parameters for fitting factors c and m

By defining calibrated TDR moisture as the dependent variable, using the derived or measured values of σ_w, σ_b, and percent clay as independent variables, and designating the four coefficients and exponents of c and *m* in **(2)** and (**3)** as unknown parameters, we numerically optimized the equation and solved for the best values of the parameters. Data used for optimization are the extracted 1-D ERT data from locations where both TDR moisture values and soil properties were obtained. The results of the optimization are later used with interpolated values of the independent variables to calculate the 2-D ERT-derived soil moisture profiles. Numerical optimization of **(4)** for the four parameters in **(2)** and (**3)** was performed using a Modified Gauss-Newton iterative numerical model in UCODE 2005, which is a universal inverse modeling program (Poeter et al., 2005). We used UCODE to find the global minima for the model

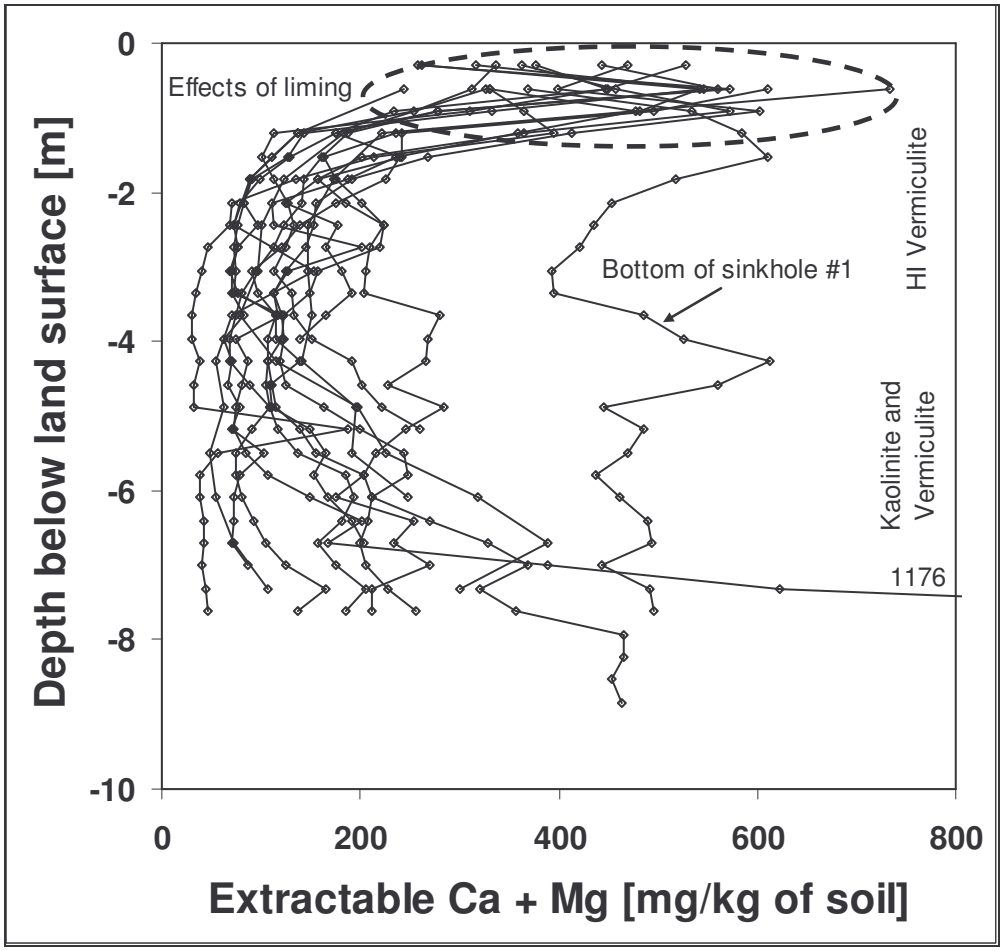

Figure 3.3 Extractable Ca and Mg vs. profile depth
Diagram illustrating the general decrease in extractable Ca and Mg to around 3m in depth for sinkhole #1. Each 1-D profile is from analyses of soil samples collected during access-tube installation in sinkhole #1. 'Bottom of sinkhole #1' indicates the profile from the lowest point in sinkhole #1. One profile had very high extractable Ca and Mg near the bottom and is shown extending off the diagram to a value of 1176 mg/kg. This may indicate the presence of an otherwise undetected carbonate bedrock pinnacle or weathered bedrock instead of fluvial sediments. Based on work by Harris (1980), we have labeled the regions which correspond with depth intervals where hydroxyl interlayered vermiculite, vermiculite and kaolinite likely dominate clay mineralogy. High Ca + Mg near the surface is probably the result of agricultural lime application and not clay mineralogy (area inside dashed oval).

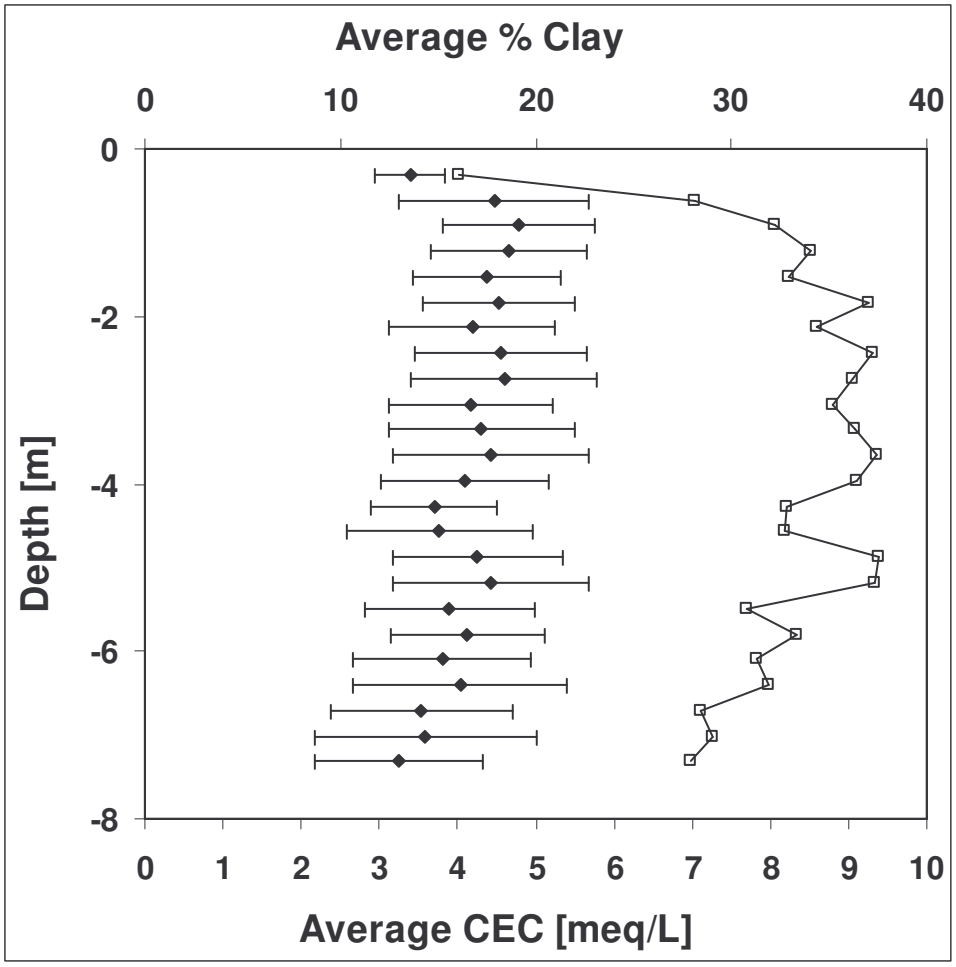

Figure 3.4 Mean CEC and % clay vs. depth
Cation exchange capacity (CEC) averaged by sample depth interval of 0.3048 m (1 ft) in sinkhole #1 (filled diamonds). Note gradual decrease in CEC with depth, is likely related to changes in clay mineralogy, decreasing organic material with depth, and changes in average clay content with depth. Error bars for CEC represent one standard deviation for each averaged depth interval. Average percent clay for the same depth intervals is shown by open squares. Number of samples = 317.

solution. We tested the UCODE's ability to find a global minimum by running the same optimization problems with several different sets of starting values for the four unknown parameters. The model converged on the same solutions regardless of starting values.

Interpolating 1-D data for derivation of 2-D moisture profiles

We used a multi-step process to obtain a final 2-D ERT-derived profile of soil moisture. The first step involves taking the 1-D calibrated TDR moisture, percent clay, and pore-water conductivity data and interpolating between access-tube derived data points using linear kriging with a horizontal to vertical anisotropy ratio of 5:1 and angle settings. By incorporating a horizontal bias in the interpolation process, the results more accurately reflect the sub-horizontal layering in the ancient fluvial sediments which was observed during sampling. Angle settings were used in profile A-A' (**Figure 3.1** and **Figure 3.5)** to more effectively model the consistent dip of soil layers in the profile. Soil layers tend to be sub-horizontal on sinkhole flanks due to draping as the underlying bedrock is removed. After the data are interpolated, 2-D grids of points with 0.5m spacing and identical node locations are produced. The 2-D ERT model is likewise converted to a 0.5m grid of bulk conductivity data using the same node locations, though without including any horizontal bias or angle settings in processing the data. With these identically spaced grids created, we tabulated the data in spreadsheets and used **(4)** to convert bulk conductivity, pore water conductivity, and percent clay into ERT-derived soil moisture values.

RESULTS AND DISCUSSION

Figure 3.5 shows the locations of access tubes with respect to the corresponding ERT profiles for sinkholes #1 and #5. In sinkhole #5 we interpreted a soil-bedrock interface based on information collected during augering and interpretation of ERT data between the access-tubes and monitoring wells. The access tubes shown also represent the locations of 1-D profiles where all soil samples were collected for the physical and chemical characterizations.

Using values we estimated or calculated for σ_w and σ_b, and measured percent clay, we tested the modified form of Archie's Law proposed by Shah and Singh (2005) by calculating soil moisture values using **(4)** with **(2)** and **(3)**, which use their values of model parameters for fitting factors *c* and *m***.** The initial results are shown in **Figure 3.6**. While these results did not show a strong correlation between θ_{TDR} and θ_{calc}, there was clearly a relationship which was not initially present between ERT values *vs.* calibrated TDR soil moisture (**Figure 3.2**)**.** Following numerical

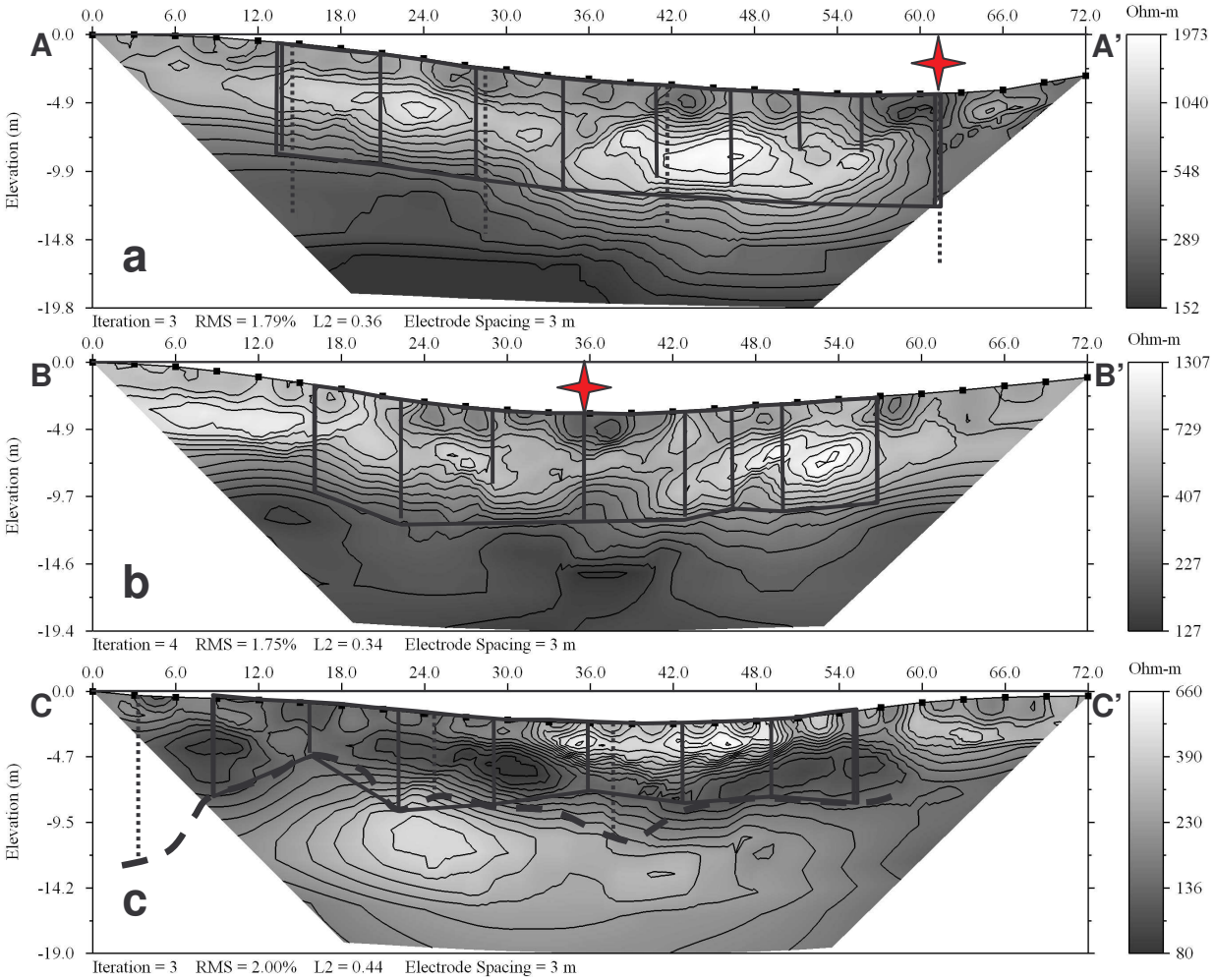

Figure 3.5 ERT profiles

ERT profiles for each transect showing contoured resistivity values, access tubes (solid vertical lines), monitoring wells (dashed vertical lines), bedrock-soil interface (bold dashed line in c)), and outlines of regions where variables were interpolated and kriged to produce profiles. a) and b) show transects across sinkhole #1 while c) is across sinkhole #5. Stars indicate the point where a) and b) intersect. A, A', B, B', C and C' represent transect endpoints as shown in **Figure 3.1**. Also note that the resistivity scales are not the same for each profile

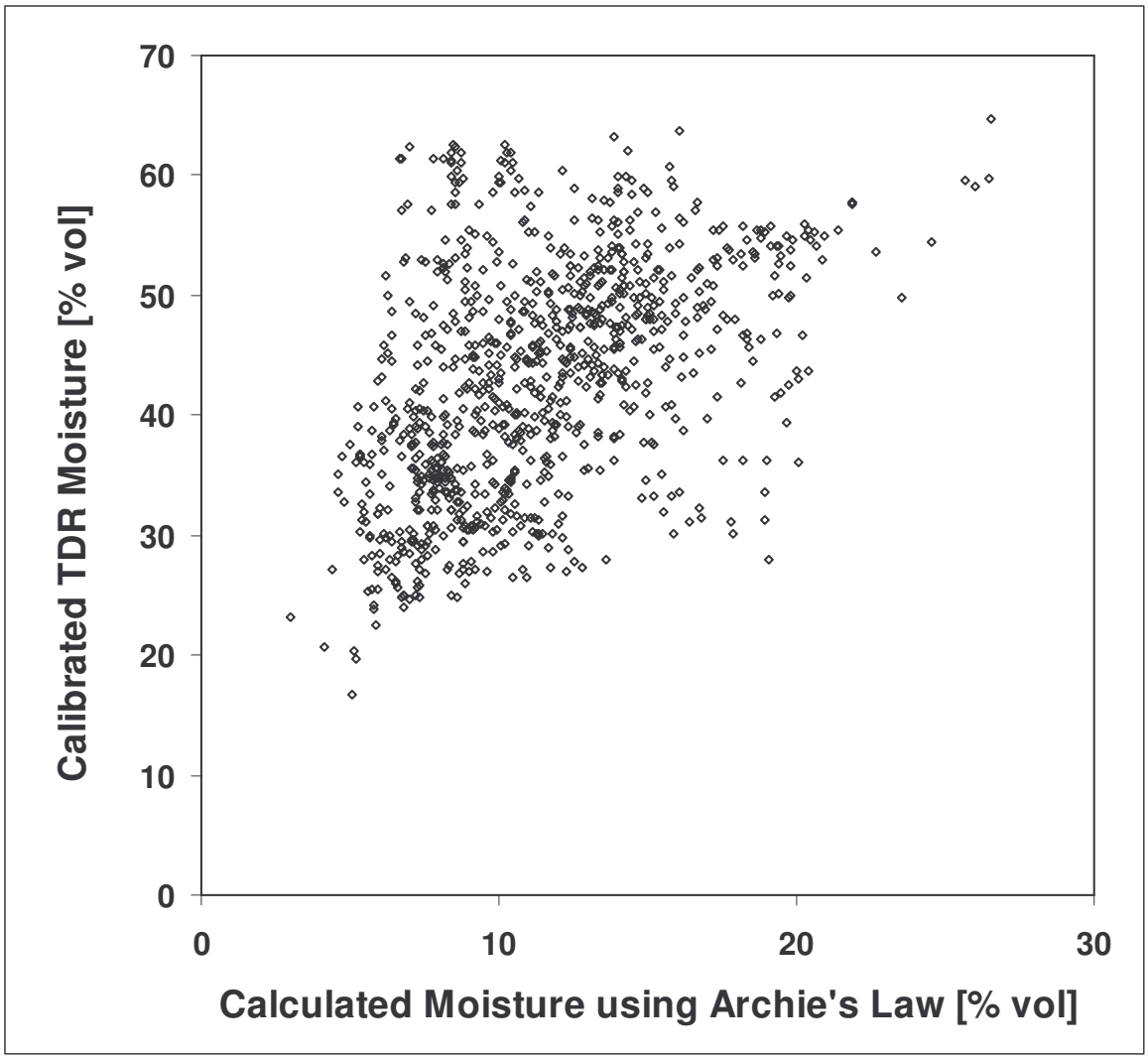

Figure 3.6 ERT moisture vs. TDR moisture
Results of using a modified form of Archie's law as presented by Shah and Singh (2005) using our data with a soluble salts estimate of pore water conductivity.

optimization of the four parameters in **(2)** and **(3)** and using the Ca + Mg proxy for σ_w**,** we derived:

$$c = 0.00873 \cdot Clay^{2.608} \quad \textbf{(5)}$$

$$m = 0.4848 \cdot Clay^{0.8183} \quad \textbf{(6)}$$

Using the numerically optimized fitting factors *c* and *m* in **(4)** gave significantly improved results (**Figure 3.7**) when compared with **Figure 3.6** and **Figure 3.2**. Between the two methods for estimating σ_w, we chose to use the Ca + Mg extractable cation proxy of pore water conductivity in our final calculations rather than the soluble salts estimate because of improved results using the cation proxy (R^2 of 0.57 vs. 0.53). We believe that the soluble salts estimate probably would have produced better results if many of the total soluble salts measurements for our soil samples were not below the instrument resolution in the 1:2 soil-water mixtures.

Shah and Singh (2005) showed that variations in the value of fitting factors *c* and *m* are related to differences in percent clay in the soil. For the fitting factors c and *m,* they reported ranges of 0.33 to 15.85 (for c) and 0.74 to 3.92 (for m). Their calculations were based on measured pore water conductivity data, which we did not have. Using the numerical optimization and our Ca + Mg proxy for σ_w, we derived **(5)** and **(6)** which resulted in fitting factors values ranging from 0.029 to 454.50 (for c) and 0.707 to 14.64 (for m). The values of the four numerically optimized parameters we use for coefficients and exponents of fitting factors *c* and *m* in **(5)** and **(6)** are different than those used by Shah and Singh (2005). We believe these range differences can be explained by the fact that our estimates of pore water conductivity are based on a proxy for σ_w rather than the true values. In the optimization process, adjustments were made to the four parameters (which then changed the fitting factor values) until the best fit between θ_{TDR} and θ_{calc} was achieved. Additionally, the fitting factors are related to the physical and chemical properties of soils and pore waters. If a proxy for the physical property pore water conductivity is used, it follows that the derived fitting factor values may not fall within the same range as those obtained using measured pore water conductivity.

Figure 3.8, Figure 3.9 and **Figure 3.10** show the results of using **(4)** with **(5)** and **(6)** to generate 2-D soil moisture profiles for three sinkhole transects and how the θ_{calc} distribution relates to percent clay, estimated σ_w, and ERT data which were used in calculations to obtain θ_{calc}. **Figure 3.8** and **Figure 3.9** show the modeled and measured distribution of data in sinkhole #1, while

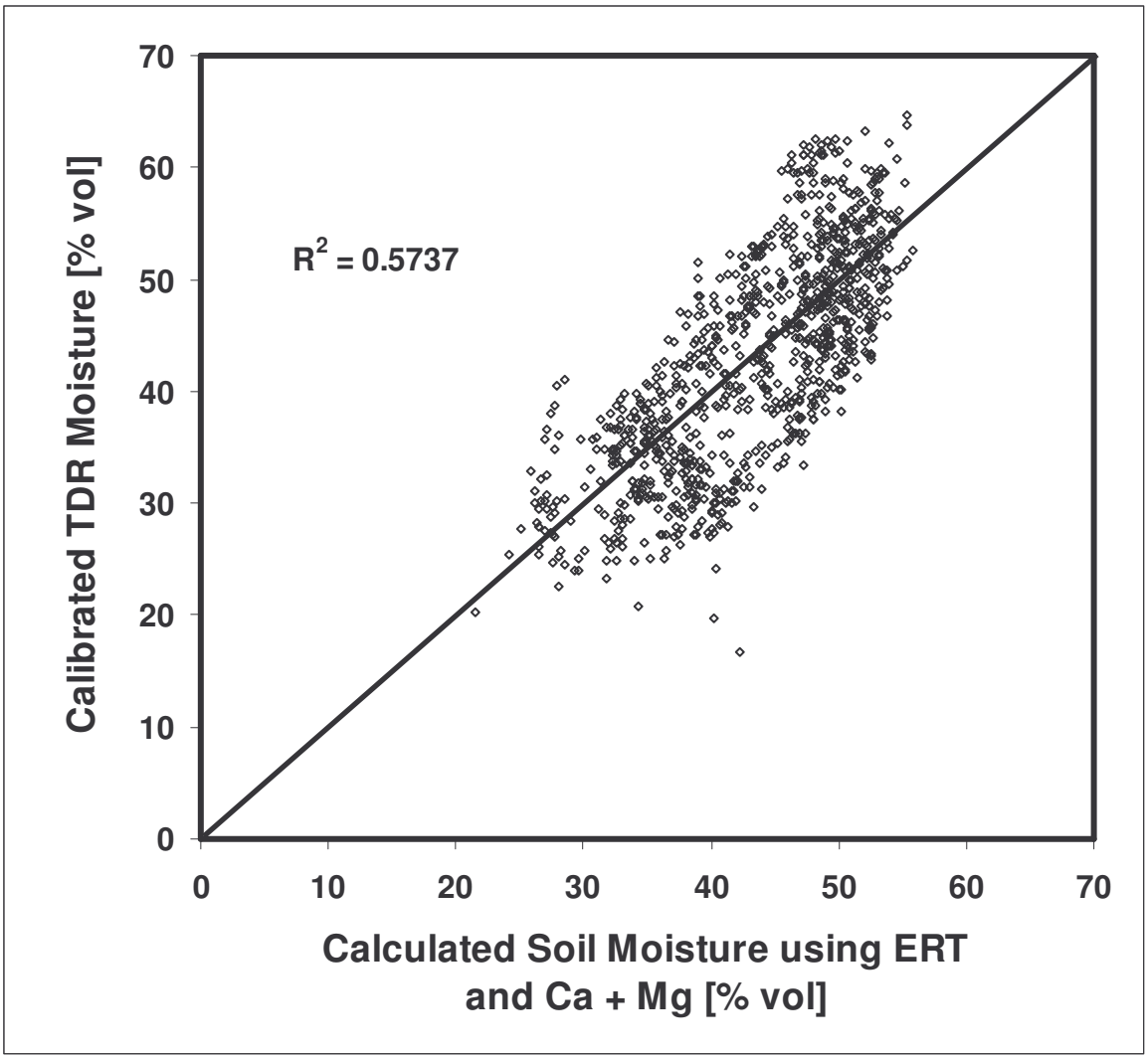

Figure 3.7 Optimized ERT moisture vs. TDR moisture
Plot showing results of using the modified form of Archie's Law to calculate soil moisture from ERT data after numerical optimization**.** These results were obtained using a Mehlich 1 extractable cation proxy (of Ca and Mg) for pore water conductivity.

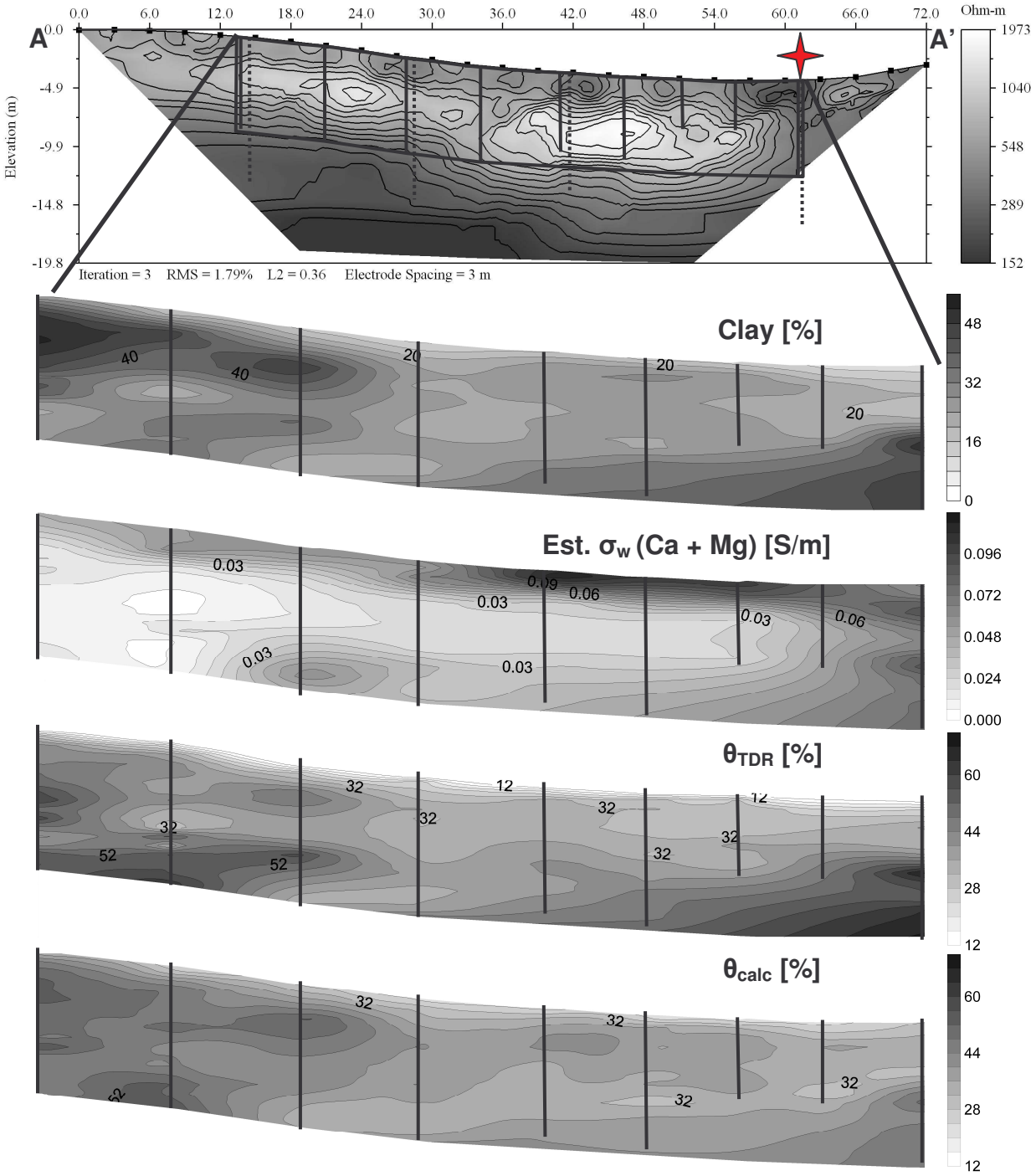

Figure 3.8 Data for sinkhole #1, profile #1
Profiles of variables interpolated between access-tubes where samples were collected from A to A' in sinkhole #1. These variables were used to produce the soil moisture profile labeled θ_{calc}. Note the similarities between this profile and the profile for θ_{TDR}. Also notice how soil moisture and ERT are related to the distribution of % clay and estimated σ_w. Note that units of [S/m] for estimated pore water conductivity are not true conductivity and are instead an estimate based on the Ca and Mg proxy.

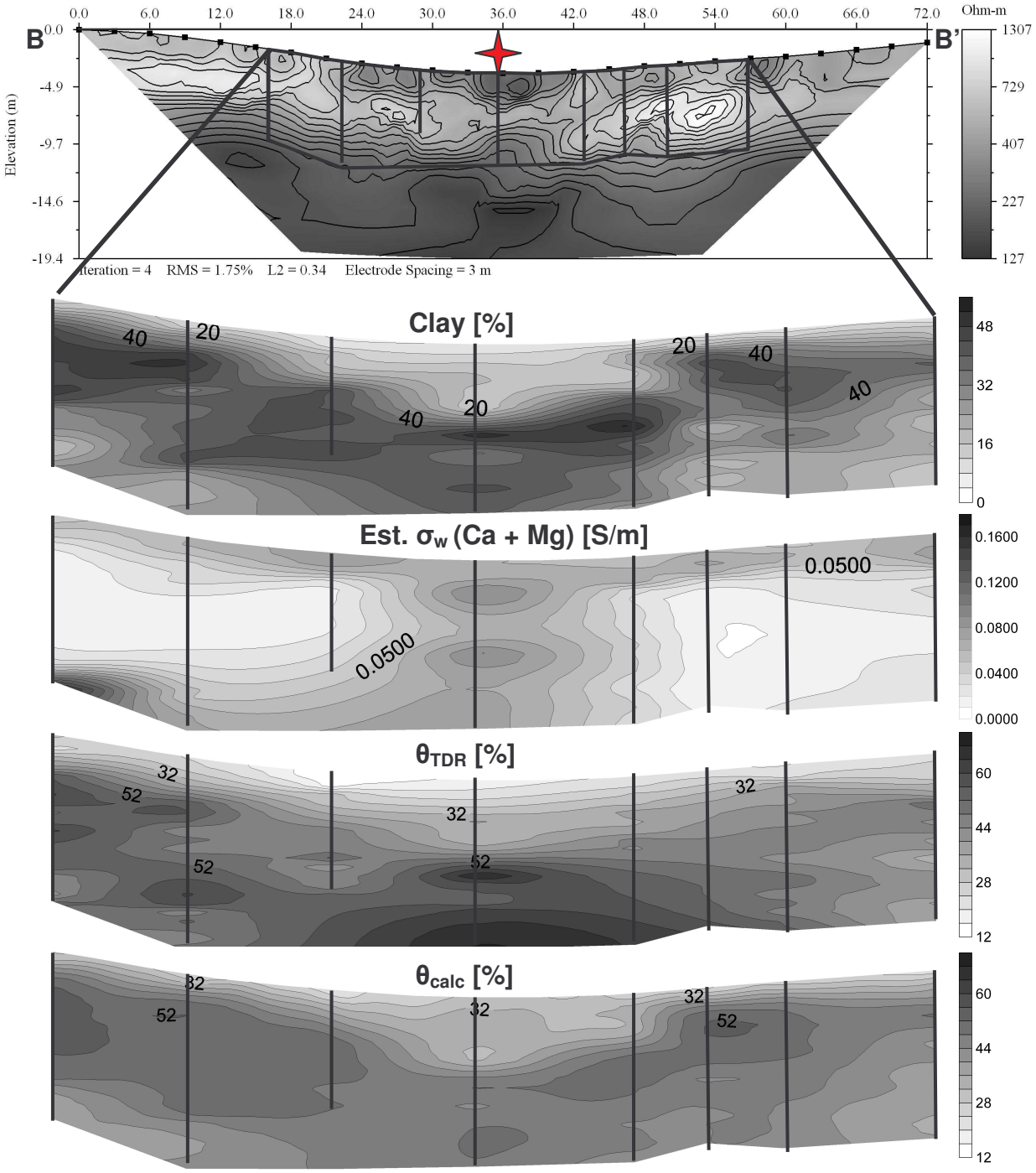

Figure 3.9 Data for sinkhole #1, profile #2

Profiles of variables interpolated between access-tubes where samples were collected from B to B' in sinkhole #1. These variables were used to produce the soil moisture profile labeled θ_{calc}. Note the similarities between this profile and the profile for θ_{TDR}. Also notice how soil moisture and ERT are related to the distribution of % clay and estimated σ_w. Note that units of [S/m] for estimated pore water conductivity are not true conductivity and are instead an estimate based on the Ca and Mg proxy.

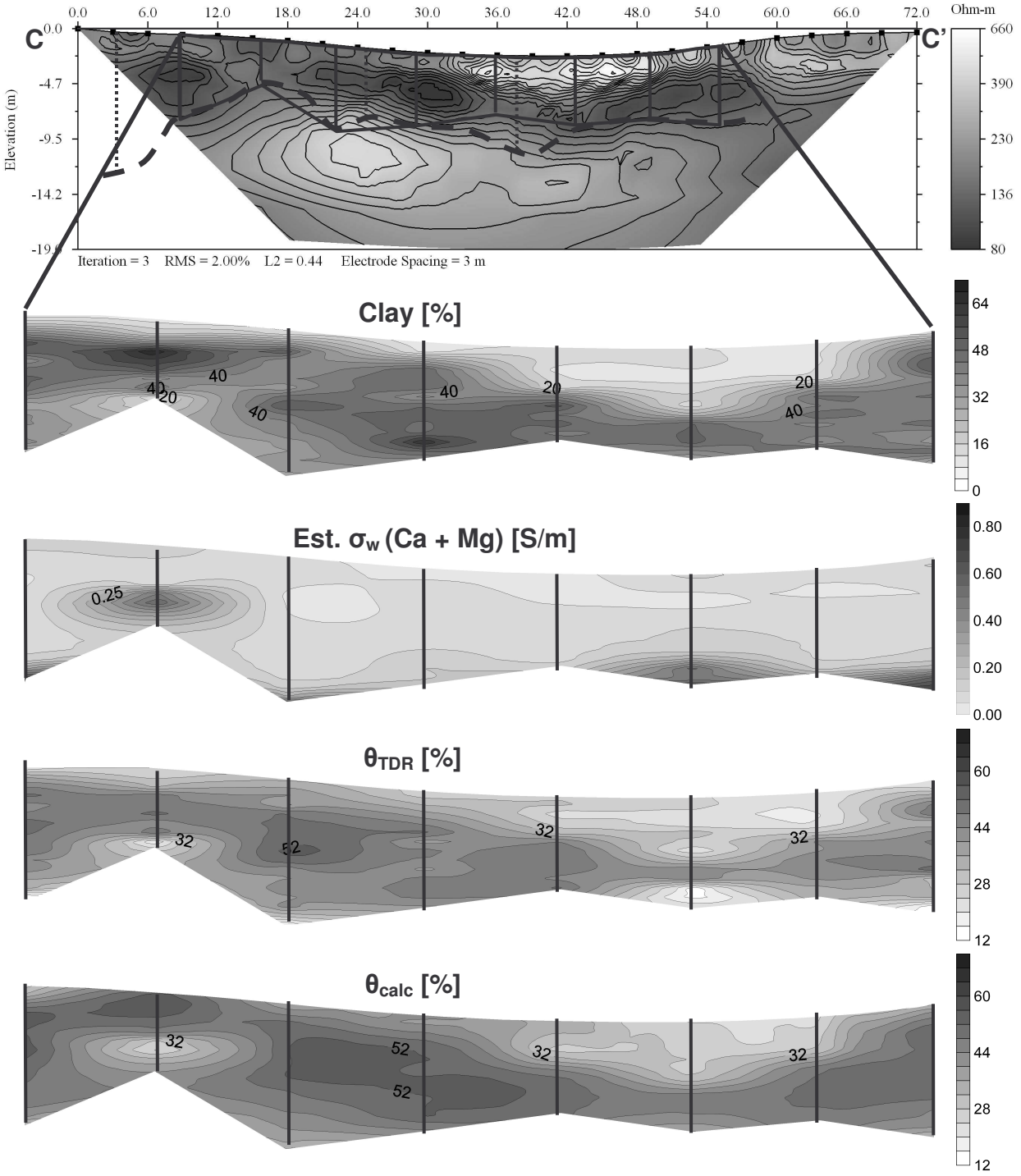

Figure 3.10 Data for sinkhole #5, profile #1
Profiles of variables interpolated between access-tubes where samples were collected from C to C' in sinkhole #5. These variables were used to produce the soil moisture profile labeled θ_{calc}. Note the similarities between this profile and the profile for θ_{TDR}. Also notice how soil moisture and ERT are related to the distribution of % clay and estimated σ_w. Note that units of [S/m] for estimated pore water conductivity are not true conductivity and are instead an estimate based on the Ca and Mg proxy.

Figure 3.10 shows these data for sinkhole #5. **Figure 3.8** is roughly perpendicular to **Figure 3.9** (see **Figure 3.1b**) and they intersect at the locations marked with a star. The general patterns in distribution of the 2-D kriged θ_{TDR} and ERT-derived θ_{calc} are very similar except for the upper 50 cm or so where θ_{calc} tends to overestimate soil moisture based on the θ_{TDR} measurements. In the near-surface, there were two important reasons for this. First, the methods we used to protect the top of our access tubes from agricultural activities resulted in the upper ~50 cm being shielded from infiltration and led to a gradual drying around the tops of the access tubes between the time of installation and the time at which these measurements were taken. The second layer of PVC (the 4 inch (10.1 cm) schedule-40 protective casing) also artificially decreased θ_{TDR}. These factors led to θ_{TDR} values which were skewed towards being drier than they actually were in the unaffected surrounding soils. Secondly, the 3 m spacing of our ERT electrode arrays resulted in lower model sensitivity to electrical properties at or just below the surface in the regions between electrodes. Additionally, the 12 inch (30.5 cm) long ERT electrodes were permanently installed 13 inches (33 cm) deep and this resulted in measurements which were skewed towards representing the damper (and more electrically conductive) soils near the bottom of the electrodes.

Also, θ_{calc} tended to produce smoother contours than are shown in the kriged θ_{TDR} data. This is primarily the result of the insensitivity of ERT models to small-scale heterogeneities (relative to the scale of ERT measurements) in soil moisture and physical properties which were clearly apparent in both θ_{TDR} measurements and in measured physical and chemical properties. **Figure 3.8, Figure 3.9,** and **Figure 3.10** allow visual comparisons between the 2-D distributions of θ_{calc} and θ_{TDR} and highlight this difference. The range of θ_{TDR} was more than twice that of θ_{calc}, which was from approximately 28 to 52 percent moisture. However, the highest and lowest values of θ_{TDR} were usually found in small regions rather that being consistently high or low over large areas. One exception is found in the lowest portions of profiles in sinkhole #1 where a region of high θ_{TDR} is not well represented by θ_{calc} (**Figure 3.9**). It is possible that the access-tube here penetrates a small-scale region of high soil moisture which is not representative of the larger-scale conditions. During augering, we observed significant heterogeneity in soil moisture at the scale of 10 cm or less. As examples, it was common to find ancient root casts or very thin layers of gravel which were acting as tiny conduits carrying water through relatively drier surrounding soils. Some of these small scale features are clearly visible in profiles of percent clay and in θ_{TDR} in **Figure 3.8, Figure 3.9,** and **Figure 3.10.**

By collecting and characterizing a large number of soil samples, we were also able to develop generalized soil profiles for each transect. In addition to characterizing soils by chemical analysis, particle size analysis and soil moisture, we also recorded detailed color information and the location of gravel and cobble-rich layers, which were not represented in the particle size analyses. In combination, these data produced an extremely complex and heterogeneous map of soils at our field site. By grossly grouping soils based on colors (which provide information about weathering history, age, and parent materials (White, 1977)) and textures, we created **Figure 3.11**. Of note is the fact that our ERT profiles (**Figure 3.5**) generally displayed patterns which could be correlated with several of the gross soil layers shown in **Figure 3.11**. As examples, the higher resistivity region near the surface in the bottom of sinkhole #5 corresponds well with an observed lens of what is essentially topsoil which eroded off the flanks and was deposited in the bottom of the sinkhole. ERT profiles in sinkhole #1 show several regions of higher resistivity values which correlate well with observed layers of very hard, dark red and high clay content soils. There are also areas where patterns in the ERT profiles appear to correlate with patterns in the distribution of percent clay, soil moisture or σ_w, though the patterns are not consistent across the entire profile. These results supported what the ERT vs. θ_{TDR} data indicated, which was that there is no simple relationship between these two parameters without first applying a model which includes the effects of certain physical and chemical parameters.

During the planning stages of this research, we assumed that the soil bedrock interface at the study site would be between 2 and 5m below the surface. This was based on verbal communications with people who had drilled to the bedrock-soil interface in nearby locations. We were surprised by the depth of soils in and around the study sinkholes - especially in sinkhole #1. One reason we initially chose ERT to image the subsurface was the fact that others have successfully imaged the soil-bedrock interface using ERT (Zhou et al., 2000). In our case, ERT did not clearly detect the interface in sinkhole #5 (**Figure 3.5** and **Figure 3.11)**. In fact, without ground-truthing by augering, we would not have determined that the bedrock-soil interface was within the depth of resolution for our ERT measurements. Many of the resistivity contrasts which were initially identified as possible soil-bedrock interfaces (in ERT profiles obtained prior to augering) were actually contrasts in soil texture, soil moisture and other physical properties. We believe there are two important reasons why we did not detect the soil-bedrock interface with ERT in sinkhole #5: 1) the Elbrook Formation is locally highly fractured

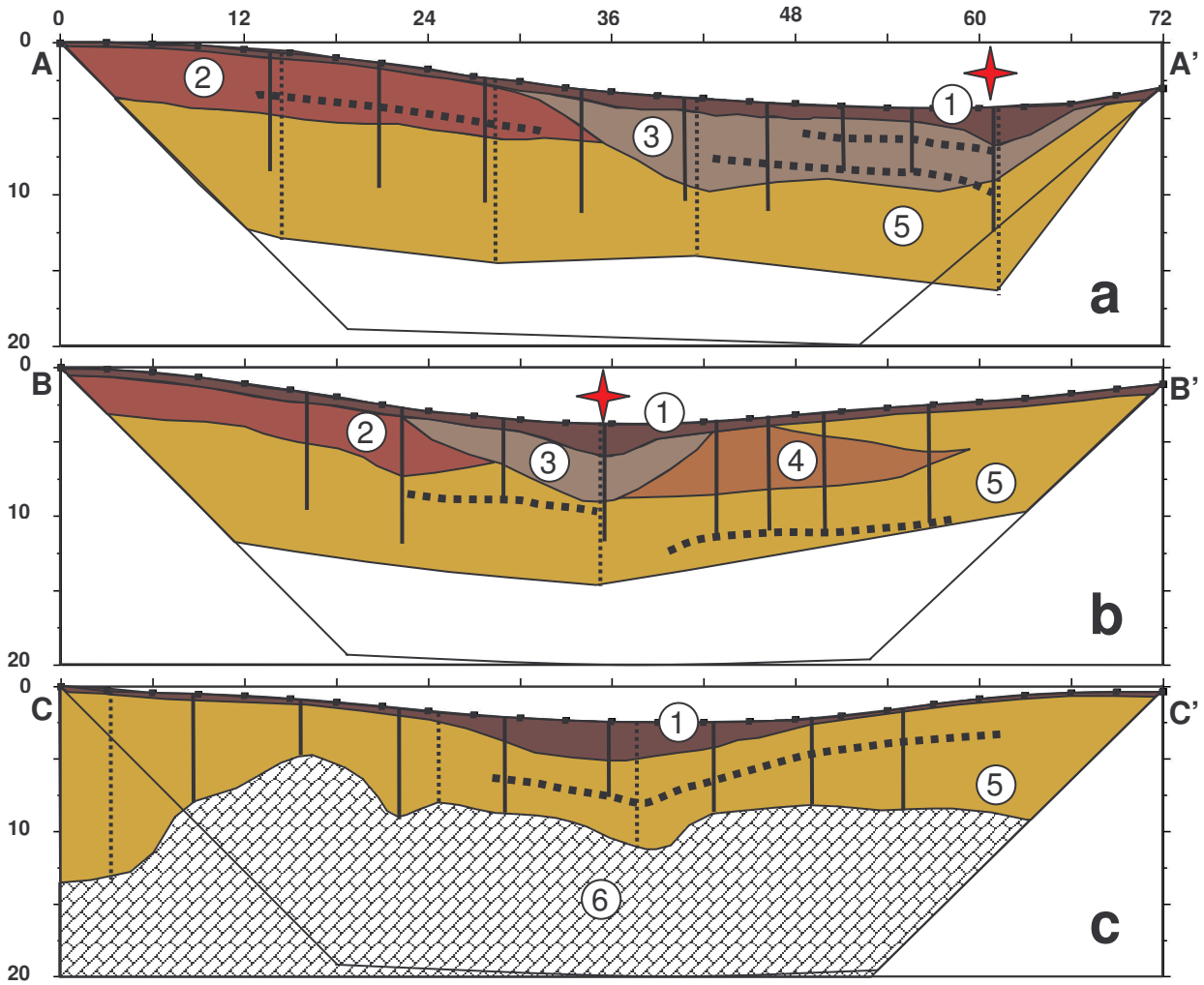

Figure 3.11 Generalized profiles of gross soil texture and color
Interpretations of gross soil texture, color, and horizonation for each transect in sinkhole #1 (a and b) and sinkhole #5 (c). Circled numbered zones: 1) represents dark yellow brown loam, clay loam, sandy loam, and silt loam (A horizons), 2) is hard and generally drier dark red clay loam, silty clay loam and silty clay (Bt horizons), 3) is light grey to yellow grey sandy clay loam, sandy loam and loam (Btg and Bg horizons), 4) is a reddish orange clay loam, silty clay loam and silty clay (Bt horizons), 5) is a brownish yellow to yellow silty clay, silty clay loam and clay loam (Bt and C horizons), and 6) is carbonate bedrock. Bold dashed lines represent interpreted cobble and gravel layers. The star in a) and b) indicates the location at which transects a) and b) intersect. Profile endpoints A, A', B, B', C and C' represent end points on transects shown in **Figure 3.1**. We emphasize that these interpretations are only based on gross soil characteristics and do not represent the true heterogeneity of the system in terms of textures, cobble and gravel content, or color. Soils in these profiles fall into all USDA soil texture classes except for sand, and are widely distributed across the USDA textural triangle with no clear patterns. Solid vertical lines represent access-tubes and dashed lines represent monitoring wells. Interpretations extend beyond the outline of our ERT profiles where we have information from monitoring wells. All units are in [m].

and weathered because of our field site's proximity to the edge of the Pulaski thrust sheet (Commonwealth of Virginia, 2003), and 2) the uppermost region of weathered bedrock has both high clay and moisture content. It is also worth pointing out that the highest resistivity values in sinkhole #5 are less than 700 Ohm-m and were actually measured in the well-drained silty soils in the bottom of this sinkhole rather than in the underlying bedrock. These are all important factors to consider when using ERT in similar geologic settings and reinforce the fact that ERT is best used in conjunction with physical data to validate interpretations.

To obtain the most accurate soil moisture models, it is important that accurate ERT measurements be collected. Obtaining ERT profiles with minimized measurement error can be difficult and may require methods for data collection in the field which are more exacting than are required for an ERT profile designed to grossly characterize features in the subsurface. Perhaps the most important factor in the field is ensuring good electrical contact between ERT electrodes and the soils. Our method of installing permanent carbon electrodes minimized measurement error and produced higher quality data than we were able to obtain using traditional metal electrodes inserted at the surface. Though it is certainly more time consuming than using metal electrodes at the surface, we recommend this method if long term studies of soil moisture are planned.

CONCLUSIONS

We have developed a new method for determining field-scale 2-D soil moisture distribution using 2-D electrical resistivity tomography (ERT) measurements with 1-D soil moisture and physico-chemical properties of the soil. Our methods are easy to apply to nearly any field site where a quantitative assessment of 2-D soil moisture distribution is desired. We have shown that these methods will produce useful results in heterogeneous settings and that meter-scale soil moisture variations can easily be detected and modeled. Our model results do not resolve small scale heterogeneities in soil moisture measured with TDR, but instead represent a smoother model which reflects the inability of ERT measurements to measure small-volume features at this scale. For example, small regions of high or low moisture as measured in a 1-D TDR moisture profile, and which span at most 30 cm, are unlikely to be resolved using an ERT array with 3m electrode spacing. Our field site contains extremely heterogeneous soil profiles because the soils are derived from weathered ancient fluvial terrace deposits. In more homogeneous

systems, lower resolution sampling of physical/chemical measurements may be required to achieve the same level of accuracy in moisture prediction.

A specific setting where our methods might be particularly useful in determining soil moisture distribution is in thick soils - especially in clay-rich soils where tools such as GPR can not be used to image subsurface features because of signal attenuation problems. Another very important application of these techniques would be to quantitatively assess volumetric moisture changes over time by collecting time-series data. Results of this type of study can be used to address important hydrogeologic questions such as how much, where, and when do infiltration and recharge occur in different unsaturated hydrogeologic settings? With the current capabilities of ERT equipment and inversion software to both collect and model 3-D ERT data, these same methods can also be applied to understanding 3-D soil moisture distribution both spatially and temporally.

Showing that extractable cations can be used as a proxy for pore water conductivity in a numerically optimized form of Archie's Law was an especially important result of this research, particularly for soils with very low soluble salts. By using extractable cations, we eliminated the difficult and time consuming task of measuring pore water conductivity and instead used data which are easy to obtain by a standard soil analysis. Depending on the soil characteristics at other sites, different extractable cations may need to be used to obtain the best results.

ACKNOWLEDGEMENTS

We acknowledge funding for this research from: US Department of Education GAANN Fellowship, Virginia Water Resources Research Center, Cave Conservancy Foundation, Cave Research Foundation, National Speleological Society, Geological Society of America, West Virginia Association for Cave Studies, and the Virginia Tech Graduate Research Development Program. We thank Ankan Basu, Mike Beck, Lee Daniels, Beth Diesel, Bruce Dunlavy, Frank Evans, Brad Foltz, Marty Griffith, Mary Harvey, Ashley Hogan, Danielle Huminicki, Stuart Hyde, Rachel Lauer, Steve Nagle, Jeanette Montrey, Wil Orndorff, Zenah Orndorff, Dave Rugh, Cori and Zachary Schwartz, Jim Spotila, Brett Viar, Dongbo Wang, and Brad White for their assistance both in the field and in the lab.

REFERENCES

Advanced Geosciences, I. 2005. EarthImager 2D.

Archie, G.E. 2003. Electrical resistivity log as an aid in determining some reservoir characteristics. Society of Petroleum Engineers reprint series: 9-17.

Auerswald, K., S. Simon, and H. Stanjek. 2001. Influence of soil properties on electrical conductivity under humid regimes. Soil Science 166:382-390.

Barker, R., and J. Moore. 1998. The application of time-lapse electrical tomography in groundwater studies. The Leading Edge October:1454-1458.

Commonwealth of Virginia. 2003. Digital Representation of the 1993 Geologic Map of Virginia, Publication 174. Department of Mines, Minerals and Energy, Division of Mineral Resources.

Daily, W., and A. Ramirez. 2000. 200 East Vadose Test Site, Hanford Washington, Electrical Resistivity Tomography. Lawrence Livermore National Laboratory, Livermore, CA.

Dane, J.H., Topp, G.C., (ed.) 2002. Methods of soil analysis. Part 4: physical methods, pp. 1-1692. Soil Science Society of America, Madison, Wisconsin.

Harris, W.G., S.S. Iyengar, L.W. Zelazny, J.C. Parker, D.A. Lietzke, and W.J. Edmonds. 1980. Mineralogy of a chronosequence formed in New River alluvium. Soil Science Society of America Journal 44:862-868.

Hauck, C., and A. Scheuermann. 2005. Comparing Time Domain Reflectometry and Electrical Resistivity Tomography Measurements for Estimating Soil Water Distribution. 11th European Meeting of Environmental and Engineering Geophysics (Near Surface 2005).

Jacobsen, O.H., and P. Schjonning. 1993. A laboratory calibration of time domain reflectometry for soil water measurement including effects of bulk density and texture. Journal of Hydrology:147-157.

Kalinski, R.J., and W.E. Kelly. 1993. Estimating water content of soils from electrical resistivity. Geotechnical Testing Journal 16:323-329.

Kalinski, R.J., W.E. Kelly, I. Bogardi, and G. Pesti. 1993. Electrical resistivity measurements to estimate travel times through unsaturated ground water protective layers. Journal of Applied Geophysics 30:161-173.

Lambot, S., J. Rhebergen, I.v.d. Bosch, E.C. Slob, and M. Vanclooster. 2004. Measuring the soil water content profile of a sandy soil with an off-ground monostatic ground penetrating radar. Vadose Zone Journal 3:1063-1071.

Maulem, Y., and S.P. Friedman. 1991. Theoretical prediction of electrical conductivity in saturated and unsaturated soil. Water Resources Research 27:2771-2777.

Michot, D., Y. Benderitter, A. Dorigney, B. Nicoullaud, D. King, and A. Tabbagh. 2003. Spatial and temporal monitoring of soil water content with an irrigated corn crop cover using surface electrical resistivity tomography. Water Resources Research 39:1138.

Mullins, G.L., Heckendorn, S. E. 2005. Draft Copy of Laboratory Procedures - Publication 452-881. Virginia Tech Soil Testing Laboratory, Blacksburg.

Poeter, E.P., M.C. Hill, E.R. Banta, S. Mehl, and S. Christensen. 2005. UCODE_2005 and Six Other Computer Codes for Universal Sensitivity, Calibration, and Uncertainty Evaluation: U. S. Geological Survey Techniques and Methods 6-A11.

Rhoades, J.D., N.A. Manteghi, P.J. Shouse, and W.J. Alves. 1989. Estimating soil salinity from saturated soil-paste electrical conductivity. Soil Science Society of America Journal 53:428-433.

Schwartz, B.F., M.E. Schreber, P.S. Pooler, and J.D. Rimstidt. *In review*. New methods for obtaining accurate access-tube TDR moisture values: a tool for understanding vadose

hydrology in deep and heterogeneous soil profiles. *In review at:* Soil Science Society of America Journal.

Shah, P.H., and D.N. Singh. 2005. Generalized Archie's Law for Estimation of Soil Electrical Conductivity. Journal of ASTM International 2:1-20.

Shuyun, L., and T.-C.J. Yeh. 2004. An integrative approach for monitoring water movement in the vadose zone. Vadose Zone Journal 3:681-692.

Titov, K., A. Kemna, A. Tarasov, and H. Vereeken. 2004. Induced polarization of unsaturated sands determined through time domain measurements. Vadose Zone Journal 3:1160-1168.

USDA-NRCS. 2006. Web Soil Survey [Online] http://websoilsurvey.nrcs.usda.gov/app/WebSoilSurvey.aspx (verified September 4, 2006).

White, W.B. 1977. Characterization of karst soils by near infrared spectroscopy. The National Speleological Society Bulletin 39:27-31.

Yao, T., P.J. Wierenga, A.R. Graham, and S.P. Neuman. 2004. Neutron Probe calibration in a vertically stratified vadose zone. Vadose Zone Journal 3:1400-1406.

Zhou, Q.Y., J. Shimada, and A. Sato. 2001. Three-dimensional spatial and temporal monitoring of soil water content using electrical resistivity tomography. Water Resources Research 37:273-285.

Zhou, W., B.F. Beck, and J.B. Stephenson. 2000. Reliability of dipole-dipole electrical resistivity tomography for defining depth to bedrock in covered karst terranes. Environmental Geology 39:760-766.

CHAPTER 4

Quantifying potential recharge through thick soils in mantled sinkholes using ERT data

ABSTRACT

We quantified potential recharge through thick soils in mantled sinkholes using differential electrical resistivity tomography (DERT). Conversion of time-series 2-D ERT profiles into 2-D modeled soil moisture profiles using a numerically optimized form of Archie's Law allowed us to monitor soil moisture differences over time. These results were combined with Penman-Monteith daily potential evapotranspiration (PET) and daily precipitation data to quantify potential recharge through thick soil profiles. Potential recharge calculated from three sets of time-series ERT data indicated that precipitation contributing to potential recharge only occurred during brief periods when precipitation exceeded PET. Over the study duration, potential recharge amounts calculated from changes in soil moisture ranged from 19% to 31% of cumulative precipitation. Spatial distribution of infiltration showed that a significant amount occurred on sinkhole flanks, though overland flow also caused higher amounts of infiltration in sinkhole bottoms. Results also indicated that soil filled sinkholes can both transmit water rapidly to an underlying aquifer and store and slowly release water as a result of slower infiltration.

INTRODUCTION

Recharge and infiltration are important hydrologic processes which are difficult to understand and quantify at the field scale. The process of water movement from the surface into the subsurface is defined as infiltration, while recharge is defined as water which is added to an aquifer (Scanlon et al., 2002). Recharge can be further separated into actual recharge and potential recharge. Potential recharge usually refers to water which has infiltrated to a depth at which it may be assumed to recharge an aquifer at some time in the future (Scanlon et al., 2002). Exceptions to this assumption are in arid regions or in areas with extremely deep unsaturated zones. Understanding where, when, and how much water recharges an aquifer is critical information for understanding groundwater quality and quantity (de Vries and Simmers, 2002). An important reason for obtaining a better understanding of infiltration and recharge is that the

ability to model transport of dissolved contaminants through the unsaturated zone requires information about where, when, and how infiltration and recharge are occurring.

Recharge occurs at variable rates via different mechanisms depending on geologic, climatic, biologic, and geomorphic settings. In many settings, recharge is a relatively slow process resulting from diffuse infiltration of precipitation through soils and underlying bedrock. One notable exception is in many karst settings where a significant portion of the recharge entering an aquifer can occur as direct recharge via sinking streams flowing through conduits which are open to the surface. While this process (sometimes referred to as rapid or point-source recharge) can quickly add large amounts of water to a karst aquifer, an extension of the same conduit system which rapidly introduced water to the aquifer may also rapidly remove it. Rapid recharge is often cited as one reason why karst aquifers are extremely sensitive to contamination, and sinkholes, in particular, are targets of concern as a potential source of significant contamination (Lee and Krothe, 2001; Stephenson et al., 1999). Sinkholes are usually considered part of the epikarst, which is the uppermost portion of a karst system and contains both unsaturated and saturated conditions and may contain a significant amount of the storage capacity in a karst system (Doctor et al., 2006; Klimchouk, 2004; Lee and Krothe, 2001; Perrin et al., 2003). The epikarst also has the ability to transmit water relatively rapidly if infiltrating water bypasses matrix flow through soils by flowing through preferential flowpaths (Maloszewski et al., 2002; Perrin et al., 2003).

In karst settings, sinkholes are often modeled conceptually as sources of rapid recharge (White, 2003; White et al., 1995). However, characterizing soil filled sinkholes as sources of rapid recharge may not be entirely accurate, and soil filled sinkholes could actually be considered an end member in a sinkholes classification scheme. This scheme can very generally be considered to range from sinkholes with no soil and an open conduit, to sinkholes containing thick clay-rich soils and no openings. Thick clay- and silt-rich soils, in particular, have the capacity to store and slowly release large amounts of water, in addition to allowing water to pass relatively rapidly through the unsaturated zone via macro-pores such as old root casts, burrows, and soil fractures (Iqbal and Krothe, 1995; McKay et al., 1993). Adding to the complication of the sinkhole system is the fact that overland flow after heavy rainfall events is funneled to the bottom of the

sinkhole where it is forced to infiltrate, overflow, evaporate, or transpire. Even small sinkholes may capture runoff from larger areas. In sinkholes with relatively unobstructed connections to conduits, recharge is rapid. However, in soil filled sinkholes without open connections to underlying conduits, runoff ponds may form temporarily and much of this water can infiltrate relatively slowly through the soils. A significant portion of this water will recharge the aquifer as somewhat delayed and temporally distributed recharge by way of temporary storage and later slow release by the soils. In this way, thick soils in the unsaturated zone over a karst aquifer can be a significant source of slowly released water which sustains base-flow in a karst hydrologic system. The diversity of infiltration processes in soil filled sinkholes ultimately means that they have the potential to provide recharge to an aquifer at slow, intermediate and rapid rates, and cannot simply be modeled as a source of rapid recharge.

Many methods have been developed for estimating or measuring recharge at different spatial scales (Scanlon et al., 2002). For large scales, recharge can be modeled using mass-balance models which may incorporate measurements of soil water, stream and spring hydrographs, well levels, precipitation, stable isotopes, and potential evapotranspiration (Das Gupta and Paudyal, 1988; Doctor et al., 2006; Sophocleous, 1991). Geographic information systems are also useful tools for regional recharge modeling, especially for use with readily available data such as soil types, topography, land cover and climatic parameters (Dripps and Bradbury, 2007). At smaller scales, tools such as lysimeters provide good estimates of recharge, though they are subject to large spatial variations in estimated recharge due to localized heterogeneities in soils and vegetation (Chapman and Malone, 2002).

Unfortunately, quantifying amounts and rates of infiltration and recharge at intermediate scales (10s to 100s of m) is extremely difficult using traditional methods. Geophysical methods are excellent tools to use at these scales because of their scalability and mobility. Electrical techniques such as electrical resistivity tomography (ERT) are particularly well suited for work in the unsaturated zone because of their ability to penetrate to useful depths with reasonable resolution in the field and their high sensitivity to changes in electrical properties resulting from changes in soil moisture (Michot et al., 2003; Sheets and Hendrickx, 1995; Sreedeep and Singh, 2005). The primary objectives of this study were to quantify the timing and amount of

infiltration and potential recharge through sinkholes with thick soil mantles. We accomplished these objectives using changes in soil moisture derived from differential ERT over a time period of approximately five months.

FIELD SITE

Our research site at the Virginia Tech Kentland Experimental Farms in Montgomery County, Virginia contains two well-developed sinkhole plains formed in ancient New River terraces **(Figure 4.1a)**. The sinkholes are generally broad and shallow, allowing easy access for agricultural activities, and contain no bedrock outcrops. Thick terrace deposits mantle sinkholes with soils characterized as weathered fluvial terrace materials deposited by the ancient New River, which have developed over the underlying Cambrian aged Elbrook Formation limestone and dolostone bedrocks. Soils are classified by the USDA-NRCS as Guernsey silt loam, Unison and Braddock soils, and Unison and Braddock cobbly soils (USDA-NRCS, 2006). Both sinkhole plains have numerous sinkholes of similar size and shape. Two sinkholes were chosen for more detailed analysis in our study. Sinkhole #1 is in a higher and older terrace deposit and contains highly weathered soils to depths exceeding 12.2 m. Sinkhole #5 is formed in a lower and younger terrace and contains soils which are not as mature. In Sinkhole #5, bedrock was reached in most augered holes at depths between 3.4 and 7.6m below land surface. Instrumentation installed at the field site consists of monitoring wells (which do not reach the saturated zone), time domain reflectometry (TDR) access-tubes used to obtain small-scale soil moisture measurements, and permanent carbon electrode arrays for ERT measurements.

Sinkhole formation at both sites appears to be the result of two mechanisms. First, soil-piping, down-slope movement and slumping are together moving soils from the surface into the subsurface. A second, and perhaps more important, mechanism seems to be dissolution of bedrock and subsequent slumping of sediments into the resulting bedrock depression. Evidence for this can be found in cobble layers and other soil layers which are laterally continuous in sinkhole flanks, but slope towards the sinkhole bottoms and become deeper below the surface with proximity to the sinkhole bottom (**Figure 3.11**).

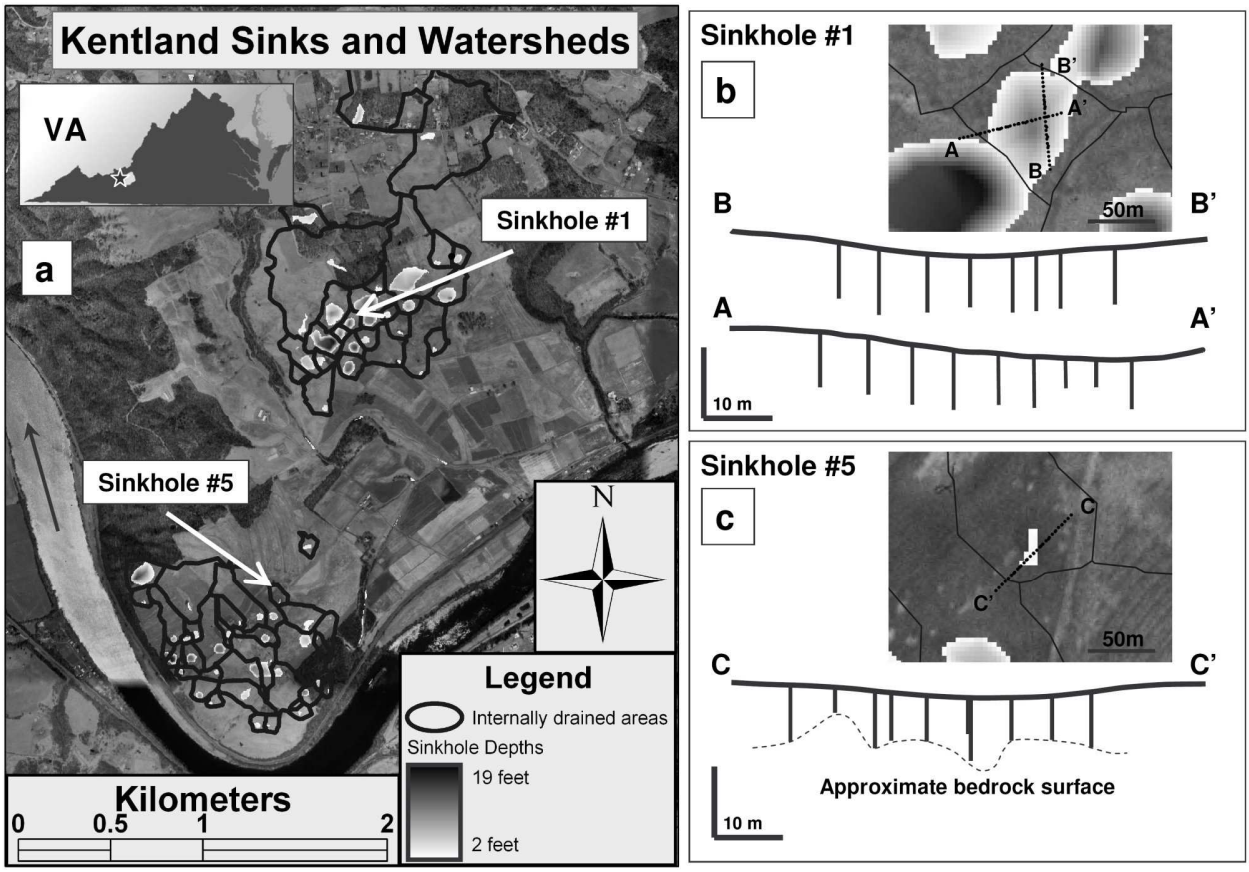

Figure 4.1 Field site and locations of ERT profiles
a) Virginia Tech Kentland Experimental Farms at Whitethorne, Virginia, USA. **Figure 4.1a** shows study sinkholes #1 and #5 and catchment areas (adjacent polygons) for each sinkhole within the two sinkhole plains. Aerial imagery © 2002 Commonwealth of Virginia. Sinkhole #1 is in the higher, older terrace. b) and c) show the location and orientation of instrumentation installed in transects across both sinkholes. Upper image in the diagrams is a map view of the sinkhole, while the lower portion of the diagrams shows profile views of monitoring wells, TDR access-tubes and other instrumentation installed along each transect. Note that depth of bedrock was not determined in Sinkhole #1.

Vegetation at the site is dominated by grasses. In the upper sinkhole #1, fields are used for hay and grazing. During the study period grass was either mowed or grazed. In the lower sinkhole #5, the site was covered by grasses and weeds which were kept mowed to < 50 cm in height.

METHODS

Our approach to quantifying potential recharge in soil-filled sinkholes involved measuring temporal variations in soil moisture derived from differential ERT measurements. In soils, potential recharge occurs when the rate of precipitation exceeds the rate of potential evapotranspiration (PET) and water moves below the root depth. By assuming a 1.5m root depth for grasses, and further assuming that soil moisture which infiltrated to depths below 1.5m had moved below the depth of influence by PET, we defined potential recharge as changes in soil moisture in the soil profiles below -1.5m (**Figure 4.2**). We compared cumulative changes in three ERT-derived soil moisture profiles with rates of cumulative precipitation and PET for the same study period to identify periods when either PET or infiltration was the dominant process. We compared the amounts of water added to the entire profile thickness vs. the portion lying below -1.5m by investigating the relationships between PET, precipitation and the amount of water added or lost within the upper 1.5m of the profiles.

ERT and soil moisture

Dipole-dipole ERT data were collected 11 times between May 17, 2006 and October 9, 2006 for each of the three different transects across the two study sinkholes **(Figure 4.1):** two in sinkhole #1 and one in sinkhole #5**.** Data were collected using permanently installed arrays of 25 carbon ERT electrodes per transect (Schwartz and Schreiber, In review) , 72m in length. We used permanent carbon electrodes to ensure very high quality ERT data and to minimize errors which would have resulted from slight variations in soil-electrode electrical contact and location if we had installed and removed electrodes each time measurements were made. Volumetric soil moisture was calculated for a portion of each of these profiles (**Figure 4.3**) by converting dipole-dipole ERT data into soil moisture using a modified and numerically optimized form of Archie's Law (Schwartz et al., *In review;* Shah and Singh, 2005) which includes the important effects of clay content on bulk soil conductivity, and a Mehlich 1 extractable Ca + Mg proxy for pore-

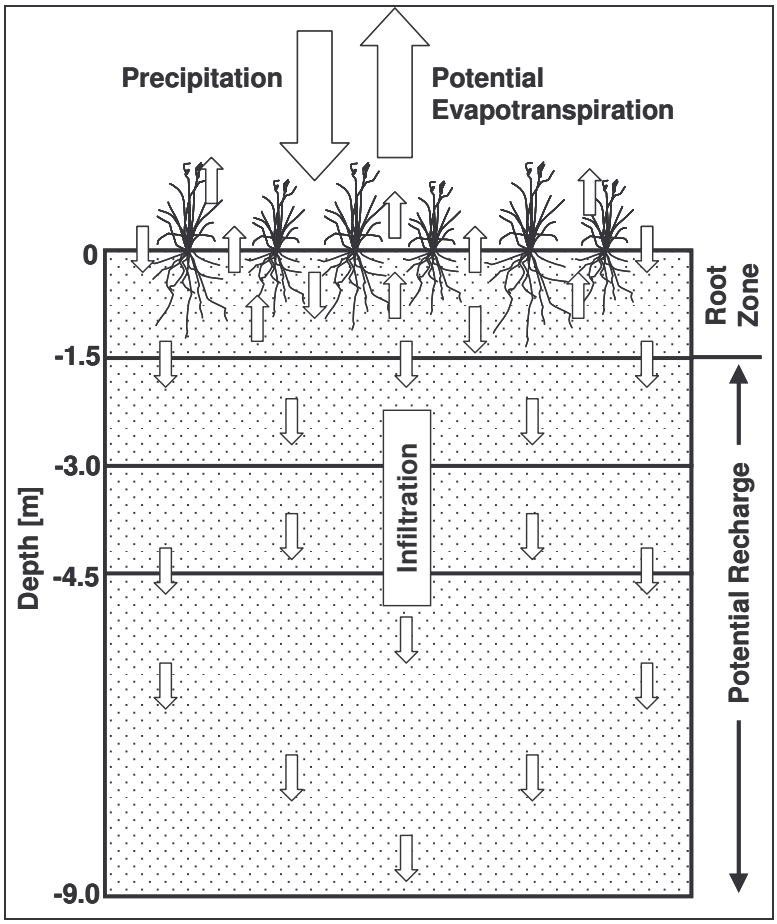

Figure 4.2 Conceptual model of vadose water movement and model layers
Conceptual diagram of the processes modeled and methods used to calculate potential recharge in unsaturated soil profiles.

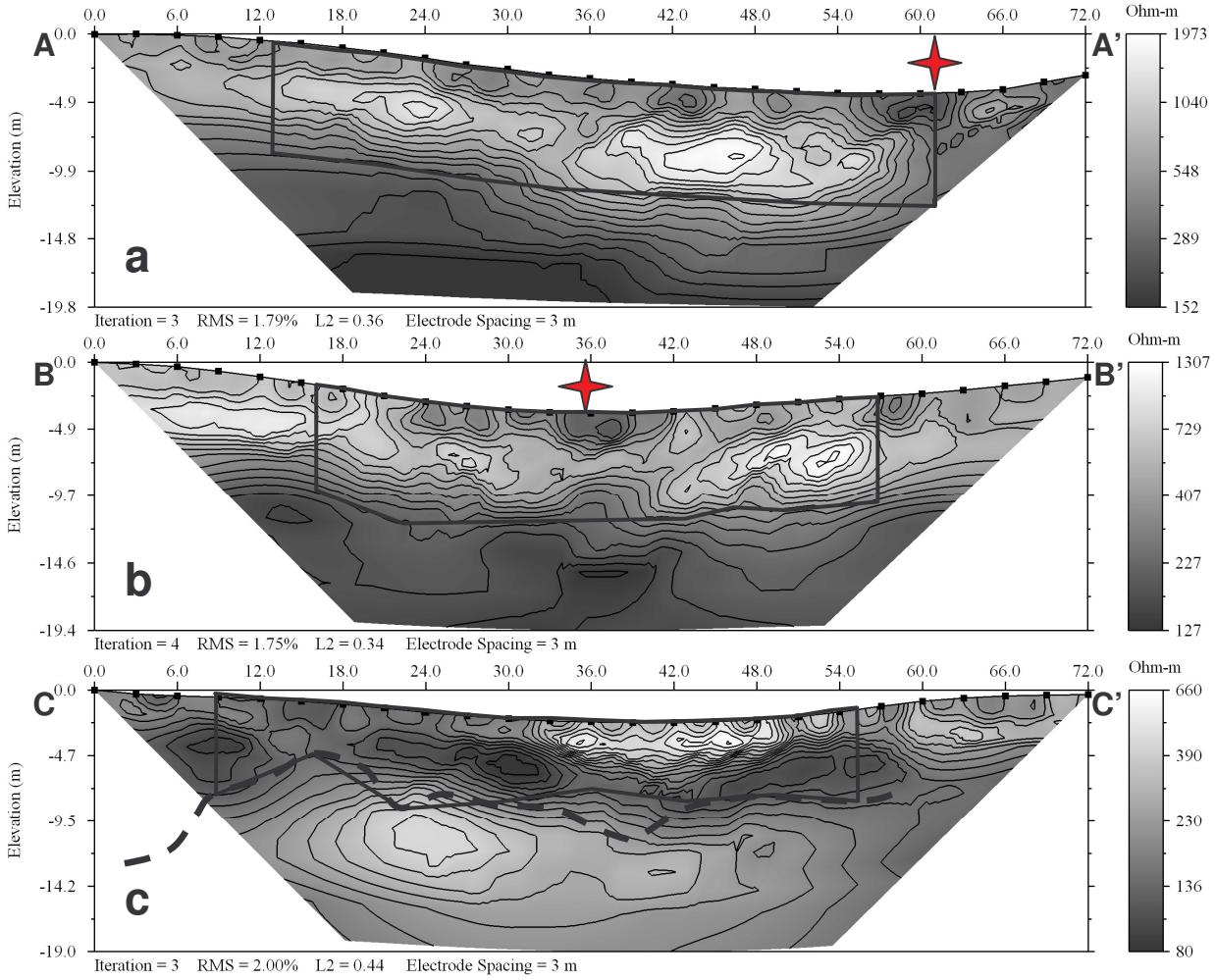

Figure 4.3 ERT profiles

ERT profiles for each transect showing contoured resistivity values and portions of each profile where time-series moisture data were modeled. a) and b) show transects across sinkhole #1 while c) is across sinkhole #5. The bedrock-soil interface in c) is shown as a dashed line. Stars indicate the point where a) and b) intersect. A, A', B, B', C and C' represent transect endpoints as shown in **Figure 4.1**. Also note that the resistivity scales are not the same for each profile

water conductivity. The proxy assumes a relationship between the dominant cation species in the soil and equilibrium pore-water conductivity.

Changes in soil moisture for 10 time intervals from May 17 to October 9, 2006 were obtained by calculating the difference in ERT-derived volumetric soil moisture relative to the initial dataset collected on May 17, 2006. These changes were calculated as m^3 of water added or subtracted from the three soil profiles (**Figure 4.3)** by assuming a 1m profile thickness. Because we calculated volumetric moisture content, conversion of these data into a volume of water added or subtracted from the profile (relative to the initial profile) was done by summing the volumetric moisture changes for each of the 0.5 x 0.5m model cells contained in a 1m thick profile.

Recharge calculations

Potential recharge was calculated by using a simple mass balance model and a 1.5m root depth (**Figure 4.2**). Increases in the soil moisture below this depth represented water which was available to potentially recharge the underlying aquifer. Decreases in soil moisture in the interval below -1.5m represented water which moved downward to the region below and could also be called potential recharge. To better understand rates of infiltration and the timing of potential recharge, we divided ERT-derived soil moisture profiles into intervals of 0 to -1.5m, -1.5 to -3.0m, -3.0 to -4.5m, and below -4.5m in depth, to monitor rates of infiltration and potential recharge based on the timing of a wetting front which moved from the upper to lower depth intervals (**Figure 4.2**). This also allowed a more detailed investigation of differences between the two sinkholes.

PET modeling and precipitation

We used the Penman-Monteith model (Allen et al., 1998; ASCE-EWRI, 2002; Howell and Evett, 2004; Snyder and Eching, 2006) with a tall grass reference to calculate daily PET at our field site. The Penman-Monteith model is the standardized method for calculating potential evapotranspiration using standard climatic data and has been shown to be widely applicable worldwide (Allen et al., 1998). If needed, the model can be adjusted for crop or vegetation conditions at a particular site which may differ from the reference crop used in the model. We used a model developed by Snyder and Eching (2006) which simulates reference

evapotranspiration for both short and tall grass canopies. Their model uses the standardized form of the Penman-Monteith equation (ASCE-EWRI, 2002) to calculate daily reference values. Required data were derived from hourly data recorded at our field site on the Virginia Tech Kentland Farms (VT, 2007), and include daily maximum and minimum temperature, average wind speed, global solar radiation (corrected to net solar radiation), and daily maximum and minimum relative humidity. Hourly precipitation data were also recorded at this weather station. Cumulative PET and precipitation were both converted into m^3 of water by multiplying the modeled or measured amount by each profile's length and assuming a profile thickness of 1m. PET was not assumed to be actual evapotranspiration (AET), and AET was not directly modeled in this study. Except for periods when the rate of precipitation is greater than the rate of PET, PET is assumed to be greater than AET.

RESULTS AND DISCUSSION

PET, precipitation, and soil moisture

Figure 4.4 shows the relationship between cumulative modeled PET, cumulative precipitation, and cumulative ERT derived changes in soil moisture in each profile over the study period. When the slope of the cumulative precipitation data is less than the slope of cumulative PET, no deep infiltration or recharge occurs. Conversely, when the slope of cumulative precipitation is greater than the slope of cumulative PET, potential recharge can occur in unfrozen soils, but only if infiltrating water moves below the depth of influence from ET processes. Three important time intervals can be described in our data based on these relationships between cumulative precipitation and cumulative PET. The first time interval is a period of drying which lasts from day-137 until day-173. During this time, most of the water removed from the soil profiles is due to ET. There is evidence that water is also being removed through the bottom of the soil profile. For example, **Figure 4.5** shows the timing of addition or removal of water from each depth interval described above. In profiles for sinkhole #1 (**Figure 4.5 a and b)** the interval between -1.5m and -3.0m showed a slight decrease in soil moisture between day-137 and day-173. There is a corresponding increase in water in the interval below -4.5m. Since both these intervals are significantly below the depth at which ET would be a factor, we concluded that this water has

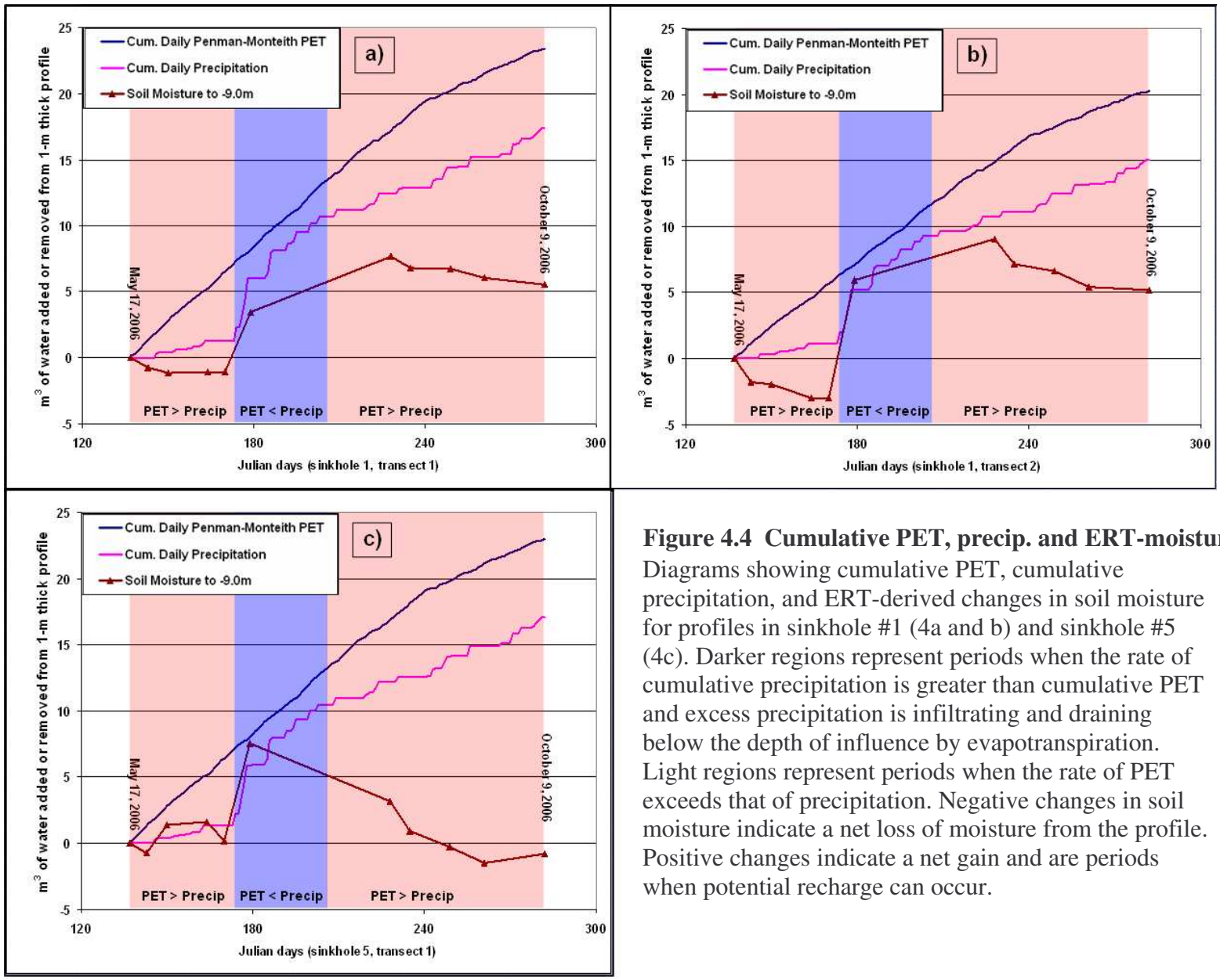

Figure 4.4 Cumulative PET, precip. and ERT-moisture Diagrams showing cumulative PET, cumulative precipitation, and ERT-derived changes in soil moisture for profiles in sinkhole #1 (4a and b) and sinkhole #5 (4c). Darker regions represent periods when the rate of cumulative precipitation is greater than cumulative PET and excess precipitation is infiltrating and draining below the depth of influence by evapotranspiration. Light regions represent periods when the rate of PET exceeds that of precipitation. Negative changes in soil moisture indicate a net loss of moisture from the profile. Positive changes indicate a net gain and are periods when potential recharge can occur.

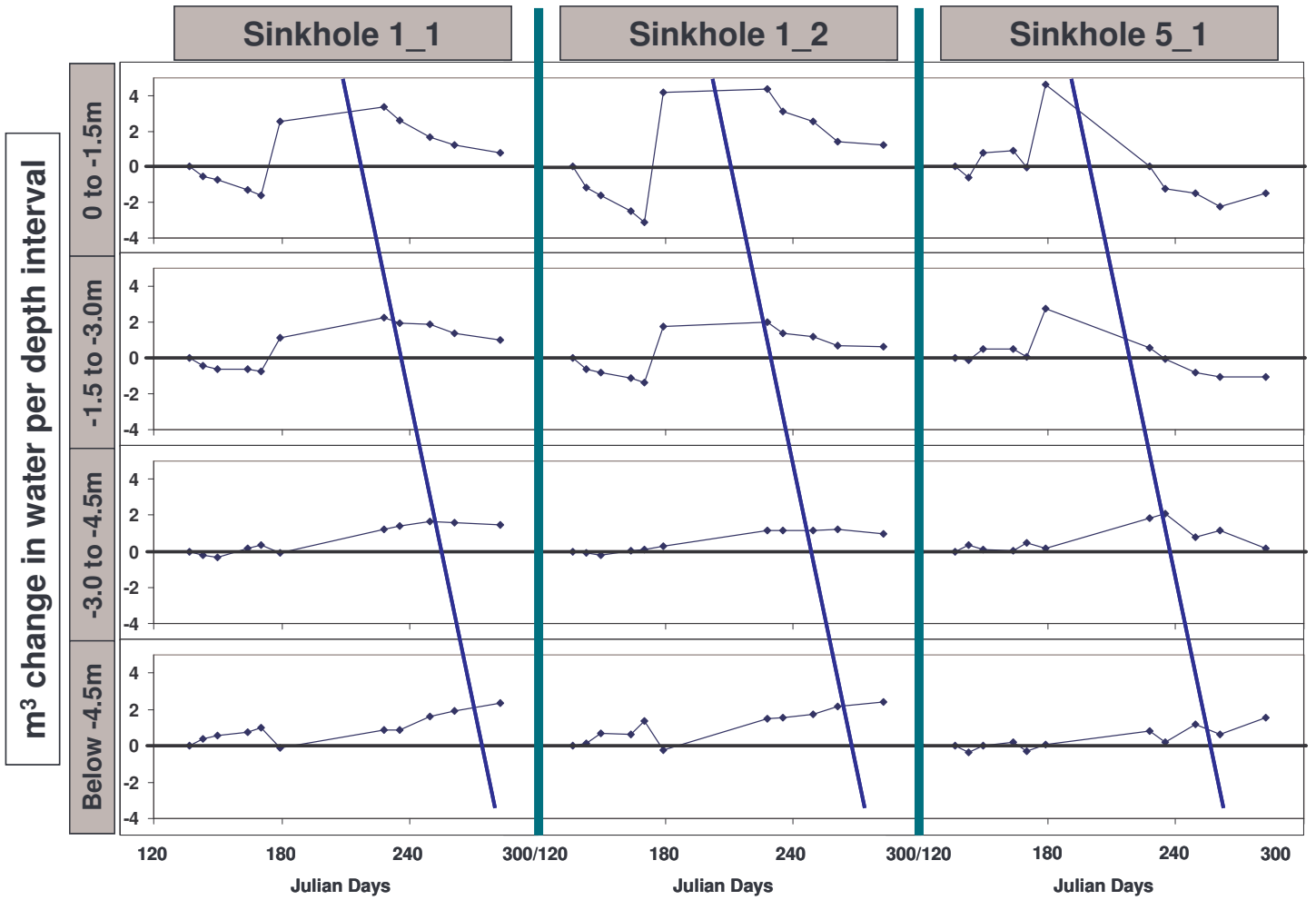

Figure 4.5 ERT-derived moisture changes by depth interval

Changes in ERT-derived soil water for each sinkhole transect by depth interval. Note a slight loss in water content in profiles for sinkhole #1, a) and b), between -1.5m and 3.0m and a corresponding increase below -4.5m. This indicates that a small amount of water was moving downward during this time interval and probably represents the motion of a wetting front from a previous rain event. Sinkhole #5 c) does not clearly show the same pattern. Diagonal lines show the progression of a wetting front as detected by the time required for water to be added to sequentially deeper intervals in the profiles.

moved downward in the soil profile. The water is likely part of a wetting front which was introduced by rainfall prior to the first ERT measurements.

On day-173, a period of significantly increased precipitation began in which the rate of cumulative precipitation was greater than or equal to the rate of cumulative PET. This trend continued until day-204 when the rate of cumulative precipitation decreased and was again less than the cumulative PET slope **(Figure 4.4)**. During this time interval, excess water infiltrated to depths below the influence of ET and could be assumed to contribute to potential recharge **(Figure 4.5 a, b and c)**.

After day-204, conditions returned to a state in which precipitation could be entirely removed from the system by ET processes (**Figure 4.4)**. Changes in ERT derived soil moisture for each 9m-thick soil profile, and analysis of changes occurring in individual depth intervals showed that moisture losses primarily occurred in the upper 1.5m of each profile (**Figure 4.5**). This supported our hypothesis that moisture above -1.5m would primarily be removed by ET during periods when PET was greater than precipitation, but water below -1.5m would continue to move downwards.

Figure 4.6, Figure 4.7, and **Figure 4.8** show the spatial distribution of increases or decreases in volumetric soil moisture over time in each 2-D profile. Patterns of change support the idea that infiltration and recharge processes are not homogeneous, especially in sites with heterogeneous soils. One pattern which was clearly apparent is that a significant amount of infiltration occurs in the topographically lowest region of the sinkholes. This is likely the result of increased infiltration during heavy rain events which caused overland flow to pond in the bottom of the sinkholes. Patterns apparent in **Figure 4.6, Figure 4.7,** and **Figure 4.8** also support the idea that large amounts of water infiltrate on the flanks of sinkholes. For example, in **Figure 4.6** and **Figure 4.7** (sinkhole #1)**,** there is an increase in soil moisture along the entire length of the profile with localized regions of higher soil moisture. **Figure 4.8** (sinkhole #5) does not show this pattern as clearly and it appears that more water has infiltrated at the lowest portion of the sinkhole. This could be due to a) either slightly different vegetation in sinkhole #5 or b) different soil characteristics (higher silt and clay content) (Schwartz et al., *In review*). Runoff and

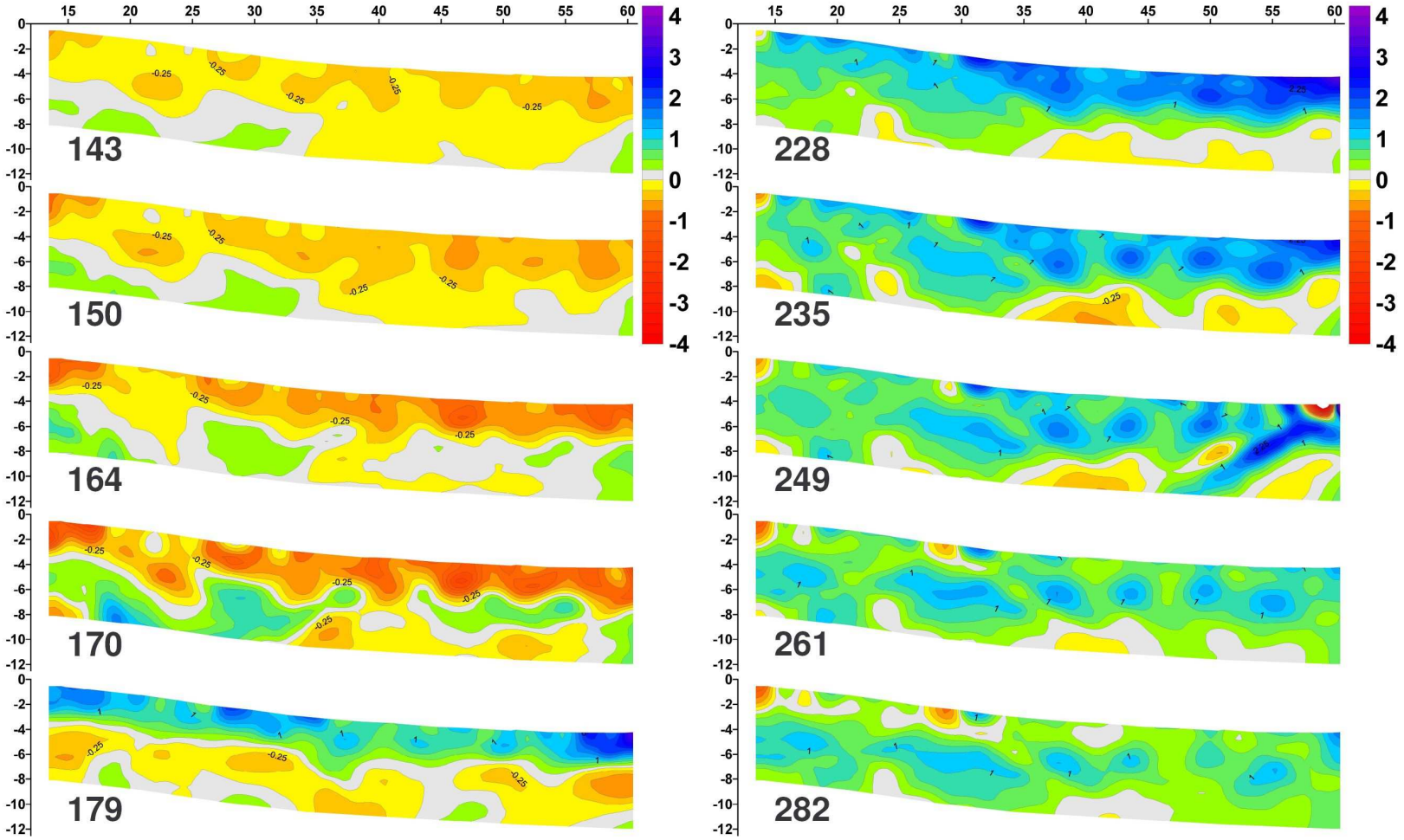

Figure 4.6 Profiles of moisture change over time in sinkhole #1, profile #1
Temporal and spatial changes in soil moisture relative to a baseline model on day-137 (May 17, 2006) in sinkhole #1, transect #1as modeled using time-series ERT data. Warm colors represent decreases in volumetric moisture content and cooler colors represent increases in volumetric soil moisture content. Scales on the X and Y axes are in [m]. Numbers in the lower left of each profile are Julian days. The baseline profile was measured on Julian day-137. Large rain events occurred between day-173 and day-187, with PET < Precip between day-173 and day-204.

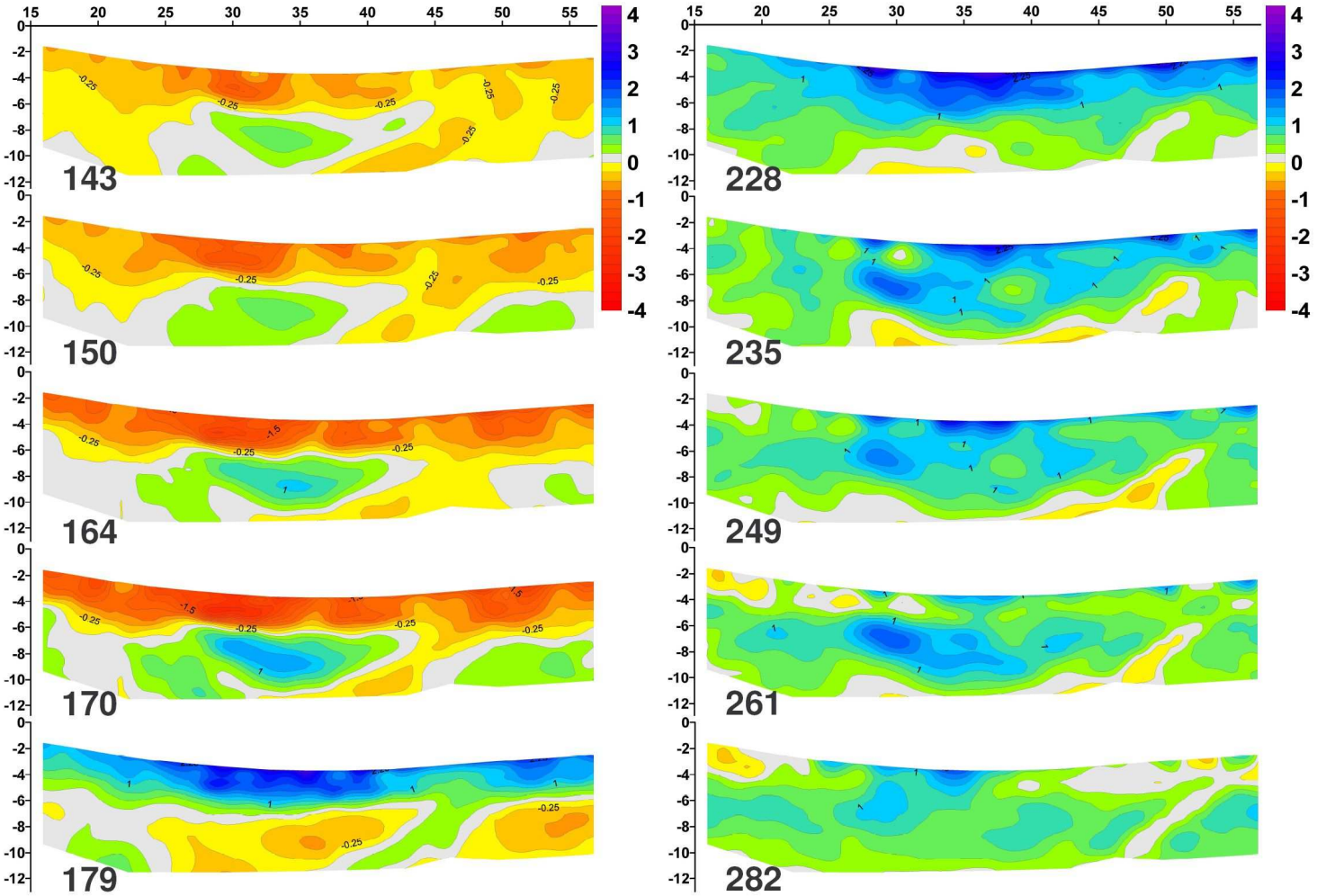

Figure 4.7 Profiles of moisture change over time in sinkhole #1, profile #2

Temporal and spatial changes in soil moisture relative to a baseline model on day-137 (May 17, 2006) in sinkhole #1, transect #2as modeled using time-series ERT data. Warm colors represent decreases in volumetric moisture content and cooler colors represent increases in volumetric soil moisture content. Scales on the X and Y axes are in [m]. Numbers in the lower left of each profile are Julian days. The baseline profile was measured on Julian day-137. Large rain events occurred between day-173 and day-187, with PET < Precip between day-173 and day-204.

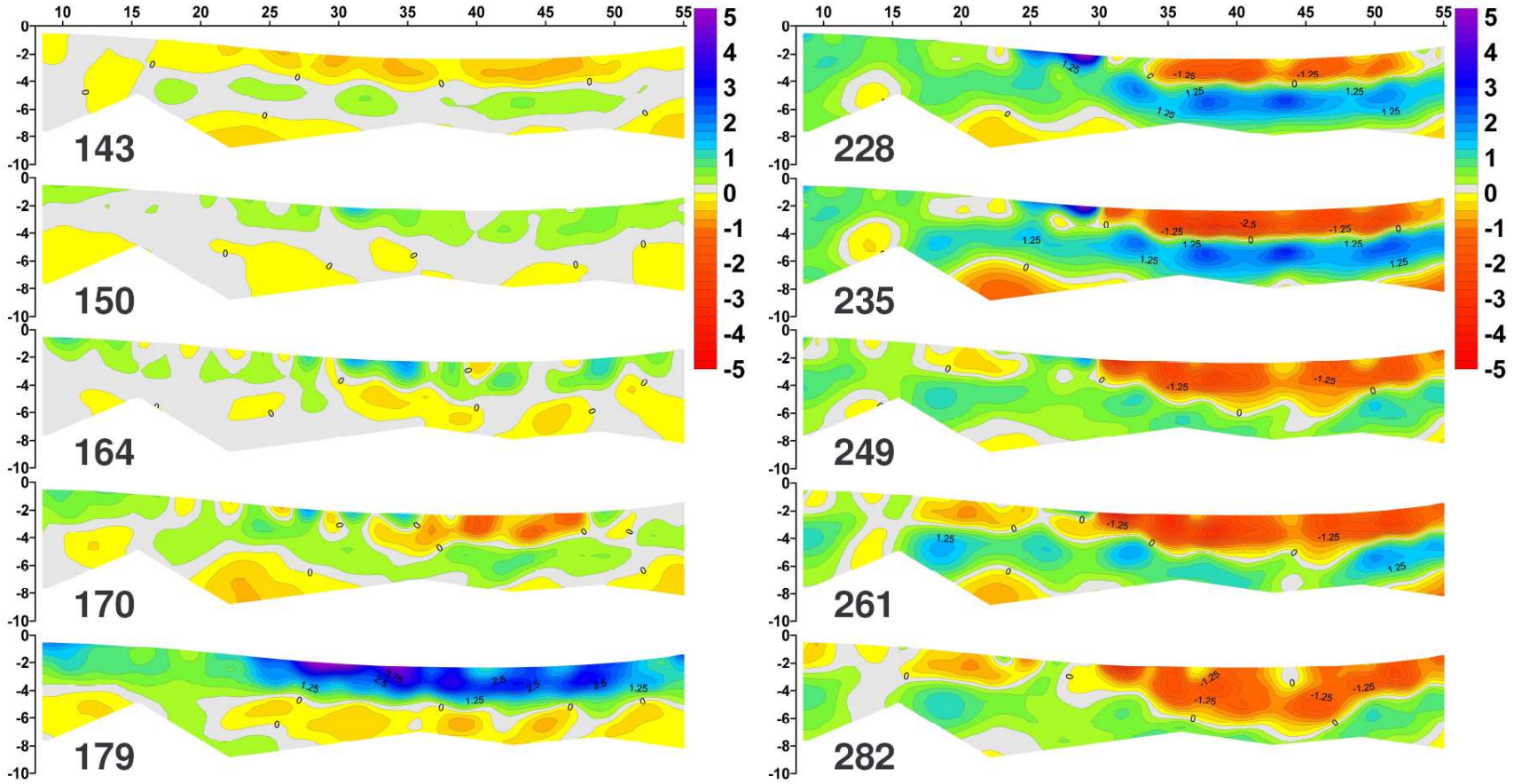

Figure 4.8 Profiles of moisture change over time in sinkhole #5, profile #1
Temporal and spatial changes in soil moisture relative to a baseline model on day-137 (May 17, 2006) in sinkhole #5, transect #1as modeled using time-series ERT data. Warm colors represent decreases in volumetric moisture content and cooler colors represent increases in volumetric soil moisture content. Scales on the X and Y axes are in [m]. Numbers in the lower left of each profile are Julian days. The baseline profile was measured on Julian day-137. Large rain events occurred between day-173 and day-187, with PET < Precip between day-173 and day-204.

ponding in the lowest part of sinkhole #5 may also have been greater than in sinkhole #1. We observed evidence of ponded water 20-30 cm deep in the lowest point of sinkhole #5 after a heavy rain. The amount of infiltration which occurs in the bottom of the sinkhole vs. the flanks is controlled by rates of precipitation (which would influence runoff), physical properties of the soils (which control rates of infiltration), type and amount of vegetation and preceding soil moisture conditions (which also influence how much and how fast infiltration occurs).

Recharge

We calculated recharge using a simple mass balance in each of the three 2-D profiles (**Figure 4.2** and **Figure 4.5**). **Figure 4.9** shows cumulative PET, precipitation, change in water content for the entire profile thickness, and change in water content for the profile below -1.5m. By assuming that any addition or removal of water to the interval below 1.5m in depth represented either recharge (by passing through the bottom of the profile) or potential recharge (by being added to the profile), we were able to quantify recharge. **Table 4.1** presents the amounts of water added to each profile below -1.5m. Our calculations indicate that between 19 and 31% of precipitation between day-173 and day-204 (June 22 to July 23) infiltrated to a depth where it can be considered potential recharge. Based on published estimates of annual recharge as a percent of precipitation (Delin and Risser, 2007), these values are reasonable. It is worth pointing out that this occurred during the summer growing season when PET was very high and recharge rates are normally very low. However, as others have shown, recharge is extremely variable temporally and is dependent upon many different factors such as geology, climate, antecedent moisture conditions, physical and chemical soil parameters, and rates of precipitation and overland flow. (Delin and Risser, 2007; Delin et al., 2007; Dripps, 2003; Nolan et al., 2007).

Unfortunately, we do not have data for the time interval between day-179 and day-228. In**, Figure 4.5** and **Figure 4.8,** we see evidence that a significant portion of precipitation which fell of sinkhole #5 probably passed quickly through the profile and was not detected by our measurements. For example, in the profile for sinkhole #5 **(Figure 4.4**), there was a rapid increase in the volume of infiltrated water in the soil profile, but by day-228 the moisture content had already decreased to approximately half of the initial increase at day-179. It is very likely that much of this water had already passed through the entire profile by day-228. In addition to

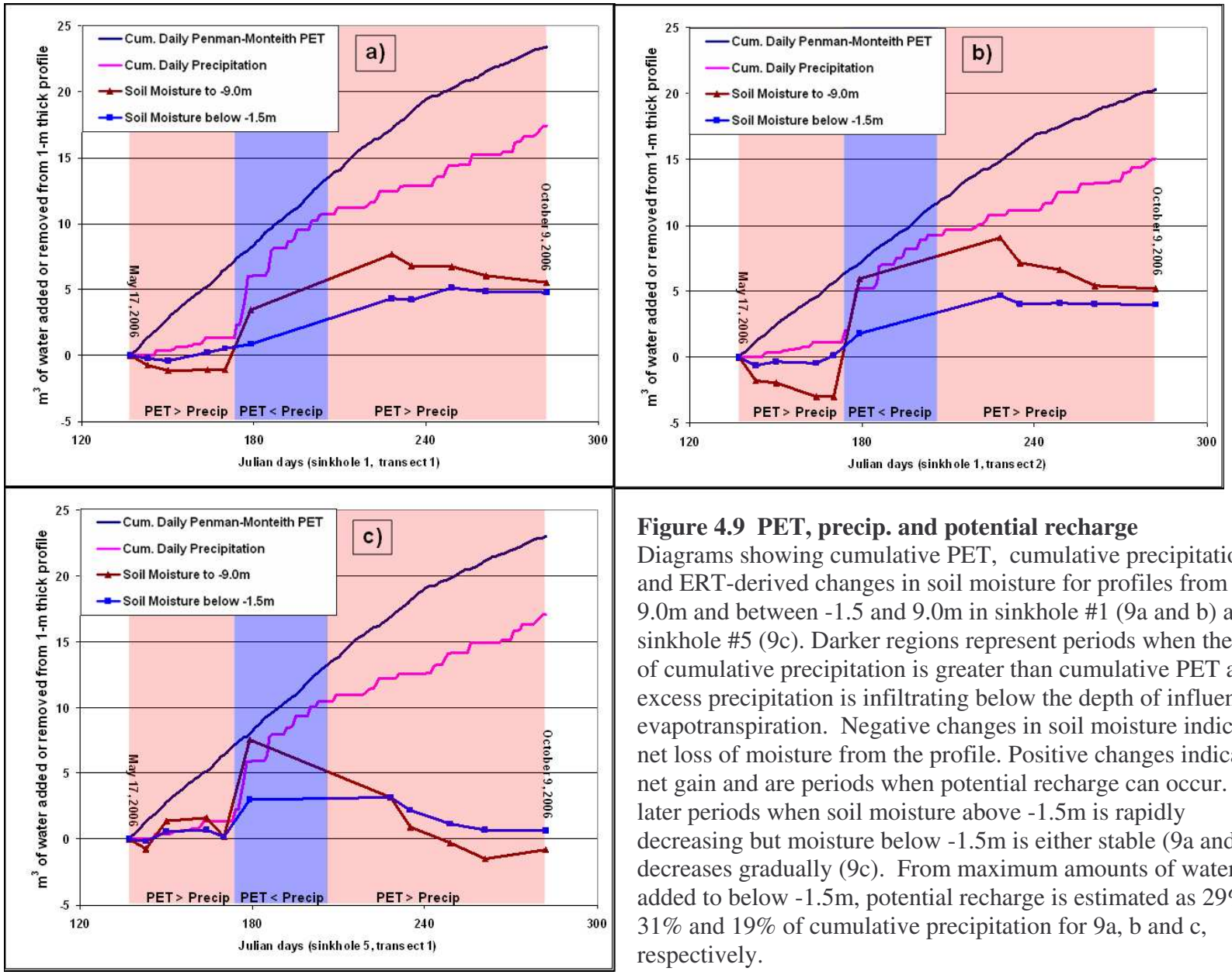

Figure 4.9 PET, precip. and potential recharge
Diagrams showing cumulative PET, cumulative precipitation, and ERT-derived changes in soil moisture for profiles from 0 to -9.0m and between -1.5 and 9.0m in sinkhole #1 (9a and b) and sinkhole #5 (9c). Darker regions represent periods when the rate of cumulative precipitation is greater than cumulative PET and excess precipitation is infiltrating below the depth of influence by evapotranspiration. Negative changes in soil moisture indicate a net loss of moisture from the profile. Positive changes indicate a net gain and are periods when potential recharge can occur. Note later periods when soil moisture above -1.5m is rapidly decreasing but moisture below -1.5m is either stable (9a and b) or decreases gradually (9c). From maximum amounts of water added to below -1.5m, potential recharge is estimated as 29%, 31% and 19% of cumulative precipitation for 9a, b and c, respectively.

measuring a much smaller percent of precipitation as recharge for this profile (**Table 4.1**) when compared to those in sinkhole #1, ERT derived moisture changes shown in **Figure 4.8** indicate that the wetting front moved through these soils much faster than it did in sinkhole #1 (**Figure 4.6** and **Figure 4.7**).

Our ERT-derived results compared well with the expected timing and amounts of infiltration and potential recharge using cumulative Penman-Monteith PET and precipitation data (**Figure 4.9a, b,** and **c**). ERT results for the three profiles show several similarities and differences. In all three profiles, the ERT-modeled increase in water content over the entire profile thickness was consistent with nearly 100% infiltration during the intense rain events. In **Figure 4.9b** and **c**, the increase in ERT-derived moisture is greater than the cumulative precipitation which fell over the profiles. We believe this is the result of overland flow from the adjacent sinkhole flanks which shed large amounts of water. Overland flow is not represented in the cumulative precipitation data shown in **Figure 4.4** and **Figure 4.9**. Enhanced infiltration at the bottom of the sinkholes was measured by ERT profiles which cross the bottom of the sinkhole. Evidence to support this hypothesis can be found in **Figure 4.9a** where the increase in ERT-derived soil moisture is nearly identical to the precipitation which fell during the intense rain events beginning on day-173, but is significantly less than the infiltration measured in **Figure 4.9b**. The profile shown in **Figure 4.9a** ends at the bottom of the sinkhole and did not measure moisture changes across the entire width of the bottom as the profile shown in **Figure 4.9b** did.

Even though the two profiles in sinkhole #1 show different amounts of water infiltrated, both **Figure 4.9a** and **b** show that similar amounts of water were added to the depth interval below -1.5 m, with approximately 30% of cumulative precipitation contributing to potential recharge. When only compared to the interval where the rate of precipitation equaled or exceeded the rate of PET (day-173 to day-204), approximately 50% of this precipitation contributed to potential recharge. Results from sinkhole #5 were different from sinkhole #1, though it appeared that a similar amount of water infiltrated and contributed to potential recharge below -1.5 m. The main difference between sinkhole #5 and #1 was that the rate at which water passed through the soil profile was much higher. This is evident by the temporal distribution of soil moisture in both the entire profile and at depths below -1.5m (**Figure 4.9c**). **Figure 4.8** clearly shows this difference

as well, with a well-defined wetting front moving downward quickly. After the rate of precipitation decreased to less than that of PET at day-204, the near-surface lost moisture rapidly (especially in silty soils filling the lowest potion of the sinkhole). By day-282, there was almost no evidence of this water remaining.

CONCLUSIONS

The most important result of this research is that we were able to model field scale spatial and temporal distribution of soil moisture in three profiles from 41 to 47 m in length and 9 m in depth using 11 sequential sets of ERT data. We did this by using a modified form of Archie's Law to convert 2-D ERT data into 2-D soil moisture and then measuring differences in modeled soil moisture content over time. This model and these methods are described in Chapter 3. From these data we derived potential recharge amounts for each profile. We also showed that these results are in good agreement with the results expected after examining the relationships between cumulative PET and precipitation over the monitored time interval.

We have shown that soil-filled sinkholes can retain and slowly transmit significant amounts of water after a recharge event. At the same time, we also saw evidence that a portion of infiltrating water probably moved through the unsaturated zone relatively quickly (but not what might be considered rapidly), especially in sinkhole #5. These results refute the assumption that all sinkholes should be treated simply as a source of rapid infiltration and recharge and suggest that for the purposes of understanding infiltration and recharge, in certain cases soil-filled sinkholes should be treated more like surrounding upland areas where diffuse infiltration dominates. However, these conclusions are not valid in cases where overland flow forces concentrated infiltration of both water and potential contaminants at the bottom of sinkholes. For the purposes of better management practices, soil-filled sinkholes should still be treated as sources of potential contamination, even though the rate of transport through the unsaturated zone may be somewhat attenuated. For the purposes of characterizing the hydrogeology of mantled sinkholes and karst settings, these results indicate that soil-filled sinkholes have a significant capacity to store and slowly release water to the underlying aquifer.

One advantage of using this hydrogeophysical method to quantify potential recharge is that it is relatively easy to apply to field scale studies. After basic soil properties have been measured, the method is non-invasive and can be used over any time interval desired. There are often large discrepancies between results of small-scale recharge estimates or measurements and regional-scale results. For field-scale studies, the methods we present are an alternative to scaling large or small scale results down or up to obtain intermediate-scale estimates.

ACKNOWLEDGEMENTS

We acknowledge funding for this research from: US Department of Education GAANN Fellowship, Virginia Water Resources Research Center, Cave Conservancy Foundation, Cave Research Foundation, National Speleological Society, Geological Society of America, West Virginia Association for Cave Studies, and the Virginia Tech Graduate Research Development Program. We thank Ankan Basu, Mike Beck, Lee Daniels, Beth Diesel, Bruce Dunlavy, Frank Evans, Brad Foltz, Marty Griffith, Mary Harvey, Ashley Hogan, Danielle Huminicki, Stuart Hyde, Rachel Lauer, Steve Nagle, Jeanette Montrey, Wil Orndorff, Zenah Orndorff, Dave Rugh, Cori and Zachary Schwartz, Jim Spotila, Brett Viar, Dongbo Wang, and Brad White for their assistance both in the field and in the lab.

REFERENCES

Allen, R.G., L.S. Pereira, D. Raes, and M. Smith. 1998. Crop evapotranspiration - Guidelines for computing crop water requirements - FAO Irrigation and drainage paper 56. Food and Agriculture Organization of the United Nations, Rome.

ASCE-EWRI. 2002. The ASCE standardization reference evapotranspiration equation. Environmental and Water Resources Institute of the American Society of Civil Engineers.

Chapman, T.G., and R.W. Malone. 2002. Comparison of models for estimation of groundwater recharge, using data from a deep weighing lysimeter. Mathematics and Computers in Simulation 59:3-17.

Das Gupta, A., and G.N. Paudyal. 1988. Estimating aquifer recharge and parameters from water level observations. Journal of Hydrology 99:103-116.

de Vries, J.J., and I. Simmers. 2002. Groundwater recharge: an overview of processes and challenges. Hydrogeology Journal 10:5-17.

Delin, G.N., and D.W. Risser. 2007. Ground-water recharge in humid areas of the United States - A summary of ground-water resources program studies, 2003-06. U. S. Geological Survey, Ground-water Resources Program, Reston, VA.

Delin, G.N., R.W. Healy, D.L. Lorenz, and J.R. Nimmo. 2007. Comparison of local- to regional-scale estimates of ground-water recharge in Minnesota, USA. Journal of Hydrology 334:231-249.

Doctor, D.H., C.E.J. Alexander, M. Petric, J. Kogovsek, J. Urbanc, S. Lojen, and W. Stichler. 2006. Quantification of karst aquifer discharge components during storm events through end-member mixing analysis using natural chemistry and stable isotopes as tracers. Hydrogeology Journal 14:1171-1191.

Dripps, W. 2003. The spatial and temporal variability of groundwater recharge. PhD Dissertation, Ph.D. Dissertation, The University of Wisconsin - Madison.

Dripps, W.R., and K.R. Bradbury. 2007. A simple daily soil-water balance model for estimating the spatial and temporal distribution of groundwater recharge in temperate humid areas. Hydrogeology Journal 15:433-444.

Howell, T.A., and S.R. Evett. 2004. The Penman-Monteith Method. USDA Agricultural Research Service.

Iqbal, M.Z., and N.C. Krothe. 1995. Infiltration Mechanisms Related to Agricultural Waste Transport Through the Soil Mantle to Karst Aquifers of Southern Indiana, USA. Journal of Hydrology 164:171-192.

Klimchouk, A.B. 2004. Towards defining, delimiting and classifying epikarst: Its origin, processes and variants of geomorphic evolution. Speleogenesis and Evolution of Karst Aquifers www.speleogenesis.info 2.

Lee, E.S., and N.C. Krothe. 2001. A four-component mixing model for water in a karst terrain in south-central Indiana, USA. Using solute concentration and stable isotopes as tracers. Chemical Geology 179:129-143.

Maloszewski, P., W. Stichler, A. Zuber, and D. Rank. 2002. Identifying the flow systems in a karstic-fissured-porous aquifer, the Schneealpe, Austria, by modeling of environmental ^{18}O and ^{3}H isotopes. Journal of Hydrology 256:48-59.

McKay, L.D., J.D. Cherry, and R.W. Gillham. 1993. Field experiments in a fractured clay till: 1 Hydraulic conductivity and fracture aperture. Water Resources Research 29:1149-1162.

Michot, D., Y. Benderitter, A. Dorigney, B. Nicoullaud, D. King, and A. Tabbagh. 2003. Spatial and temporal monitoring of soil water content with an irrigated corn crop cover using surface electrical resistivity tomography. Water Resources Research 39:1138.

Nolan, B.T., R.W. Healy, P.E. Taber, K. Perkins, K.J. Hitt, and D.M. Wolock. 2007. Factors influencing ground-water recharge in the eastern United States. Journal of Hydrology 332:187-205.

Perrin, J., P.-Y. Jeannin, and F. Zwahlen. 2003. Epikarst storage in a karst aquifer: a conceptual model based on isotopic data, Milandre test site, Switzerland. Journal of Hydrology 279:106-124.

Scanlon, B.R., R.W. Healy, and P.G. Cook. 2002. Choosing appropriate techniques for quantifying groundwater recharge. Hydrogeology Journal 10:18-39.

Schwartz, B.F., and M.E. Schreiber. In review. Linking field scale electrical resistivity tomography and time domain reflectometry derived soil moisture.

Schwartz, B.F., M.E. Schreber, P.S. Pooler, and J.D. Rimstidt. *In review*. New methods for obtaining accurate access-tube TDR moisture values: a tool for understanding vadose hydrology in deep and heterogeneous soil profiles. *In review at:* Soil Science Society of America Journal.

Shah, P.H., and D.N. Singh. 2005. Generalized Archie's Law for Estimation of Soil Electrical Conductivity. Journal of ASTM International 2:1-20.

Sheets, K.R., and J.M. Hendrickx. 1995. Noninvasive soil water content measurement using electromagnetic induction. Water Resources Research 31:2401-2409.

University of California. 2006. PMday. Release revised November 2006. University of California, Davis CA.

Sophocleous, M. 1991. Combining the soilwater balance and water-level fluctuation methods to estimate natural ground-water recharge: practical aspects. Journal of Hydrology 124:229-241.

Sreedeep, S., and D.N. Singh. 2005. Estimating unsaturated hydraulic conductivity of fine-grained soils using electrical resistivity measurements. Journal of ASTM International 2:1-11.

Stephenson, J.B., W.F. Zhou, B.F. Beck, and T.S. Green. 1999. Highway stormwater runoff in karst areas - preliminary results of baseline monitoring and design of a treatment system for a sinkhole in Knoxville, Tennessee. Engineering Geology 52:51-59.

USDA-NRCS. 2006. Web Soil Survey [Online] http://websoilsurvey.nrcs.usda.gov/app/WebSoilSurvey.aspx (verified September 4, 2006).

VT. 2007. Virginia Tech College Farm Operation weather data [Online]. Available by College of Agriculture and Life Science http://www.vaes.vt.edu/colleges/kentland/weather/ (verified November 1, 2007).

White, W.B. 2003. Conceptual models for karst aquifers. Speleogenesis and Evolution of Karst Aquifers 1:11-16.

White, W.B., D.C. Culver, J.S. Herman, T.C. Kanes, and J.E. Mylroie. 1995. Karst Lands. American Scientist 83:450-460.

Table 4.1
Results of recharge calculations showing amount of water added to each profile below -1.5m (derived from ERT data), amount of precipitation which occurred over each profile, and percent of precipitation which infiltrated below -1.5 m and can be assumed to represent recharge. Time interval represented is between May 17 and October 9, 2006, but note that potential recharge only occurred over the time interval from day-173 to day-204.

Sinkhole # and profile	Recharge (m^3)	Precipitation (m^3)	Recharge as % of precipitation
#1, profile 1	5.1	17.4	29
#1, profile 2	4.7	15.1	31
#5, profile 1	3.2	17.1	19

CHAPTER 5

FUTURE RESEARCH

Introduction

Over the course of research for this dissertation, data were collected which were not used or presented in results discussed in the previous chapters, but were instead used for initial sinkhole characterization and to provide background data for later more in-depth research. The following pages discuss some of this work by research topic and outline future work which could build on the work already done at this field site.

Numerical modeling

The data presented in Chapter 4 for the summer and early fall of 2006 showed measurable increases in ERT-derived soil moisture in all three sinkhole profiles **(Figures 4.7, 4.8 and 4.9)**. However, a similar study which only measured ERT changes in sinkhole #1, profile #1 was conducted during fall of 2005 (**Figure 5.1**). When these results are compared to the results of the 2006 study, it is apparent that antecedent moisture conditions are very important in determining how much precipitation infiltrates. During spring and summer of 2005, below average precipitation was recorded at the site **(Figure 5.2)**, which led to drier than normal antecedent moisture conditions at the time the 2005 study began. This likely was a significant factor which contributed to a continuous loss of soil moisture over the study period (September 5, 2005 to January 9, 2006) (**Figures 5.1** and **5.3).** Additionally, rain events which did occur during this time interval were not as intense as those which occurred during the 2006 study and most of the water was probably held within the root zone and removed relatively quickly by evapotranspiration (ET) before it could infiltrate to below the root zone and become potential recharge.

Without precipitation during the winter and spring of 2006, the very short periods of intense rainfall received during summer of 2006 may not have infiltrated to the depths that they did (below root depths) and the overall trend would have been either one of little change in soil moisture or of continued soil moisture loss via both ET and potential recharge moving slowly

downward. It would be interesting to examine in more detail how antecedent soil moisture impacts the spatial and temporal distribution of soil moisture using numerical modeling.

To study long-term variations in seasonal infiltration and potential recharge in soil-filled sinkholes, ERT-methods could be used. However, high-resolution long-term data collection would be required, which would be an onerous task. As an alternative, a 2-D unsaturated zone hydrologic model such as HYDRUS-2D (Simunek et al., 1999) can be constructed to simulate unsaturated flow, which will provide information on long term changes in soil moisture and recharge. The model would include hydraulic parameters derived from the measured soil properties, precipitation, potential evapotranspiration (PET), and periodic ERT-derived moisture data. ERT-derived soil moisture distribution can be used as both initial conditions for the model and as calibration data for later time-steps in the model results. By combining numerical methods with ERT-derived data, the accuracy of the model will be significantly improved and long-term estimates of infiltration and recharge can more easily be simulated. I plan to continue these sinkhole moisture studies by performing the study outlined above.

Compare results from inside a sinkhole with a similar study outside a sinkhole

The work I have already presented focused on infiltration and potential recharge within two soil-filled sinkholes. These results give some indication that these processes might differ when compared to non-sinkhole environments with thick soils. However, to really make comparisons between what occurs in a sinkhole and outside of a sinkhole, a similar study will need to be done on an upland area around a study sinkhole. This work is not possible with the data I have already collected and would require additional instrumentation. This may be the subject of a future research proposal.

Compare results from a soil-filled sinkhole with a soil-filled sink containing an open drain

Another useful study would be to monitor infiltration and recharge in soils in a sinkhole which also contains an open drain. This experiment would allow a comparison between infiltration and slow recharge in the soil-filled sinkhole vs. runoff and rapid infiltration in the sinkhole with an open drain.

Process 3-D ERT data

I collected nearly 100 ERT profiles in six different sinkholes at Kentland Farms. These profiles were arranged is order to facilitate 3-D inversion at a later date when I might have access to 3-D inversion software. I will soon have access to this software and plan to use these data to generate true 3-D models of resistivity in the sinkholes. For sinkholes #1 and #5, in particular, I have detailed physical data which will help me interpret these models in terms of general soil properties and depth to bedrock.

Soil profile characterization

Depending on interest from potential collaborators, I may continue to investigate the physical and chemical properties of the 470 soil samples I collected at depths up to 9m. Ancient New River terrace deposits which mantle the karst plains at the Virginia Tech Kentland Experimental Farms have not been well characterized at depths below 3m. The samples I collected preserve information which can be used to better understand the age, weathering history, parent materials, and depositional environments of the sediments which now form the soils found in these terraces. As an example, some work has been done to characterize mineralogy of clays and other size fractions of these soils (Harris et al., 1980). This research suggested that clay mineralogy changes with depth and soils transition from containing more hydroxy-interlayered vermiculite near the surface, to more kaolinite with increasing depth. If this is true, and the trend in increasing kaolinite with depth continues or remains constant, this could be useful in efforts to further refine the extractable cation model of pore-water conductivity used in the modified form of Archie's Law which is discussed in Chapter 2.

References

Harris, W.G., S.S. Iyengar, L.W. Zelazny, J.C. Parker, D.A. Lietzke, and W.J. Edmonds. 1980. Mineralogy of a chronosequence formed in New River alluvium. Soil Science Society of America Journal 44:862-868.

Simunek, J., M. Sejna, and M.T.v. Genuchten. 1999. The HYDRUS-2D software package for simulating two-dimensional movement of water, heat, and multiple solutes in variably saturated media. Version 2.0, IGWMC - TPS - 53. International Ground Water Modeling Center, Colorado School of Mines, Golden, Colorado:251pp.

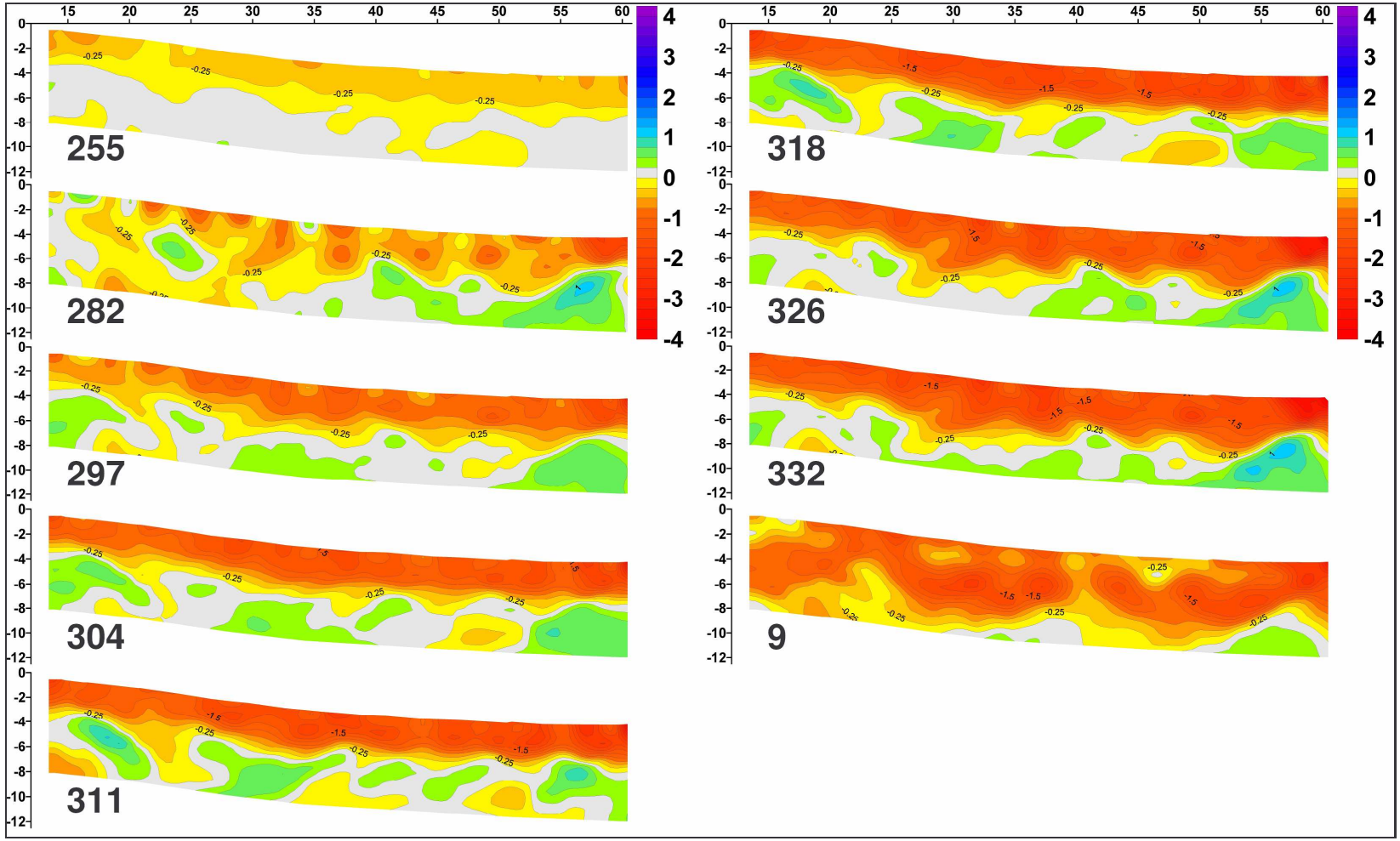

Figure 5.1 ERT-derived changes in soil moisture during fall of 2005

Temporal and spatial changes in soil moisture from Sept 5, 2005 to January 9, 2006 in sinkhole #1, transect #1 as modeled using time-series ERT data. Warm colors represent decreases in volumetric moisture content and cooler colors represent increases in volumetric soil moisture content. Scales on the X and Y axes are in [m]. Numbers in the lower left of each profile are Julian days. The baseline profile was measured on Julian day-248. These profiles show that 1) rainfall during this period did not significantly contribute to potential recharge, and 2) that much of the observed decrease in moisture below -1.5m in depth is the result of continuous downward movement of moisture over time, which resulted in relative decreases in soil moisture during the study.

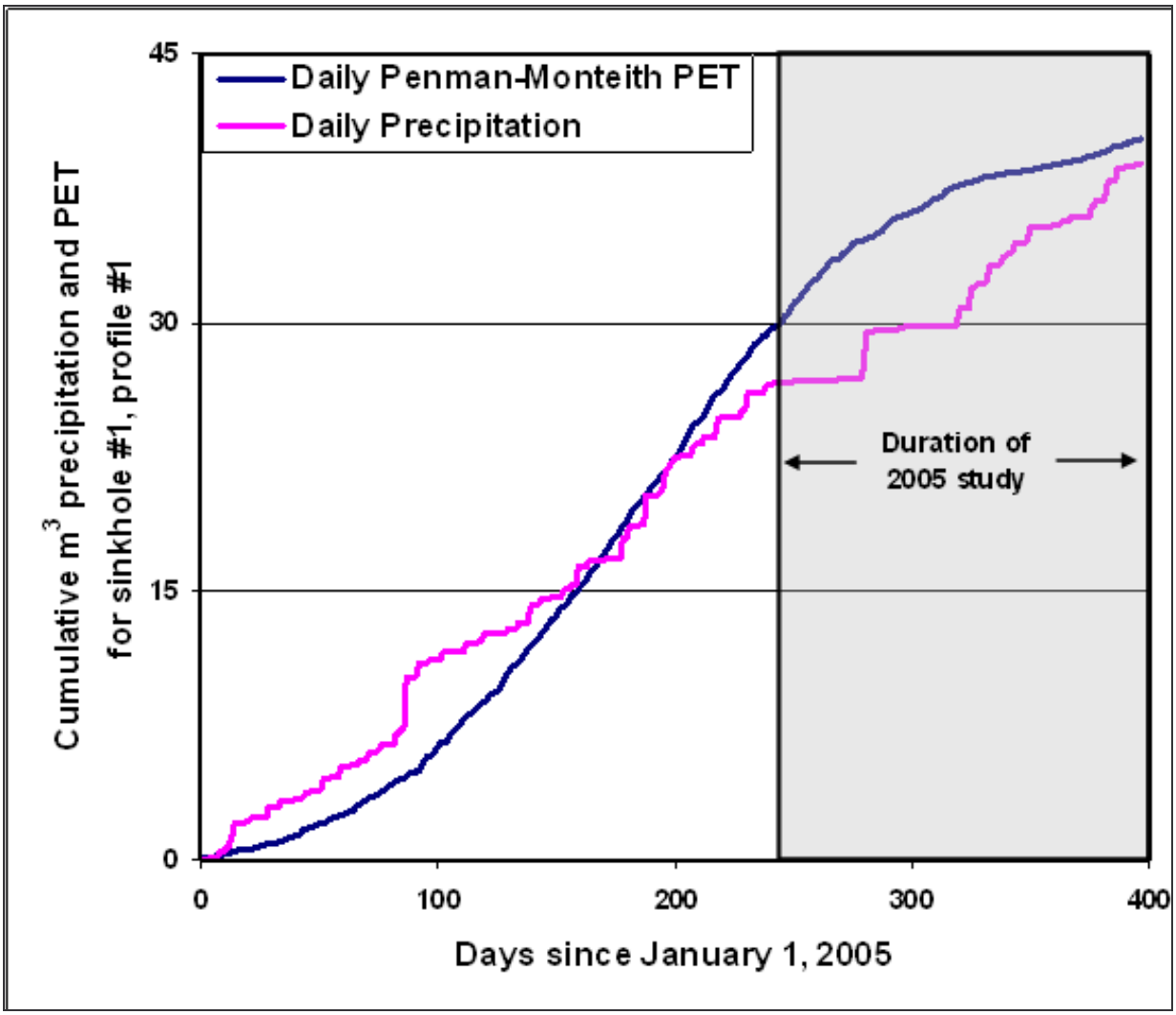

Figure 5.2 Cumulative precipitation and PET during 2005
Diagram showing cumulative precipitation and Penman-Monteith modeled PET for sinkhole #1, profile #1. Note that for much of the year prior to the 2005 study the rate of PET exceeded the rate of precipitation.

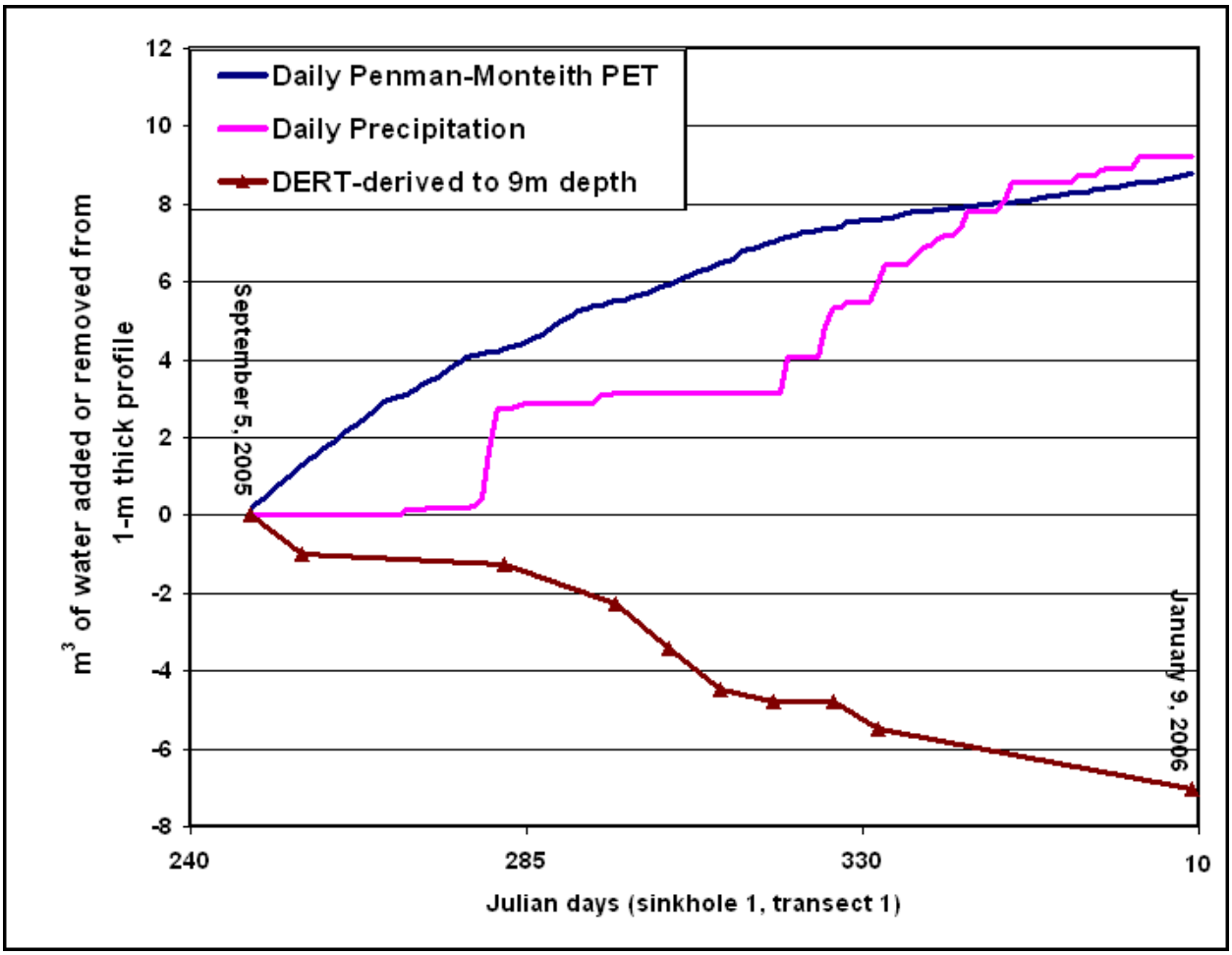

Figure 5.3 Cumulative precip, PET, and ERT-moisture for 2005 study
Diagram showing loss of volumetric soil moisture in sinkhole #1, profile #1 between September 5, 2005 and January 6, 2006 as modeled using ERT-derived changes in soil moisture. Also shown are cumulative precipitation and modeled Penman-Monteith PET for the same period.

VITA

Benjamin F. Schwartz

EDUCATION

Virginia Polytechnic Institute and State University, Blacksburg, VA
Ph. D. Geosciences, *expected fall 2007.*
Dissertation: *Quantification of Infiltration and Recharge through Soil-filled Sinkholes using Electrical Resistivity tomography and Time Domain Reflectometry*
[Advisor: Dr. Madeline Schreiber]

Radford University, Radford, VA
B. S. Geology, May 2003 - *Summa cum Laude*

Professional Experience

2001 - 2003 Full time summer employee for Virginia Department of Conservation and Recreation, Division of Natural Heritage, Karst Program in Radford, VA. Primary duties included delineation of karst drainage basins in VA with dye tracing, water sampling, geologic field observations and interpretation. Managed and compiled data in a GIS and wrote annual progress reports for the project.

2000 - 2001 Part time employee at Anderson and Associates Surveyors and Engineers, Blacksburg, VA. Performed high precision GPS surveys in SW VA. Position also required extensive CAD work.

1995 - 1999 CNC machinist for Nicholson Precision Instruments, Gaithersburg, MD. Specialized in prototyping and machining small close tolerance parts made with aluminum, plastics and exotic materials. Also specialized in precision mold making and molding of complex silicone rubber gaskets. Managed all daily operations of an independent satellite machine shop.

1991 - 1995 Party chief, rodman and courthouse researcher for Jeffery Hiner, Land Surveyor, Monterey, VA. Primary duties related to rural land surveying.

Teaching and Mentoring Experience

2007 Supervising and mentoring a geology major during a 4-credit undergraduate research project at Virginia Tech dealing with analysis of discharge data recorded at an ebb and flow karst spring. Objectives include flow period characterization, choosing an appropriate method for time-series analysis, developing a model to predict flow periods based on average discharge, writing a final report, and presenting results at the 2007 Geological Society of America annual meeting in Denver.

Fall 2005 Wrote a field guide for, organized, and led a two-day karst hydrology field trip to Bath County, VA for a graduate level Karst Hydrology class at Virginia Tech. The field trip was a critical link between classroom exercises, instruction, and discussion and the 'real-world' aspects of karst geology and hydrogeology. The trip included a trip into one of the largest caves in Virginia to observe a karst hydrologic system from the inside.

Spring 2004 Laboratory Instructor for Groundwater Hydrology, Virginia Tech. Taught labs for upper-level undergraduates and graduate students. Re-organized and edited several lab sections

and wrote new lab sections for a karst hydrology lab exercise and field trip, as well as a hydrogeophysics lab section that included demonstration and application of Electrical Resistivity Tomography equipment to characterizing shallow hydrogeology.

Fall 2003 Laboratory Instructor for three sections of Physical Geology, Virginia Tech. Duties included writing and administering exams and quizzes, and assigning all grades.

Virginia Tech Service

2004 - 2006 Member (2004-2005) and Chair (2005-2006) of Graduate Student Liaison Committee, Virginia Tech Department of Geosciences. Responsibilities included: communicating graduate student concerns and issues to the department; assisting with developing annual questionnaires for anonymous graduate student feedback; and working with the Graduate Student Research Symposium (GSRS) committee to make the GSRS more beneficial to both graduate students and faculty.

2006 Assisted with the departmental graduation ceremony and party, including setting up and removing equipment, tables and chairs.

Spring 2005 Assisted the Laboratory Instructor for Groundwater Hydrology with two field-centered lab exercises.

2005 Taught the Geophysics laboratory instructor how to set up and operate the department's Electrical Resistivity Tomography equipment.

2004 - 2005 Assisted with annual fall field trips for incoming graduate students, Virginia Tech Department of Geosciences. Described local karst hydrology and geology at several stops on the field trip, as well as described my research at the VT Kentland Farms.

2003 - 2005 Assisted with yearly karst field trips for Groundwater Hydrology class. Duties included driving vans and helping to describe karst hydrology and geology at several stops

Professional Service

2005 Assisted with a four-day Project Underground (describe/define this) workshop and field trip for VA earth science teachers where the primary emphasis was on how to incorporate karst science into SOL materials. Presented an invited talk about my research on sinkhole hydrology and hydrogeophysics and discussed how this current research could be incorporated into classroom materials.

2003 - present Project co-manager: Powell Mountain Karst Preserve. Responsibilities include: managing access for research and exploration to several caves (including the longest and deepest cave in VA) lying within the PMKP – owned by the Cave Conservancy of the Virginias (CCV); managing and compiling all field notes, scientific data and maps for the project in hard copy and digital formats; and compiling annual reports of activities and accomplishments for the CCV and the National Forest Service.

1997 – 2003 and 2006 – 2007 Director - Board of directors for Butler Cave Conservation Society. Responsibilities include a variety of duties related to operating a non-profit organization, as well as serving on many committees.

1993 - present Director - Board of directors for Virginia Speleological Survey. Duties include coordinating and managing research and exploration in several regions of Virginia

Grants and Awards

2007 $145 Southeast Division Geological Society of America travel grant.

2007 $13,386 Cave Conservancy of the Virginias. *The Role of Epikarst in Controlling Recharge, Water Quality and Biodiversity in Karst Aquifer Systems of Virginia*

2007 $20,000 Virginia Water Resources Research Center grant. *The Role of Epikarst in Controlling Recharge, Water Quality and Biodiversity in Karst Aquifer Systems of Virginia*

2007 VT College of Science Runner-up Award for Outstanding Grad Student of the Year.

2006 $15,000 Cave Conservancy Foundation's Ph.D. Graduate Fellowship in Karst Studies. *A multi-method approach to characterizing sinkhole hydrogeology and recharge mechanisms in agricultural settings.*

2006 $90 Southeast Division Geological Society of America travel grant.

Fall 2006 Full Research Assistantship and other funding - co-wrote grant proposal with Dr. Madeline Schreiber. Submitted to: Virginia Water Resources Research Center.

Spring 2006 Byron N. Cooper Graduate Fellowship award. Full Research Assistantship funding for one semester. Dept. of Geosciences, Virginia Tech.

2005 $5,000 Cave Research Foundation's annual Karst Research Fellowship. Presented annually to one student who proposes an outstanding karst-related research project.

2005 $2,000 National Speleological Society's Ralph W. Stone Award and Fellowship.

2005 $2,000 Geological Society of America research grant.

2005 $100 Geological Society of America travel grant.

2005 Award: GSA outstanding research proposal. One of 19 from 720 applications.

2005 $250 and award: GSA Hydrogeology Division outstanding research proposal. One of three.

2005 $300 Research grant from West Virginia Association for Cave Studies.

2005 $250 Research grant from Virginia Tech Graduate Research Development Program.

2004 Awarded a US Dept. of Ed. GAANN Fellowship. Provided full Research Assistantship funding and some travel and equipment funds for three semesters.

2004 $100 Geological Society of America travel grant.

2003	$4,600 Research grant from Cave Conservancy of the Virginias for equipment. *Can Cave Sediments Predict Past Flood Magnitudes?*
Spring 2003	Deans Scholar – Geology Department – Radford University
2000	$5,000 Cave Conservancy Foundation's Undergraduate Fellowship in Karst Studies.
1999	Fellow award - National Speleological Society.

Peer-reviewed Publications

Schwartz, B. F., Schreiber, M. E. and Rimstidt, J. D., 2006, Calibrating access-tube TDR soil moisture values using measured physical and chemical soil parameters. Submitted to *Soil Science Society of America Journal.*

Schwartz, B. F. and Schreiber, M. E., 2005, New Applications of Differential Electrical Resistivity Tomography and Time Domain Reflectometry to modeling infiltration and soil moisture in agricultural sinkholes. Proceedings of the *10th Multidisciplinary Conference on Sinkholes and the Engineering and Environmental Impacts of Karst.* September 2005.

Other Publications

Orndorff, W., Hypes, R., Lucas, P., Fagan, J, Zokaites, C., Orndorff, Z., Lucas, C., **Schwartz, B.**, 2005, Protecting Virginia's Caves and Karst through the Environmental Review Process. Proceedings of the *National Cave and Karst Management Symposium*, November 2005.

Schwartz B. F., Schreiber M. E., and Orndorff W., 2004. Hydrologic characterization of sinkholes in agricultural settings: Implications for best management practices. *Proceedings of the 2004 Virginia Water Resources Research Symposium*, Blacksburg, Virginia, Oct 4-6, 2004.

Schwartz, B. F., 1999, Exploring Barberry Cave. *National Speleological Society News*, September, v. 57 no. 9. A report documenting the history of exploration in Barberry Cave, Bath County, Virginia.

Schwartz, B. F., 1999, Project Caving and Permanent Rigging. *National Speleological Society News*, October, v. 57 no. 10. A technical report dealing with solutions to problems encountered with rigging in long-term project caving.

Schwartz, B. F., 1993 - present, Reports, maps and articles in *The Virginia Cellars,* the official publication of the Virginia Speleological Survey.

Publications in preparation

Schwartz, B. F., Orndorff, W. D., Futrell, S. M., Lucas, P. C., The Caves and Karst of Virginia. Chapter for Caves and Karst of North America. A book being published prior to the 2009 International Congress of Speleology held in Kerrville, Texas.

Ficco, M. J., Davis, N. W., White, W. B., **Schwartz, B. F.** Geology of the Chestnut Ridge Cave System, Bath County, Virginia. Book chapter being prepared for a publication compiling and presenting 50 years of research and exploration by the Butler Cave Conservation Society in the Burnsville Cove, Virginia.

Schwartz, B. F., Schreiber, M. S., Comparison and evaluation of Time Domain Reflectometry and Electrical Resistivity Tomography as tools for modeling soil moisture at the field scale. In preparation.

Schwartz, B. F., Schreiber, M. S., Quantifying Potential Recharge through Thick Soils in Mantled Sinkholes Using ERT Data. In preparation.

Conference Presentations

Hyde, S., **Schwartz, B.**, Lucas, P., 2007, Characterizing discharge signals and flow mechanisms at a Virginia ebb and flow karst spring. Poster presentation at the *Geological Society of America annual meeting,* October, 2007

Schwartz, B., Schreiber, M., 2007, Field scale soil moisture measurements using TDR-calibrated ERT data. Oral presentation at the *Geological Society of America annual meeting,* October, 2007

Schwartz, B., Schreiber, M., 2006, Examining temporal changes in soil moisture in a karst sinkhole using differential ERT and TDR. Oral presentation at the *Virginia Water Science and Technology Symposium*, November, 2006

Schwartz, B., Schreiber, M., 2006, Integrating Differential Electrical Resistivity Tomography and Time Domain Reflectometry as a tool for modeling soil moisture and infiltration in sinkholes. Oral presentation at the *Geological Society of America annual meeting,* October, 2006

Schwartz, B., 2006, An update on Omega Cave System: the last 6 years of exploration and discovery in Wise County, Virginia. Oral presentation at the *National Speleological Society annual meeting,* August, 2006

Schwartz, B., Schreiber, M., 2006, Integrating Differential Electrical Resistivity Tomography and Time Domain Reflectometry as a tool for modeling soil moisture and infiltration in sinkholes. Poster presented at the *SEG 2006 Hydrogeophysics Workshop.* August, 2006

Schwartz, B. F., 2006, Techniques for measuring soil moisture in sinkholes. Oral presentation at the *Graduate Student Research Symposium*, Virginia Tech Dept. of Geosciences, March, 2006

Schwartz, B. F. and Schreiber, M. E., 2005, Using TDR and 2D Differential ERT to monitor changes in soil moisture in mantled agricultural sinkholes. Oral presentation at the *Geological Society of America Annual meeting,* October, 2005

Schwartz, B. F., 2005, A multi-method approach to characterizing sinkhole hydrogeology and recharge mechanisms in agricultural settings. Oral presentation at the *Graduate Student Research Symposium*, Virginia Tech Dept. of Geosciences, March, 2005

Schwartz, B. F., Schreiber, M. E., Orndorff, W. D., 2004, Hydrologic Characterization of Sinkholes in Agricultural Settings. Oral presentation at the *Geological Society of America annual meeting,* November 2004.

Schwartz, B. F., Schreiber, M. E., Orndorff, W. D., 2004, Hydrologic Characterization of Sinkholes Using a Multi-method Approach. Oral presentation at the *Virginia Water Resources Research Center symposium,* October 2004.

Schwartz, B. F., Schreiber, M. E., Orndorff, W. D., 2004, Hydrologic Characterization of Sinkholes Using a Multi-method Approach. Poster presented at *Geological Society of America NE-SE meeting,* March 2004.

Orndorff, W. D**., Schwartz, B. F.**, Orndorff, Z. W., 2004, Patterns of Karst Hydrological Systems Developed in Ordovician-aged Carbonates of the Southwestern Virginia Valley and Ridge. Oral presentation at the *Geological Society of America NE-SE meeting,* March 2004.

Schwartz, B. F., 2004, Hydrologic characterization of sinkholes using a multi-method approach. Oral presentation at the *Graduate Student Research Symposium*, Virginia Tech Dept. of Geosciences, March, 2004

Invited Presentations

Schwartz, B. F., March, 2007, Integrating Differential Electrical Resistivity Tomography and Time Domain Reflectometry as a tool for modeling soil moisture and infiltration in sinkholes. Weekly seminar speaker at USGS, Reston, Va.

Schwartz, B. F., November, 2006, Karst, hydrology and geophysics - (How to turn a sinkhole into a complex hydrogeophysical problem). Weekly seminar speaker at Eastern Tennessee State University, Department of Physics, Astronomy and Geology, Johnson City, TN.

Schwartz, B. F., 2006, Karst, hydrology and geophysics - (How to turn a sinkhole into a complex hydrogeophysical problem). Weekly seminar speaker at Appalachian State University, Department of Geology, Boone, N.C.

Non-thesis Research

2006 - *Characterizing a complex ebb-and-flow karst spring in Bath County, Virginia*. We are currently collecting field data that will allow us to investigate relationships between average flow rates and several overlapping ebb-and-flow signals. Mechanisms for causing this behavior are also being investigated and modeled.

2003 - *Delineation of the subterranean Doe Creek, Clover Hollow, Sinking Creek and Little Stony Creek drainage basins in Giles County, Virginia, with the use of multiple fluorescent water tracers.* This research project fulfilled a research requirement for the Karst Hydrology course offered through Western Kentucky University and the Center for Cave and Karst Studies.

2002 - *Features controlling the speleogenesis, and the speleogenetic sequence, of Doe Mountain Cave in Giles County, Virginia*. This project fulfilled a research requirement for the Karst Geology course offered through Western Kentucky University and the Center for Cave and Karst Studies.

2003 - *Current: Can Cave Sediments Predict Past Flood Magnitudes?* This project is in progress and is investigating the relationship between flow velocities needed to move boulders through hydraulic lift tubes, and the magnitude of catastrophic flood events required to achieve this.

2002 - Independent Study Project: *Analysis of an Igneous Intrusion in a Highland County, Virginia, cave.*

2002 - *Microgravity survey across a portion of Hatteras Island, NC.* – This study measured extremely small variations in gravity across the island and is part of a larger geo-physical and hydrological study of this barrier island.

General Speleology:

- Eighteen years of experience in studying, exploring, surveying, and documenting caves.
- Many published maps and written works on caves, and caving techniques and equipment, in Virginia, other states, and other countries.

Professional Affiliations

Geologic Society of America
American Geophysical Union
National Speleological Society